INFORMATION TO USERS

This manuscript has been reproduced from the microfilm master. UMI films the text directly from the original or copy submitted. Thus, some thesis and dissertation copies are in typewriter face, while others may be from any type of computer printer.

The quality of this reproduction is dependent upon the quality of the copy submitted. Broken or indistinct print, colored or poor quality illustrations and photographs, print bleedthrough, substandard margins, and improper alignment can adversely affect reproduction.

In the unlikely event that the author did not send UMI a complete manuscript and there are missing pages, these will be noted. Also, if unauthorized copyright material had to be removed, a note will indicate the deletion.

Oversize materials (e.g., maps, drawings, charts) are reproduced by sectioning the original, beginning at the upper left-hand corner and continuing from left to right in equal sections with small overlaps. Each original is also photographed in one exposure and is included in reduced form at the back of the book.

Photographs included in the original manuscript have been reproduced xerographically in this copy. Higher quality 6" x 9" black and white photographic prints are available for any photographs or illustrations appearing in this copy for an additional charge. Contact UMI directly to order.

UMI

A Bell & Howell Information Company
300 North Zeeb Road, Ann Arbor MI 48106-1346 USA
313/761-4700 800/521-0600

Université d'Ottawa · University of Ottawa

Spatially-Explicit Regional Flood Frequency Analysis Using L-Moment, GIS and Geostatistical Methods

by

JEAN-LUC DAVIAU

M.A.S.c. Thesis
submitted to the School of Graduate Studies and Research
under the supervision of

DR. KAZ ADAMOWSKI

in partial fulfilment of the requirements for the degree of
Master of Applied Sciences, Civil Engineering*

at the

University of Ottawa
Ottawa, Ontario, Canada
July 1998

* The Master of Civil Engineering Program is a joint program with Carleton University administered by the Ottawa-Carleton Institute for Civil Engineering

Abstract

Each year, floods cause many deaths, displace thousands from their homes and are responsible for several billions of dollars in damages. Lacking efficient means of digital data storage and processing, previous regional flood frequency analyses seldom considered the spatial dimension of the problem explicitly. As a result, insufficient use was made of spatial autocorrelation; of associations with other variables or of topological inter-relationships such as proximity (near a water body), containment (within a 2nd order watershed) and orientation (bearing and azimuth). Spatially-implicit methods also tended to marginalise the importance of flood-generating mechanisms – which vary continuously in space – and which combine at each location to yield the total flood risk.

In this study, the most current nonparametric and L-moment (parametric) methods for flood frequency analysis (FFA) are supplemented by geostatistical and GIS techniques. Three spatial approaches are adapted for FFA: scientific visualization of random fields; characterization of spatial associations; and hierarchical spatial models of flood parameters. Three spatial models are investigated for the L-moments of flood observations: the L-skew is taken as an average within regions (polygons); the L-coefficient of variation is modelled using kriging (continuous space); and the L-mean is estimated locally (point) or from maps if local records are unavailable. L-moments are used to estimate the parameters probability distributions used to describe floods.

Average daily maximum (AM) flood flows for Central and Eastern Canada are analysed – extending an earlier study (Bobée *et al.*, 1996). Nonparametric methods are used to test the statistical properties of the data, to estimate their at-site probability density function and to describe flood timing. L-moments are used to compute the L-mean, L-coefficient of variation and the L-skew of flood times and flows. They are also used to identify discordant sites in a region, to test regional heterogeneity, to obtain the signal-to-noise ratio, and to identify a suitable (parametric) distribution for the data.

Geostatistical techniques are used to quantify spatial auto-correlations and to estimate L-CV using spatially-explicit kriging methods. Due to the extensive area covered, the earth's curvature must be accounted for in mapping geostatistical results – this is done using a GIS. GIS techniques are also used to visualize spatial associations between flood parameters and several meteorological and physiographic variables. A measure of spatial contrast is developed and used to diagnose homogeneous regions for L-skew.

Exploratory data analysis were used to reveal spatio-temporal patterns in the flood generating mechanisms. The behaviour of the multimodality index (MMI) developed herein was diagnosed and its usefulness as a summary measure of nonparametric PDF was confirmed. In combination with the direct visualisation of Julian flood dates (instead of less intuitive seasonal statistics), the MMI served as a good diagnostic tool to identify areas where multiple mechanisms are likely. Traditional unimodal parametric flood distributions must be used with caution (or in the context of a classified FFA) in such areas.

The spatial contrast measure developed herein was used to diagnose a complex but continuous homogeneous region for L-skew (initially delineated using L-moments and flood timing). Re-definition of the size and shape of the region's boundaries based on the spatial contrast can result in smaller heterogeneity L-statistics, indicating an improved regionalisation model. This was supported by an examination of spatial patterns in L-CV and other indicator variables such as vegetation and snow.

The methodologies of previous regional flood frequency analyses and regional GIS studies, which were combined for the purpose of the current study, are discussed and further integrated in the last section.

Gray-scale maps are required by thesis publishing standards. Une version de ce résumé est disponible en Français.

Acknowledgments

I am truly grateful to my family for supporting me throughout this period – particularly my wife, Julie, whose thesis "widowhood" did not cause her to lose her sense of humour. My supervisor, Dr. Kaz Adamowski, was encouraging of my interests in GIS, geostatistics and teaching even though they were time-consuming. His thoughtful contributions to our hydrology manual, conference paper and to this thesis document have greatly improved my technical and academic writing skills.

I am thankful to the staff of the geological department for welcoming me as one of their own: from the department's administrator, Helen DeGough; to the GIS lab supervisor, Jean-Francois Tardif and to professor Grahame Bonham-Carter who guided my GIS pilot project and thoroughly supported my cross-disciplinary approach. I also thank my own faculty's engineering computing supervisor, Steve Symons and the administrators Paulette, Bonnie and Noella who guided me both on and off-campus.

I value the advice and encouragement I received from David Harvey, John Power, Claude Faucher and Paul Pilon of Environment Canada. A GIS study requires large amounts of data for which I am indebted to Richard Post and Matthew Craig (watershed, land-use and climate data) and Dr. Shin-Yung (HYDAT flow data) of Environment Canada. Some data was re-used from the National Sciences and Engineering Research Council (NSERC) strategic grant in which I participated.

Funding for part of this work was provided by NSERC strategic grant G15430 and this is gratefully acknowledged. I also recognize the support of Lisa Andrews at Tydac Technologies for the grant of an academic licence of the SPANS™ GIS: this thesis would not have been possible without it. The completion of the thesis was supported by my employer, Dr. Alan Fok of Environmental Hydraulics Group, to whom I am truly grateful.

Contents

List of Figures

List of Tables

Notation

Greek Characters:

λ_1 = First sample L-moment, analogous to the mean.
λ_2 = Second sample L-moment, analogous to the standard deviation.
λ_3 = Third sample L-moment, analogous to the coefficient of skewness.
λ_4 = Fourth sample L-moment, analogous to the coefficient of kurtosis.
β = Probability weighted moment.
ε = Bias.
$\gamma(h)$ = Variogram ordinate at lag h.
μ, σ = Mean and standard deviation.
τ_2 = Ratio of the L-moments λ_2/λ_2. Also termed L-CV.
τ_3 = Ratio of the L-moments λ_3/λ_2. Also termed L-skew or L-skewness.
τ_4 = Ratio of the L-moments λ_4/λ_2. Also termed L-kurtosis.
ζ = Buffer width as a proportion of the feature being dilated.

Roman Characters:

a = Range of a variogram in geostatistical analysis.
A, B = Probabilistic events.
b = Estimate of a probability weighted moment.
C_0 & C_1 = Used to express the nugget effect (C_0) and sill ($C_0 + C_1$) of a variogram.
C_{ij} or $\mathbf{C}$ = Covariance between locations i and j (C_{ij}) or covariance matrix $\mathbf{C}$.
C_w = Contrast, the natural logarithm of the odds ratio, O_r.
D = Discordance statistic.
$\mathbf{D}$ = Vector of distances between samples and the location to be estimated.
f(x) = Probability density function. Also abbreviated as pdf.
F(x) = Cumulative distribution function. Also abbreviated as cdf.
h = Smoothing factor used in nonparametric probability density estimation OR lag used to evaluate auto- or cross-correlation in geostatistical analysis.
H_i = Heterogeneity statistics based on observed and simulated regions.
K(x) = Kernel function used in nonparametric estimation (usually Gaussian).
N, n = Number of floods in the population (N) or the observed sample (n).
O, O_r = Odds (O) and odds ratio (O_r).
P = Probability.
r = Order of a moment or L-moment, e.g.: second order is the variance.
$R(x_0)$ = Random function error in X at the location where an estimate is required.
$\mathbf{S}$ = Sample covariance matrix based on $\mathbf{u}$.
T_{ij} = Area cross-tabulation totals (usually obtained from a GIS area analysis).
$\mathbf{u}$ = Vector containing the first three L-moment ratios.
V_i = Variability of L-parameter groupings with respect to simulation results.
$V(x_i)$ = Random function variate (flood parameter) at a sampled location.
w or $\mathbf{w}$ = OK or UK weights (w) or weight vector ($\mathbf{w}$).
X or x = Random variable (X) or flood flow (x).
Z = Goodness of fit statistic for various parametric distributions.

Abbreviations

A/P	=	Elongation ratio (area to perimeter), in km.
AM	=	Average annual maximum daily flow.
API_i	=	Antecedent Precipitation Index. Subscript denotes number of days.
ATI_i	=	Antecedent Temperature Index. Subscript denotes number of days.
BLUE	=	Best linear unbiased estimator – kriging estimates are BLUE.
CFA	=	Consolidated frequency analysis software by Environment Canada.
CI	=	Confidence interval of a flood estimate.
DA	=	Drainage area of a watershed.
$DIST_{sub}$	=	Distance from a point or line (subscript) obtained by buffering.
EDA	=	Exploratory Data Analysis – used to reveal patterns in the data.
EL	=	Elevation in metres above mean sea level (amsl).
ENSO	=	El-Nino – Southern Oscillation.
FFA	=	Flood frequency analysis.
GEV	=	Generalized extreme value distribution.
GIS	=	Geographical information system.
GLO	=	Generalized logistic distribution.
GPA	=	Generalized Pareto distribution.
GSLIB	=	Geostatistical software library at Stanford University.
HT	=	Heavy-tailed [probability density function].
i.i.d.	=	Independently and identically distributed.
L-____	=	L-statistics analogous to conventional mean, coefficient of variation, skewness and kurtosis.
LAT	=	Latitude in decimal degrees.
LAND	=	Land cover and/or land use.
LONG	=	Longitude in decimal degrees. Also expressed as LONG.
MM	=	Multi modal [probability density function]. An indicator for the number of flood-generating mechanisms active at the flow gauge.
MMI	=	Multi modality index. Summarizes the proportion of probability assigned to modes (i.e. mechanisms) other than the primary mode.
MSE	=	Mean square error, sometimes expressed as a root (RMSE).
NMODES	=	Number of modes of the nonparametric probability density function.
NPEAK	=	Net peak height for a given mode in a probability density function.
NSERC	=	National sciences and engineering research council.
OK	=	Ordinary Kriging. Spatial estimation analogous to regression.
P	=	Mean annual precipitation. Subscript denotes total, rain or snow.
PD	=	Partial duration or peaks-over-threshold flood series.
pdf	=	Probability density function.
PWM	=	Probability weighted moment.
ROI	=	Region of influence. Hydrologically-similar group to which a flow gauge belongs. Alternative to geographically homogeneous regions.
SEE	=	Standard error of estimate.
SPANS™	=	Spatial analysis software by Tydac (GIS used in this study).
TCEV	=	Two-component extreme value distribution (for bimodal data).
UM	=	Unimodal [probability density function]. Single mechanism likely.

Chapter 1

INTRODUCTION

1.1 Motivation

Floods are the most destructive of natural hazards (Wallis, 1988), either in terms of property damage or loss of human life. Consequently, flood frequency analysis (FFA) is a dynamic field of research in which new theories are continuously applied, including fractal theory (Ribeiro-Correa and Rouselle, 1996), neural networks (Daniell, 1991) and others. Critics point-out that new techniques do not necessarily improve flood estimates (Klemeš, 1993). Three principles have been proposed to avoid such pitfalls: increased use of "regional" or spatial data; improved representation of flood-generating mechanisms; and heightened focus on the nature of the extreme events being estimated (NRC, 1988).

As regards the second principle, the author participated in an NSERC strategic project in which a systematic comparison of regional FFA methods was made (Bobée *et al.*, 1996a & 1996b). During this study, the importance of using simulation techniques such as bootstrap (Ouarda *et al.*, 1995; Fortin *et al.*, 1997) or Polya resampling (Bobée *et al.*, 1993) for comparing different FFA methods was stressed. The third principle was addressed by using nonparametric methods to characterize the effect of climate on flood-generating mechanisms. The author also undertook a pilot GIS project to quantify the spatial influence of snow on floods and reported the findings at a conference (Daviau *et al.*, 1994).

The foregoing led the author to hypothesize that the three principles could be unified by extending regional FFA techniques to include the spatial dimension explicitly (the temporal dimension can already be handled explicitly using time series or partial duration analysis). The consequences of spatially explicit FFA are perhaps best explored by re-examining the fundamental nature of the flood estimation problem.

Broadly speaking, the flood risk to human communities can be defined in terms of the frequency and magnitude of exceptionally large flows (or high water levels) resulting from any combination of climactic forcing (thunderstorms, snowmelt, ice) on the particular physiographical attributes of a drainage basin (soil types, land use, slopes); as modified by the topology of its river network (marsh and lake storage, flood routing, river confluences, tidal deltas). Both climactic forcing and watershed state are time and space-dependent phenomena – as are the interconnections between floods and human settlements. Several flood-generating mechanisms can occur at a given location but each may act at different temporal and spatial scales.

Time can be handled using a discrete scale (annual maxima, AM) or on a continuous basis. Many FFA assume AM floods to be time-independent and calculate measures of location (mean), spread (CV) and shape (skew) using the method of moments (or L-moments: L-mean, L-CV and L-skew). The L-moment approach has been used extensively at the University of Ottawa – the principal results of this work are reviewed and applied in this thesis.

The spatial dimension of flood phenomena can likewise be treated as points (single-site FFA), polygonal regions (regional FFA) or in a continuous, spatially-explicit manner. Previous regional FFA have tended to be spatially-implicit: latitude, drainage area and other spatial indicators were assigned to point locations, then used as dependent variables along with meteorological and other parameters in regressions, numerical simulations or cluster analysis (Hosking and Wallis, 1996). By restricting the use of spatial data to scalar measures (e.g.: latitude), these methods failed to address autocorrelation and topological information. Such restrictions were often due to the limited availability of tools to handle spatial data explicitly.

Regional FFA techniques, on the other hand, grouped gauges from neighbouring locations into statistically homogeneous regions. Regional flood estimation methods gave smaller errors when applied to these regions than to either the entire study area or to the site data alone. Regressions were used to relate physiographic or meteorological data, available at points, to flood parameters. The shape parameter of floods was often assumed to be constant within each region, resulting in discontinuities at boundaries. In a notable exception, Waylen and Woo (1984) plotted the probability distribution parameters from several gauges as trend surfaces for Northern Ontario; however, this was still an implicit method since the only spatial information used were the latitude and longitude of the gauges.

This thesis extends regional FFA methodology by treating at-site flood parameters as spatially-continuous random variables. This is accomplished using more spatially-explicit techniques than have been used in the past: geographic information systems (GIS, from the field of geography) and geostatistical theory (from the geological and mining engineering fields). Analytical GIS is a fundamentally visual and data-centred discipline within which different methods can be compared to each other, or to themselves, at different spatial and temporal scales. As a result of its multi-disciplinary evolution, it is well-suited as a framework for data processing and modelling (Bonham-Carter, 1994). Geostatistical theory is a rigorous, spatially-explicit set of methods used to describe random variables and fields (Isaaks and Srivastava, 1989). It is analogous to regression in the spatial dimension.

To the best of the author's knowledge, the explicit spatial estimation of floods' L-moments using geostatistics and the use of GIS to investigate the impact of snow and to guide homogeneous region delineation have not been treated elsewhere in the literature.

1.2 Objectives

The objectives of this thesis are as follows:

1) To critically review the methodologies and results of previous annual maxima regional flood frequency studies in central and eastern Canada (including the recent NSERC study in which the author participated). The review will focus on:

   - The manner in which spatial dimension was handled in previous studies.
   - The techniques used to delineate homogeneous regions in previous studies.

2) To use GIS and scientific visualization techniques to characterize the spatial variation of the principal flood-generating mechanisms and parameters by:

   - Developing a numerical "multimodality index " (MMI) to describe the shape of nonparametric probability density functions (pdf);
   - Developing an objective method to classify a pdf as: unimodal (UM), heavy-tailed (HT) or multimodal (MM);
   - Calculating statistics which describe the time distribution of floods; and,
   - Mapping the above information using a GIS to characterize spatial patterns.

3) To investigate spatially-explicit methods of flood characterization and information transfer using GIS and geostatistical techniques, including:

   - To diagnose hierarchically-defined homogeneous regions for L-skew and L-CV using a spatial contrast measure developed herein in combination with existing L-moment diagnostic statistics for regions;
   - To quantify spatial associations between L-CV and independent variables such as vegetation, precipitation and distance from major water bodies; and,
   - To obtain point estimates of L-CV for any location within the study area. This is a useful result in that it can provide flood estimates at sites where flow data is unavailable.

1.3 Scope

Within the range of third-order drainage areas selected for this study, 10 to 100,000 ha, flood parameters will be assumed to be scale-invariant. Some researchers have hypothesized that flood magnitudes can be described using fractal or multifractal measures (Turcotte, 1994). Indeed, flood risk is probably not constant at different scales: there is growing evidence that continental teleconnections such as ENSO (Gingras & Adamowski, 1995) and global climate change can affect flood risk at much smaller spatial scales by modifying the time and spatial distribution of precipitation. In this thesis, a sub-continental scale will be used in which planetary or continental effects, e.g.: global warming trend and ENSO, will not be considered.

While each flood-generating mechanism may act at a different scale, (e.g.: dissipating hurricanes, thunderstorms or ice-jams), and some may act at several scales simultaneously, their impact will only be considered from a third-order basin perspective in this thesis. Although each basin's many mechanisms could be composited to obtain the range of their action as large-scale phenomena, this will not be done here due to time constraints. Instead, it will be assumed that only two flood-generating mechanisms are responsible for the flood observations: snowmelt and "other" (usually various types of rainfall).

Since periods of record are generally short and due to the large number of sites considered in this study, it was not possible to statistically model each flood-generating mechanism separately in what is known as a classified FFA. The effect of multiple-mechanisms will be handled implicitly by considering their impact on the nonparametric multimodality index (developed herein) and the L-CV of each drainage basin. In an earlier pilot project, L-CV was shown to have an inverse spatial association with snow (Daviau *et al.*, 1994). This relationship will be formalized in this study.

While other unimodal probability distributions such as the generalized Pareto (GPA) could be used, the generalized extreme value (GEV) distribution will be used to

estimate flood frequency at each site. In terms of data sources, the analysis will be conducted on average daily AM flood series only. Partial duration (PD) flood series and instantaneous maximum flows will not be considered, nor shall the effects of hydraulic rating curves or tidal bores, which can introduce error in flow estimates. Historic and paleoflood information will also be neglected. Meteorological maps from the digital Canada Climate Normals have been used as-is in order to save time – contouring point data would perhaps have resulted in more detailed maps (e.g: more map classes).

The method of L-moments is used to obtain the at-site moments, to estimate the parameters of the GEV distribution and to test the homogeneity of regions by means of numerical simulations. Although this method has several advantages, it is recognized that other methods such as regression, maximum-likelihood or the nonparametric approach could have been used instead in some cases. Indeed, nonparametric methods are used as a screening tool and the geostatistical method of estimation called kriging is analogous to regression.

Geostatistical techniques will be applied in a thorough manner but not to the full extent possible. For example, the variograms models describing the spatial variation of L-CV, L-skew and snow pack depth allow for directional anisotropy but are otherwise simple, incorporating no more than two nested structures. It is recognized that more advanced GIS methods for map modelling (weight-of-evidence Bayesian method) and geostatistical estimation (conditional simulation studies) could have enriched the results but their use was not possible due to time constraints.

Chapter 2

LITERATURE REVIEW

The cross-disciplinary nature of this thesis required an extensive review of the flood-frequency, GIS and geostatistical literature. FFA has a long history in civil engineering because it is a central theme in water resources. However, geostatistics and GIS techniques are only now beginning to be applied for FFA. This section reviews the development of FFA techniques from single site to regional methodologies and indicates the ways in which floods may be treated as spatially continuous phenomena.

The principal hypothesis to be tested herein is whether the flood parameters called L-moments can be treated as regionalised variables, e.g.: quantities which vary according to location and whose behaviour is somewhere between a truly random and a deterministic variable (Bonham-Carter, 1994). Such variables are the object of geostatistics and are amenable to treatment within a GIS.

2.1 Single-Site Flood Frequency Analysis

2.1.1 Parametric Approaches

All parametric techniques attempt to fit a theoretical probability distribution to the observed flood data series. In recent years, increasingly sophisticated numerical methods have been developed to the estimate parameters of theoretical or "parent"

distributions under the assumption that the observed data represent a sample drawn from such a population. This is usually done using either the maximum-likelihood technique or the method of moments. The latter method, which equates the sample moments to the population moments, has been used most widely.

Arguably the most powerful implementation of this approach is by means of L-moments which are linear (L-) combinations of ranked statistics. These can be obtained directly from the data, without the use of plotting-position estimators or probability-weighted moments (Hosking and Wallis, 1995; Wang, 1996). The L-moment approach used herein has the following advantages: its widespread application; robustness to outliers; virtual lack of bias (Vogel and Fennessey, 1993) and the maturity of its theoretical underpinnings. It has also been extended for use in regional FFA (Hosking and Wallis, 1993; Pilon and Adamowski, 1992).

The four steps in single-site FFA using L-moments parallel those of classical FFA. Each is summarized below along with appropriate cautionary notes:

1) Select a sample. Parametric methods require flood observations to satisfy several assumptions, namely: that they be statistically independent from each other; have no significant trends or discontinuities (stationarity); and be drawn from a homogeneous population with a unique pdf. These are often abbreviated as: independently and identically distributed or i.i.d. (Watt *et al.*, 1989).
   - Abnormally small or large observations should be checked for gross errors and tested to determine whether they should be treated as statistical outliers. Such outliers are often due to a different flood-generating mechanism.
   - Historical flood information can significantly increase the accuracy of estimates and should be used whenever possible (Pilon and Adamowski, 1993). Historic floods, which are often the largest on record, may also belong to a different population.

2) Infer population properties. The most likely parent distribution must be identified using probability plots (graphical method), L-moment ratio diagrams or goodness-of-fit tests such as the Z L-statistic (Hosking and Wallis, 1993).
   - A unimodal probability distribution must not be selected if the data appear to be the result of multiple flood-generating mechanisms (see discussion below).

3) Fit a theoretical distribution. This is done by estimating the L-mean, L-standard deviation and L-skewness and using these to calculate the parameters of the probability distribution chosen in the previous step.

- If multiple flood-generating mechanisms exist, it is difficult to fit any distribution based on at-site data alone (see discussion below).

4) Estimate the design floods. For each return frequency, e.g.: once in every 20 years (or 1:20), the fitted probability distribution equation is used to estimate the flood magnitude. Depending on requirements, one may also calculate the standard error of estimate (SEE) and/or the confidence interval (CI) for the flood estimate.
   - If average daily maximum flows were used in the analysis, it is sometimes necessary to convert these to instantaneous daily maximum flows using a suitable relationship.
   - Caution must be exercised not to extrapolate too far beyond the period of record, e.g.: an estimate of the 500-year flood based on 20 years of record is likely to be unreliable (Klemeš, 1993).

The results of nonparametric tests used to verify the assumptions made in the first step are described in Appendix A and in section 4.2). In step 2, Gingras (1993) has shown that multimodality in the data can be diagnosed based on both the time of the year in which each flood occurs and a plot of the pdf obtained using nonparametric methods.

Several studies in North America (Pilon *et al.*, 1991b; Gingras and Adamowski, 1992) and around the world (Rao and Hamed, 1994; Karim and Chowdhury, 1995; Önöz and Bayazit, 1995) have shown that the GEV distribution is one of the most flexible and reliable distribution to use – with cautions for Australia (Vogel *et al.*, 1993a) and the Southwestern United States (Vogel *et al.*, 1993b). The GPA distribution has also been recommended by many researchers (Ashkar and Ouarda, 1996). Since departures from unimodality can have a greater impact on flood estimates than distribution choice, this topic is not emphasized herein. The GEV distribution will be used in this thesis.

In step 3, a dilemma arises which cannot be resolved for at-site analyses using (typically) short periods of records (20 years). If floods are the result of more than one flood-generating mechanism then unimodal distributions, including the GEV, can not describe them adequately (Chow and Watt, 1990; Gingras, 1993). Multimodal distributions such as the two-component extreme value (TCEV) or the Wakeby have a greater number of parameters (4 and 5, respectively).

Alternatively, splitting the flood series in two by classifying each observation as belonging to either the primary or the "other" mechanism(s) requires the evaluation of at least four parameters to fit two distributions (Singh, 1987). Since the number of available observations at each site is fixed, it is difficult to obtain accurate estimates for a large number of parameters (Maidment, 1993). Users of parametric methods must therefore accept either poor parameter estimates or the use of an unsuitable distribution when analysing flood series with a significant departure from unimodality.

The presence of outliers and multimodality in flood data points to the fundamental problem in FFA: how can the information obtained from each observation be used to describe flood-generating mechanisms most efficiently? Short of increasing the number and duration of observation sites or of locating historical flood data, additional information can be obtained in two ways: by pooling data from other nearby sites (regionalisation) and/or by using proxy variables such as precipitation to improve estimation (Rossi and Villani, 1994). Since both flood observations and proxy variables vary continuously across space, geostatistical and GIS techniques can be applied to improve spatial information transfer.

From a spatial perspective, most outliers and observations in the tails of multimodal pdf are artefacts which result from flood-generating mechanisms' overlapping areas of influence – floods which are deemed unusual merely because they fall outside the assumption of a unimodal pdf (Gingras and Adamowski, 1993). If the analyst's perspective shifts from traditional at-site (or multi-site) to spatially-continuous analysis, many of these same observations can be considered as "normal" floods resulting from one of several flood-generating mechanisms which can occur in a given watershed.

2.1.2 Nonparametric Approaches

Nonparametric methods describe the statistical properties of observations in the most direct way possible, e.g.: without using intermediate parameters. This has led to the development of several tests to verify statistical assumptions about data: that it has no trends, is random, homogeneous and independent. These must be satisfied before

either parametric or nonparametric analysis can proceed, therefore most FFA software suites such as Consolidated Frequency Analysis (CFA) incorporate such tests (Pilon and Harvey, 1994). The results of these tests for the flood data used in this thesis are given in Appendix A.

Nonparametric methods can also be used to estimate the pdf directly from observations, without making any assumptions as to its shape or the number of modes (Adamowski, 1985). The procedure used herein is analogous to building a histogram by placing a kernel function (itself a pdf) centred at each observation, then summing and normalizing the area to obtain the overall pdf. Bardsley (1989) indicated that this requires the evaluation of a non-informative bandwidth parameter, h, but this is done automatically by software such as CFA using a cross-validation procedure.

Using a nonparametric pdf to estimate design floods (i.e.: floods with a specific return period) has several advantages over parametric methods (Alila, 1987):

- While parametric methods' estimates are most reliable where the majority of observations are available (in the middle of the range), nonparametric methods are equally sensitive to all observations, resulting in less biased flood estimates.
- In parametric methods, each observation is used to estimate the distribution parameters. Consequently, a large change in a small observation can affect estimates for the very larger and rarer floods which are of interest in FFA – a nonsensical result (Klemeš, 1993). This does not occur using nonparametric methods.
- Nonparametric methods can estimate the probability of flooding even if the observations are the result of several flood-generating mechanisms, e.g.: multimodal pdf. They are therefore applicable in areas where such mixtures occur.

Furthermore, since each mode in a multimodal pdf may correspond to different flood-generating mechanisms, nonparametric pdf plots can be used as a diagnostic tool during the identification of a parent distribution (in parametric methods). By matching the statistical properties of the nonparametric pdf plot to those of a suitable parametric distribution (e.g.: GEV for unimodal or heavy-tailed and Wakeby for multimodal), the population assumption underlying parameter estimation can be respected more closely.

For each site considered herein, nonparametric methods will be used to characterize the primary mechanism or mode (snowmelt in the north and rainfall in the south) and all other mechanisms under the "secondary" category.

Directional statistics (also known as seasonality or circular statistics) express the average at-site flood timing as the magnitude of a vector whose azimuth is the Julian flood date. Recently, directional statistics have also been used to characterize different flood-generating mechanisms by noting the time of occurrence of floods within each year (Burn *et al.*, 1997). This is also a nonparametric method. A more accurate assignment of floods to mechanisms is possible using the antecedent precipitation index (API) (Waylen and Woo, 1984) and/or the antecedent temperature index (ATI) (Alila, 1987) – however the significant effort entailed is only worthwhile if the resulting series are to be analysed separately. Like Magilligan and Graber (1996), the purpose for characterizing flood-generating mechanisms in this thesis is exploratory.

Extending the approach of Gingras and Adamowski (1993), the above information will be used to diagnose homogeneous regions for the flood parameters under study (L-CV and L-skewness) using nonparametric density estimation. Gingras (1993) identified a need for objective methods to categorize nonparametric pdf as unimodal (UM), heavy-tailed (HT) or multimodal (MM). Such a method, which also counts the number of significant modes, is developed herein. Finally, at site values of L-CV for multimodal sites tend to be larger due to the wider range of the observations. Large values of L-CV were previously shown to be negatively associated with snow (Daviau *et al.*, 1994). The strength of this relationship will be quantified in this thesis.

2.2 Regional Flood Frequency Analysis

2.2.1 Review of Regional FFA Methodologies

Traditionally, regional FFA methodologies have pooled data from several sites grouped together either as "homogeneous regions" (usually spatially-contiguous) or "regions of influence" (not necessarily contiguous), within which flood characteristics were considered hydrologically similar. The three steps involved in regional flood frequency analysis (Kite, 1977) are shown below with emphasis on the L-moment method:

1) Determine homogeneous regions and test their spatial variability [at-site analogue: select a sample and test its temporal variability]. L-moment D and H statistics; nonparametric pdf plots and the timing of floods can be used to diagnose regions.
   - Multimodal pdf or outliers may indicate improperly defined regions.
   - Check that unexplained variance is smaller than for entire study area.

2) At-Site Frequency Analysis yielding either L-moments, distribution parameters or flood quantiles (depending on the method). For each watershed, indicator variables are also compiled in three categories: geographic (LAT, EL, DA, A/P); physiographic (S, land use); and meteorologic (ATI, API, P, S) for use in the next step.

3) Regional Relationship Development, traditionally resulting in regression equations for the L-moments, distribution parameters or flood quantiles in terms of the indicator variables obtained in the second step. Since regression does not account for spatial autocorrelation, kriging can be considered as a more thorough replacement method for this purpose (see section 2.3.3).

Floods estimated using regional relationships usually have lower mean squared errors (MSE) than at-site estimates except where long periods of record are available, in which case the opposite may be true. Rather than using either at-site or regional parameter estimates alone, Bayesian methods have been suggested to weight the relative importance of at-site vs regional information (Tung and Mays, 1981; Kuczera, 1983). This is usually a concern for L-CV since the L-mean almost always better estimated at-site while the regional average estimate of L-skew is most often used for consistency (it is difficult to estimate L-skew from short samples).

In this thesis, spatially-explicit methods are used to optimize each of the three steps in regional FFA. A spatial visualization technique is introduced to optimize regions' shape and size in step 1 (based on the pilot study mentioned above). Rather than point values, maps are used to represent indicator variables such as snow in step 2. Furthermore, unbiased estimation techniques for L-moments are used to obtain at-site estimates (Hosking and Wallis, 1995). Rather than regression in step 3, a spatially-correlated surface is obtained for L-CV using kriging; and geostatistical techniques are used to measure the association between L-CV with snow and other variables. It would have been desirable to use of ATI & API criteria to obtain separate or "classified" snowmelt and rainfall PD flood series in step 2, but this was not possible due to time constraints.

The objective of regional FFA is to make the best compromise between spatial and temporal variability. The total variance of regionalised parameter values is a function of both at-site temporal variability; inter-station correlation; and spatial disturbance (Rossi and Villani, 1994). Larger numbers of sites with longer records decrease total variance, but the benefits decrease in densely sampled areas due to temporal and spatial inter-station correlations.

These authors and others suggest clustering techniques to reduce total variance by subdividing a study area into a successively larger number, m, of regions using a step-wise procedure (Burn *et al.*, 1997). This results in a smaller MSE for each region than for the entire study area. However, cluster analysis cannot account for anisotropic spatial correlation and allows for sudden changes in parameters between overlapping regions of influence (ROI), which are often discontinuous (Hosking and Wallis, 1996).

Instead, this study seeks to minimize total variance in two steps: first, the time dimension is summarized by estimating at-site L-moments; and second, spatial relationships are handled explicitly for each parameter using GIS and geostatistical techniques such as kriging. Both L-moment and kriging techniques provide measures of estimation variance.

As noted above, nonparametric methods can handle mixed populations at single sites but they have not been adapted to pool data from nearby sites. Previous nonparametric regional studies have used regression to express the at-site flood quantiles in terms of basin and meteorologic variables in a region (Gingras, 1993). This incorporates information about floods from all mechanisms since each flood affects the at-site pdf and quantiles. Due to its strengths in dealing with multimodal flood data, the investigation of improved regional FFA procedures for the nonparametric method is a promising area of research – but one which lies outside the scope of this thesis.

2.2.2 Previous Regional Flood Frequency Studies

Regional FFA done at the University of Ottawa

One of the objectives of this thesis is to summarize the findings of previous regional FFA studies for the current study area. Table 2.1 summarizes how the space and time dimensions were handled (discrete or continuous) and how flood-generating mechanisms were characterized in each previous study. These are also shown graphically in Appendix C, Figure C9 b.

In his 1987 M.A.Sc. thesis, Alila investigated nonparametric kernel estimation techniques and showed that a bimodal pdf generated by two distinct flood-generating processes could be decomposed by classifying individual flood observations using a combination of ATI and API. His 1993 Ph.D. thesis recommended regional rainfall distributions for **Canada**, for which L-skewness remains constant over large areas. In Gingras' several studies of **New Brunswick** floods, the combined effects of climate and physiography were shown to result in several flood-generating mechanisms such as tropical storm tracks in the south; rainfall and snowmelt in the central areas; and snowmelt alone to the north. Gingras and Adamowski (1992) showed that L-moment methods had identified the (unimodal) GEV distribution, yet nonparametric pdf were mostly bimodal or multimodal. In his 1993 Ph.D. thesis, Gingras later developed a nonparametric regional FFA methodology and applied it to this data set.

Table 2.1: Treatment of Spatial and Temporal Scale; Flood-Generating Mechanisms in Previous Regional FFA

Authors	Yr	Region	No. Stns.	Stn-Yrs	Space	Time	Causes of Floods
Waylen, P. and Woo, M.K.	1984	Northern Ontario (ONT)	48	1000+	trend surfaces for flood parameters	annual maxima	• classified by API, ATI
Alila, Y. (M.A.Sc.)	1988	Ontario (ONT)	2	129	n/a	annual maxima	• pdf shape, R.H. tails • classified by API, ATI
Pilon, P.J.; Alila, Y. and Adamowski, K.	1991	Newfoundland (NFLD)	23	623	homo. regions	annual maxima	• MAP & timing • L-skew simulations
Pilon, P.J. and Adamowski, K.	1992	Nova Scotia (NS)	25	1036	homo. regions	annual maxima	• UM population • L-skew simulations
Gingras, D. and Adamowski, K.	1992 1993	New Brunswick (NB)	53	1383	homo. regions (effect of scale investigated)	annual maxima	• pdf shape (UM, BM, HT) and climate • timing of floods
Gingras, D. (Ph.D.)	1993	New Brunswick	53	1383	homo. regions	annual maxima	(as above)
Alila, Y.; Adamowski, K.; Pilon, P.J. and Kowalchuck, M.Z.	1993	Saskatchewan - Nelson River Basin (SASK, MAN)	230	2800	homo. regions	annual maxima	• pdf shape (UM, BM, HT) and climate • timing of floods
Daviau, J.L.; Gingras, D.; Adamowski, K. and Pilon, P.J.	1994	Ontario & Quebec (ONT, QUE)	183	3600+	homo. regions (effect of snow on L-CV studied)	annual maxima & partial duration	• pdf shape (UM, BM, HT) and climate • timing & geography of floods (using GIS)
Liang, G.C.; Gingras, D.; Adamowski, K. and Pilon, P.J.	1994	Ontario & Quebec (ONT, QUE)	183	3600+	homo. regions	annual maxima & partial duration	• classified PD series by pdf shape, timing
NSERC Strategic Grant[1] (GREYHYS)	1996 a, b	Ontario & Quebec (ONT, QUE)	183	3600+	homo. regions and ROI	annual maxima & partial duration	• annual and spring series analysed
Ouarda, T. & Ashkar, F.	1997	Ontario	183	3600+	homo. regions	partial duration	• classified PD series based on flood timing.
Daviau, J.L. (M.A.Sc.)	1998	Eastern Canada (MB, ONT, QUE, NB, NS, NFLD)	450	15,000 +	continuous (GIS and kriging). Fixed scale.	annual maxima	• pdf shape and climate. • timing & geography of floods (using GIS)

[1] See Table 2.2 for details on the methods used and compared in this study.

Pilon *et al.* (1992) applied the regional L-moment method to **Nova Scotia** and found that the province could be treated as a single homogeneous region with a single value of L-skewness. In another 1991 study for **Newfoundland**, these authors showed that the high proportion of sampling error due to random variations (noise) in L-CV and L-skew, determined from simulation studies, indicated that average values should be used throughout the province. The GEV distribution was recommended for both maritime provinces. Alila *et al.* (1993) studied the timing of floods as well as their nonparametric pdf for the **Saskatchewan-Nelson** river basin and identified three types of flood distributions: unimodal (UM), bimodal (BM) and heavy-tailed (HT). Their spatial extents were shown to correspond to climatic zones.

The above techniques were dubbed "regional estimation methods" REM_2 (nonparametric), REM_4 (L-moments) and "determination of homogeneous regions" DRH_4 (combined nonparametric and L-moments) and applied to **Ontario and Quebec** in the context of an NSERC strategic grant (Bobée *et al.*, 1996a and b). A number of other approaches were also compared systematically, as shown in Table 2.2.

Table 2.2: Methods Compared in the 1996 NSERC Study.

Delineation of Homogeneous Regions $[DHR]_i$			Regional Estimation Method $[REM]_i$		
ID	Description of Method	Gauged / Ungauged	ID	Description of Method	At-Site info used?
DRH_{11}	Burn's region of influence (ROI)	G	REM_1	Index Flood (GEV estimated by PWM)	Y
DRH_{12}	Modified ROI	G	REM_2	Nonparametric & OLS	N
DRH_{13}	ROI (ungauged)	U	REM_3	PD & multiple regr.	Y
DRH_2	Canonical Correlation	G,U	REM_4	L-moments	Y
DRH_3	Correspondence Analysis / Hierarchical Clustering	G,U	REM_5	Regression methods (incl. nonlinear)	N
DRH_4	L-Moments and Nonparametric	G,U	REM_6	Index Flood (GPA est. from PD series)	Y
			REM_7	Index Flood (EXP est. from PD series)	Y

After (Bobée *et al.*, 1996a & b).

Based on the inter-comparison criteria, the best-performing estimation method was the index-flood GEV using probability-weighted moments (REM_1) and the homogeneous regions as determined by canonical correlation analysis (DRH_2). However, the following should be noted:

- The REM_1 approach is very similar to the method of L-moments (REM_4), which has been shown to be superior in a separate study (Vogel and Fennessey, 1993). L-moment results were not available due to computational difficulties during the bootstrap.
- The nonparametric method (REM_2) was recommended for general application at gauged sites (it did not handle ungauged sites in a manner amenable to bootstrap re-sampling at the time of the study and was therefore ruled-out for such sites).
- The author believes that the effectiveness of DRH_2 (which was recommended) should be re-evaluated since it used the 10 and 100-year quantiles to define regions – yet these same quantiles served as the evaluation criteria. For gauged sites, the REM_1 was insensitive to the choice of DRH while for ungauged sites DRH_4 was consistently rated the best (after DRH_2).

Based on the above, it can be concluded that the combined use of nonparametric and L-moment methods to delineate homogeneous regions and to estimate floods is an acceptable alternative, especially since DRH_4 results in spatially-contiguous regions which are appealing from a pragmatic perspective. This combination of methodologies is further investigated in this thesis in order to determine whether a spatially-continuous treatment of the flood-generating phenomena may improve flood estimates.

Liang *et al.* (1994) showed that while two classified PD series were considered homogeneous by L-moment tests, the overall PD series was not. They also showed that unimodal pdf for PD series could correspond to either unimodal or multimodal pdf for the corresponding AM series and vice-versa. It was suggested that the number of modes in a PD series may be threshold-related. Daviau *et al.* (1994) confirmed Gingras' earlier finding that the regionalisation method described above as DRH_4 resulted in regions which were less heterogeneous than the entire study area. They also identified an inverse association between L-CV and snow.

Regional FFA done Elsewhere

Sangall and Kallio (1977) completed a regional FFA of **Southern Ontario** which identified nine homogeneous regions south of the Ottawa River – Georgian Bay line. The regions were assembled from whole drainage basins based primarily on physiographic information (soils and slopes) combined with mean annual runoff. Gingras' 1993 delineation (see section 4.5) generally agree with these regions.

Waylen and Woo (1984) classified AM floods into snowmelt or rainfall categories and fitted a compounded Gumbel distribution (one for each flood series) for 48 sites in **Northern Ontario.** Rather than determining homogeneous regions, they fitted continuous trend surfaces to the at-site parameter estimates for each series. Depending on location and climate, their approach clearly showed which flood-generating mechanism could be expected to dominate – enabling designers to estimate not only the design flood but also the season in which it was most likely to occur.

Zrinji *et al.* (1996) applied the hierarchical "region of influence" approach to **Central Canada,** covering an area almost identical to an earlier study which had used spatially-contiguous homogeneous regions (Alila *et al.*, 1993). The resulting pattern of ROIs for L-CV were very similar to those of the earlier study; however a simulation study supported the authors' claim of improved flood estimates. In a 1997 study of the same areas, Burn *et al.* used a hierarchical clustering algorithm incorporating seasonality measures and inter-site distance which resulted in spatially-contiguous but overlapping regions (this approach is discussed further in section 2.2.3).

Watt *et al.*'s 1989 "Hydrology of Floods in **Canada**" discusses at-site and regional FFA at length and provides an excellent overview of the flood-generating mechanisms active in each region of the country. This publication provides extensive references and addresses design flood criteria; special flood conditions such as ice jams; and deterministic flood estimation methods.

2.2.3 Hierarchical Regionalisation of Flood Parameters

The occurrence of floods can be viewed from complementary perspectives ranging from discrete to continuous treatments of time and space. Historically, FFA has progressed from at-site AM flood series (point in space, discrete time), through homogeneous regions (interval) and finally to (spatially-continuous) trend surfaces and classified PD flood series (continuous time). In this study, the continuous perspective is examined first so that it can guide the development and application of techniques used to obtain at-site estimates and to combine them with appropriate regional information.

This approach is similar to current "hierarchical regionalisation" methods in which the region of applicability for the highest moment ratio (usually L-skew) is subdivided into smaller sub-regions for the next lower ratios (L-CV) in the hierarchy until the lowest level (L-mean) is reached. Variables are estimated either as an average value (noise) or modelled against other variables (signal). Structural relationships between each L-moment ratio and meteorological or physiographic variables have been proposed to increase the size of the database (e.g. rainfall L-skew as proxy for floods) or to describe the ratio's systematic variation over the study area (by regression or kriging).

Characterizing Flooding Mechanisms' Spatio-Temporal Distribution

Adamowski (1985) identified mixed populations using nonparametric methods and cautioned that most distributions used in traditional (parametric) FFA were unimodal and could not deal with such flood series. Gingras and Adamowski (1993) showed that each flood-generating mechanisms could be related to a mode of each site's nonparametric pdf by relating it to a monthly partitioning of floods' time of occurrence. In a regional context, this implies that a region with homogeneous flood characteristics must have similar pdf shapes (e.g.: flood-generating mechanisms) at most sites.

Taking a continuous view, each flood-generating mechanism can be considered to operate within its own "homogeneous region", with shifting boundaries in time and space (e.g.: the flood-generating mechanism may influence at-site pdf shapes over different areas and scales and during specific seasons).

Floods' time of occurrence is best described using Julian days either directly or as "seasonality" statistics (Burn *et al.*, 1997). Magilligan and Graber (1997) recently examined the hydroclimatologic and geomorphic controls on the timing and spatial variability of floods in **New England** using GIS and geostatistical techniques. They showed that seasonality statistics, used as indices of flood generating mechanism, could be predicted using multiple regression analysis and surrogate variables for climate (latitude (LAT) and distance from the coast ($DIST_{coast}$)) and physiography (elevation (EL) and drainage area (DA)). It was found that autumn floods, believed to result from dissipating tropical storms, diminished as distance from the coast and elevation increased.

Using the parametric method of moments, flood characteristics are reflected in the shape of the pdf – which is in turn summarized by successively higher moments usually standardized and expressed as ratios. The mean is a measure of location; the coefficient of variation is a measure of spread; the coefficient of skew is a measure of asymmetry; and the kurtosis is related to the thickness of the tails.

Multiple modes resulting from several flood-generating mechanisms are reflected by a wider spread and thicker right-hand tails which result in larger values of L-CV and L-skew. In such cases, distributions such as the Wakeby or TCEV (or classified FFA) can be used to estimate floods. Gingras (1993) showed that the L-moment ratios for floods in New Brunswick lie outside the feasible space for the TCEV.

In this thesis, snowmelt and rainfall are differentiated as flood-generating mechanisms from which UM, HT or MM populations (and pdf) mixtures arise. It is postulated that the presence of multiple mechanisms is reflected in multimodal pdf shapes and in higher values of L-CV. The spatial extent of the snowmelt mechanism is shown using snow as a support variable. Thus, the spatial variability of L-skew and L-CV can be related to the degree of mixing of these populations as well as their geographical dependence on physiographic and climatic factors.

Inferring At-Site Flood Frequency from Regional Information

Over the last 30 years, FFA has progressed from a single gauge to a regional focus in which various methods are used to combine at-site and regional information (Rossi, 1994). In Dalrymple's index flood methodology, at-site estimates of the 2 year or "index" flood (which can be reliably estimated from short records) are multiplied by a point on the regional "growth curve". The curve is composed of an average, for each site in the region, of the ratios of less frequent floods to the index flood. The method's simplicity and power led to its widespread application over two decades and the general approach was still recommended by a recent NSERC study (Bobée, 1996 b). However, it can only handle unimodal populations and treats L-CV as a constant for each region. Furthermore, sharp changes at boundaries between regions are unrealistic from a climatic viewpoint.

Pilon *et al.* (1991b) extended the index flood method's use of the sampling error structure to L-moments by means of simulations and distinguished between the signal (systematic variations) and noise (sampling error) components within each region. Such simulations indicate whether each L-moment ratio (e.g.: L-CV, L-skew) should be regressed against indicator variables (strong signal) or whether an average value should be used for the entire region (mostly noise). Based on this approach, each L-moment ratio could be held constant or allowed to vary systematically within the study area (or one of its subdivisions into homogeneous regions).

Rossi *et al.* (1994a & b) suggested that the tendency towards a constant number of independent rainfalls of a given duration per year points to a corresponding constancy in annual floods. This physical interpretation of flood generating mechanism implies that rainfall and flood homogeneous regions coincide, enabling the use of the more extensive rainfall information to define homogeneous flood regions. The author showed how information can be transferred from rainfall data to the GEV and TCEV flood distribution parameter estimates. The snowmelt mechanism was not discussed.

They then applied this three level hierarchical approach to Southern Italy and used it to estimate the three L-moment ratios (which can be used to estimate the parameters of probability distributions):

1) L-skew was estimated as an average for the entire study area (treated as a homogeneous region). This was done because spatial variability was less than (temporal) sampling variability and inter-station correlation was minimal.

2) L-CV was estimated as an average for each subdivision of the study area (themselves treated as homogeneous regions). Moderate spatial variability required either homogeneous sub-regions and/or a relationships between L-CV and physiographic or meteorological parameters. It was found that when L-CV's spatial variation is significant and appears to be [spatially] correlated, kriging can reveal the pattern (e.g: orographic influences) and explain some of the variation.

3) L-mean was estimated using a regression of the log-transformed at-site estimates against a series of physiographic and meteorologic variables. This parameter exhibits considerable spatial variability, hence the use of regional information is of limited benefit – yet it has a primary impact on the design flood estimates.

The authors note that regionalisation amounts to a compromise between space and time errors and give a corresponding expression for the MSE: more sites reduce the time variability but increase spatial variability and inter-site correlation. This is analogous to cluster analysis methods (such as Hosking and Wallis, 1996) for subdividing homogeneous regions. The authors suggest using LAT & LONG variables to obtain geographically-contiguous regions.

The above progression towards spatially-continuous estimation from at-site "points" to discrete, statistically-homogeneous regions or "areas" and thence to continuous random fields is the methodology advocated in this thesis. It is an extension of the previous work done at the University of Ottawa.

As an alternative to geographically-contiguous regions, Zrinji *et al.* (1996) developed hierarchical region of influence (ROI) methods in which each L-moment ratio could be pooled across different locations. However, in a recent paper (1997), they advocate the use of LAT & LONG variables to obtain geographically-contiguous regions. The objective of cluster analysis is to decompose the total observed (or simulated) variance

into explained (within homogeneous sub-regions) and unexplained components. This reduces the overall MSE but remains either a non-spatial method (or a spatially-implicit method when LAT and LONG are used as indicators of location). Average parameter values are still used within each homogeneous region.

2.3 GIS and Geostatistical Estimation Techniques

2.3.1 Spatial Classification of Analytical Methods

Analytical methods can be classified in terms of whether the spatial attributes of the data are used explicitly or not and whether the resulting output is graphical or not (Bonham-Carter, 1994). Table 2.3 illustrates what is meant by this thesis' title: "*Spatially-Explicit* Regional Flood Frequency Analysis". With few exceptions, previous regional FFA used spatially-implicit statistics (classes II and III), but not spatially-explicit statistical techniques (classes I and IV).

Table 2.3: Spatial Classification of Analytical Methods

Type of Output	Spatial Attributes Used?		
	Not Necessarily	Always	
MAP	• reclassification & generalization • area cross-tabulations • map modeling (pixel-based) • Boolean or fuzzy overlays I	• spatial (neighbourhood) filtering • topological modelling (buffering) • surface modelling (kriging) • mathematical morphology IV	Map Modelling
TABLE or other data view	II • table & aggregation modelling • descriptive statistics (box & scatter plots, L-moments) • area analysis, correlations • cluster analysis • time series analysis	III • spatial autocorrelation, variogram analysis and model fitting. • cluster analysis with (LAT, LONG) • spatially-correlated time series (STARMA models).	Statistical Modelling
	Conventional Statistics	Spatial or Geostatistics	

Adapted from (Bonham-Carter, 1994).

Most of the methods in classes I and IV are often described as map modelling or GIS techniques, with the exception of surface analysis (geostatistics) and mathematical morphology. Class IV techniques can account for spatial autocorrelation, scale and topological relationships. Topological attributes include shape, containment and adjacency which can be used to answer queries such as: how many elongated basins have a north-eastern alignment or are located at least 200 km from any ocean?

GIS or map modelling techniques can be further classified into single or multiple map methods. Single map analytical techniques include visualization, generalization, contouring, dilation or buffering, and spatial re-sampling. Multiple map analytical techniques include area cross-tabulations, boolean and fuzzy logic models as well as Bayesian methods using prior and posterior evidence maps (weight-of-evidence method).

In previous regional FFA, spatial data was summarized at observation points (gauges) and only inter-site distance was used as a spatial attribute (with a few exceptions). In the present study, traditional methods are augmented with spatially-explicit methods of "map analysis" which utilize topological attributes and geostatistical techniques.

2.3.2 Analytical Techniques used in GIS Studies

Overview of Geographic Information Systems

The purpose of GIS is to provide support for making decisions based on spatial data sets. Analysts accomplish this goal using six fundamental capabilities of GIS: organization of multiple datasets; visualization; spatial query and measurement; combination of different types of data; analysis of maps and/or tables; and prediction using modelling (Bonham-Carter, 1994). These techniques are applied to multiple sets of geocoded spatial data layers which are in register (i.e.: overlap correctly) and to which non-spatial or attribute data is related by means of database tables.

Time is represented either as multiple map 'layers' or as multiple values held in tables. Spatial elements are represented using point, line, polygon and pixel primitives. A GIS

uses spheroids and map projections to accurately represent the earth's surface in two dimensions. The principal strength of GIS is its ability to organize information for the most powerful spatio-temporal processors available – human minds.

GIS Literature for Regional Resource Characterization

At present, only one FFA study of flood timing has used GIS techniques (McGilligan and Graber, 1997). Even Kaden's (1993) classification of the applications of GIS to water resources omits FFA. While it is not possible to present an overview of the GIS literature concerning FFA, papers dealing with spatio-temporally distributed events (Beller, 1991), which are fundamentally similar to floods, are reviewed.

Knapp (1997) mapped western USA's regional fire frequencies and showed their association with areas with large elevation differences and low grass cover. GIS-derived basin characteristics were used to model droughts in Puerto Rico, reducing SEE by 20% (Garcia-Martino *et al.*, 1996). The spatial variability of hydrologic droughts for 19 mid-western basins over 41 years was analysed using GIS methods, revealing both spatial and temporal trends (Changnon, 1996). Pitlick (1994) developed relationships between the mean annual flood and several physiographic variables for five regions in the western USA.

Several studies document the creation and management of spatial hydrologic datasets around the world, e.g. in Germany (Streit *et al.*, 1996). These studies generally document the early stages of national GIS programs and tend to focus on custodial rather than analytical issues. Others illustrate the use of specific GIS software as deterministic models – i.e: the open-standard GIS: GRASS (Mitasova *et al.*, 1995). Still others use GIS to support spatially distributed, deterministic hydrologic models which are of limited relevance for the present analysis (Schultz, 1993; McDonnell, 1996).

The 1994 ASTM standard for GIS metadata (e.g.: data's origin, processing steps and quality) was reviewed by Nebert (1994). Several theoretical investigations of GIS modelling errors have been published. Ward *et al.* (1991) developed a model for spatio-temporal data quality with supporting error visualization plots. Kemp (1993)

addressed the need to match analytical techniques to appropriate spatial data models. Hunter and Goodchild (1995) suggested ways to deal with errors in spatial data bases. Verregin (1994 & 1996) studied error propagation through the buffer operation for probability surfaces and provided tools to quantify such errors.

GIS Techniques used in the Present Study

Analytical GIS studies are analogous to statistical studies in that they can be classified as either exploratory or descriptive. The former type increase our understanding of spatially-distributed phenomena using visualization and measurement (or query) techniques. Such inductive reasoning is the second objective of this thesis: *"to use GIS and scientific visualization techniques to characterize the spatial variation of the principal flood-generating mechanisms"*.

Exploratory data analysis will consist of mapping floods' multimodality and seasonality indices; and using a GIS to characterize their spatial patterns. The following GIS techniques will be used to achieve this:

- Visualization of the spatial and temporal coverage of the data used in this study.
- Map measurements and measures of association for specific flood parameters.

Descriptive GIS studies aim to quantify or even model spatial processes in terms of independent variables in the form of evidence maps. Such deductive reasoning is the third objective of this thesis: *"to investigate spatially-explicit methods of flood characterization and information transfer using GIS and geostatistical techniques"*.

For this purpose point, line and area data is converted to the study area's geographic projection and **organized** into maps which overlap correctly [bold face denotes a fundamental GIS capability]. Once analysts have familiarized themselves with the data by **visualization** and **query** (or measurement), the "base" maps are **transformed** into evidence maps using various **combinations**.

Modelling with GIS begins by stating the conceptual model, which describes the typical characteristics of the phenomenon under study (floods) and provides an interpretation of the physical processes from which it is believed to have resulted, e.g: flood-generating mechanisms (Bonham-Carter, 1994). From the issues discussed in previous sections, the conceptual model for this study can be stated as follows:

> *Throughout the study area, floods are principally generated by snowmelt, rainfall or a combination of the two. The causes of floods at each geographical location have an impact on the L-moment ratios, which can therefore be treated as regionalised variables using geostatistical methods. While L-skew may be shown to remain constant over large areas, low values of L-CV are associated with high amounts of snow and may also be affected by geographical, physiographic and meteorologic factors.*

The conceptual model will be tested by quantifying the relationships it postulates after verifying whether L-skew (or even L-CV) can be held constant within "homogeneous regions" using a spatial contrast measure developed herein. The following techniques will be used to model L-CV:

- To obtain continuous surfaces from the point estimates of L-CV, a geostatistical technique called kriging (described in section 3).
- To quantify spatial associations between L-CV and other spatial variables provided as map coverages, matrix overlay and area cross-tabulation techniques will be used.

The above techniques operate on data in the form of evidence maps. Evidence maps serve as independent variables in the **analysis** used to create GIS or geostatistical models. Once suitable models have been identified and diagnosed, they can be used to make **predictions** (Aronoff, 1989; Bonham-Carter, 1994). They are created during the initial (and most time-consuming) step in a GIS study in which the spatial database is assembled as described in section 4.2.

2.3.3 Geostatistical Analysis

Overview of Geostatistics

Geostatistics adapts classical regression techniques to deal with spatially-continuous or "regionalised" variables – whose values change with spatial location and whose behaviour is somewhere between a deterministic and a random variable (Bonham-Carter, 1994). It includes techniques to quantify spatial autocorrelation using variograms; to model parameter surfaces with or without dependent variables (kriging); to assess the variance of estimates; and to investigate the theoretical properties of data by means of (spatial) stochastic simulation studies (Desbarats, 1996; Journel, 1996).

Although geostatistical theory was initially developed by mining and geological engineers, it is increasingly being applied in other fields, including hydrology (deMarsily and Delhomme, 1989; Cressie, 1993; Cromer, 1996). The three principal issues to be resolved in geostatistical estimation are (Isaaks & Srivastava, 1989):

1. Is an estimate required over a large area or at a specific point?
2. Is a single value (e.g: average) or an entire distribution required?
3. Is the area used to obtain the estimate (its "support") similar to those of the area for which predictions are to be estimated?

In a manner analogous to nonparametric FFA, an adaptive kernel algorithm has been proposed as a more direct estimation tool for probability surfaces (Brunsdon, 1995). However, this study follows the geostatistical mainstream and employs variogram and kriging techniques.

Variogram Model Building

The first step in a geostatistical study is the characterization of spatial autocorrelation in several directions and for various lag distances to obtain an experimental variogram. This plot is then modelled using any number of positive-definite functions. In cases where spatial autocorrelation is anisotropic, variograms can be composed of 'nested

structures' or multiplicative models which represent zonal (sill changes with direction) or geometric (range changes with direction) anisotropy. These can be formulated using re-scaled ranges which allow the range to vary with direction (Srivastava, 1996).

For co-regionalised variables, (possibly anisotropic) variograms are required for each variable as well as a cross-variogram for each pair of variables. The positive-definite analytical models fitted to each variogram and cross-variogram must be identical at each level of a nested structure, if one is used (Isaaks & Srivastava, 1989; Deutsch and Journel, 1992).

Kriging and Co-Kriging

Kriging is a method for estimating the value of a spatial variable (and, simultaneously, the spatial variance of such estimate) at discrete points or over small areas (blocks) based on a random function model of the observed spatial variability. Kriging estimates account for distance from the point being estimated, for clustering of observations in the search neighbourhood and for spatial autocorrelation (Rouhani, 1996).

All kriging methods are based on variogram models, which are directly related to the data's (spatial) autocorrelation function or variogram. They also provide the global variance of estimates and honour data values at the observation points (Deutsch and Journel, 1992). The basic method, 'ordinary kriging or OK', assumes that the variable being estimated is constant within the region considered. Restrictions on the maximum range and number of neighbouring observations used for each estimate often result in a re-scaling of the local means which is sufficient to account for gradual trends.

Klemeš' (1993) injunction to de-emphasize "the pursuit of high mathematical rigour" applies here: geostatistical models are not intended to shift the focus away from the causes of floods and their practical interpretation.

Chapter 3

THEORETICAL DEVELOPMENT

3.1 Introduction

In traditional regional FFA, flood parameters resulting from at-site analysis are usually grouped into spatially-implicit homogeneous regions or clusters. Multiple flood-generating mechanisms are seldom considered. In this study, estimation proceeds hierarchically from higher to lower moment ratios (see section 2.2.3). In this section, improved spatial techniques are developed for each level:

1) Prior to estimation, exploratory data analysis using a GIS is used to visualize and quantify associations between flood parameters (or indices) and geographical, physiographical and meteorological variables. Indices summarizing the observed pdf (obtained by nonparametric methods) and flood timing are developed for use as indicators of flood-generating mechanisms (see section 3.2).

2) If flood parameters can only be treated as average values, a spatial contrast statistic is developed to verify whether parameter values within "homogeneous regions" are significantly different from those in surrounding areas (see section 3.4).

3) If the signal to noise ratio is high enough to permit relationship development (section 3.3), a more spatially continuous treatment is attempted. Kriging techniques are used to obtain continuous surfaces for flood parameters. Snow pack depth can be used as a support variable to improve parameter estimates in sparsely gauged areas using co-kriging techniques (see section 3.5).

Consequently, flood parameters are modelled as spatially-explicitly as possible: from regional averages or relationships to continuous surfaces for the entire study area.

3.2 Nonparametric Methods

3.2.1 Estimation of the At-Site Probability Density Function

Parametric methods assume that a specific, often unimodal, theoretical distribution function can completely describe observed flood series. In fact, the probability distribution of an observed flood series, f(x), is unknown and may be the result of several flood-generating mechanisms (or sub-populations). For this reason, nonparametric methods have been developed to characterize floods at each site without assuming that a particular distribution applies (Adamowski, 1985).

Nonparametric kernel density estimators, themselves a probability function K(x), are used to estimate the probability density function, $\hat{f}(x)$, in a process analogous to the construction of a histogram but with two differences: each kernel is centred on an observation and a smoothing factor, h, is estimated from the data (analogous to class widths). The overall density function is obtained by summing each of the kernel functions:

$$\hat{f}(x) = \frac{1}{nh}\sum_{i=1}^{n} K\left(\frac{x - x_i}{h}\right) \quad \ldots\ldots (1)$$

where n is the number of flood observations, x, at the site. Adamowski and Feluch (1990) investigated several alternative kernel functions, including the asymmetric Epanechnikov kernel, but found no significant improvement in tail estimation over the conventional Gaussian kernel. Based on a cross-validation procedure by Silverman (1986), Adamowski *et al.* (1989) showed that a consistent and asymptotically optimal estimate of h can be obtained by solving the following equation numerically ($i \neq j$):

$$\sum_{i=1}^{n}\sum_{j=1}^{n} e^{\frac{d_{ij}}{4}}\left[\left(1 - \frac{4\sqrt{2n}}{h} e^{\frac{d_{ij}}{4}}\left(\frac{x_i - x_j}{h} - 1\right)\left(\frac{x_i - x_j}{h} + 1\right)\right) - 1\right], \quad d_{ij} = \left(\frac{x_i - x_j}{h}\right)^2 \qquad (2)$$

3.2.2 Statistics to Summarize Probability Density Function Shapes

The several hundred nonparametric pdf estimated in this study must be reduced to numerical indices before they can be transformed to maps. A C^{++} method has been programmed to obtain two summary indices: the number of local maxima or modes (NMODES) and the proportion of area located in the right-hand tail and/or modes (see Appendix B). The algorithm counts only the number of peaks whose net height exceeds a user-selectable proportion of the principal peak (5% in this study).

The presence of heavy right-hand tails or of multiple modes in a pdf may indicate multiple flood-generating mechanisms. In its simplest form, the multiple-mechanism index (MMI) developed herein is defined as the ratio of the total area under the pdf (unity) to that under the principal mode or mechanism:

$$\text{MMI} = \frac{\text{probability of flooding due to all mechanisms (unity)}}{\text{probability of flooding due to the principal mechanism}} \quad \ldots\ldots (3)$$

Thus, a unimodal pdf resulting from a normal flood population would have MMI= 1.0 while two equal and distinct modes would yield MMI = 2 (MMI $\geq$ 1). The difficulty lies in filtering the influence of the principal mechanism from the total pdf in a manner that is rational and which can be calibrated using numerical simulation studies.

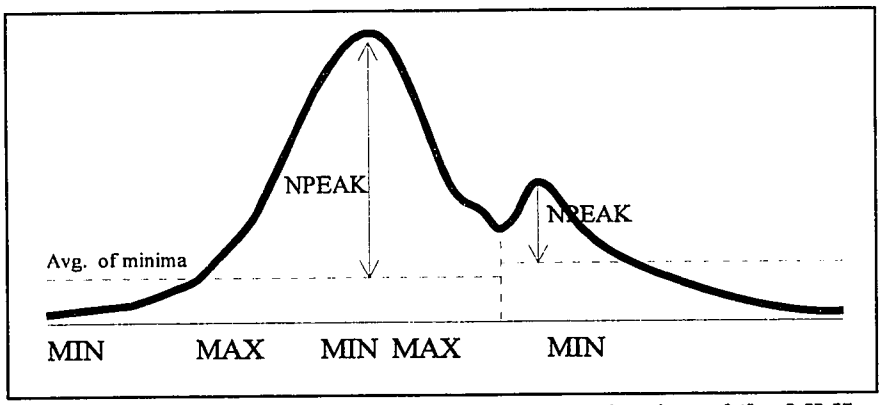

Figure 3.1:Definition Sketch of PDF for Determination of the MMI

Figure 3.1 is a sketch of a typical multimodal pdf. The MMI is calculated in three steps. First, the "raw" area underneath each mode (between each adjacent minimum) is obtained from the pdf. Secondly, the net size of each mode is computed as: $NPEAK_i = MAX_i - (MIN_i + MIN_{i+1})/2$. Finally since smaller modes' areas are often due in part to the influence of larger and nearby peaks, larger modes are allowed to capture some of the area of their smaller neighbours based on the proportion of their net peaks and on the degree of closure between them. Each mode's probability is adjusted using the following formula:

$$A_i' = \begin{cases} A_i + a' \dfrac{NPEAK_N}{NPEAK} \left(\dfrac{MIN}{MAX} \right)^{b'} A_N, & MAX > MAX_N \\ A_i \left[1 - a' \dfrac{NPEAK}{NPEAK_N} \left(\dfrac{MIN}{MAX_N} \right)^{b'} \right], & MAX \le MAX_N \end{cases} \qquad \ldots\ldots\ldots\ldots (4)$$

where N is the left or right neighbour and MIN lies between the two maxima being compared. The parameters a' and b' can be used to calibrate the factors accounting for the relative importance (N/N) and closure (MIN/MAX) between nearby modes, respectively. Their default value is one.

The closure term accounts for the horizontal separation between modes implicitly – widely separated peaks tend to have near-zero MIN which result in negligible probability adjustments. The relative peak ratio term is necessary to handle the frequent case where observations are not tightly clustered about the centre of each mode, resulting in some overlap between observations belonging to different modes. Modes whose net peaks are less than 5% (user-adjustable) of the principal peak are ignored by both the mode counting and the MMI algorithms.

3.2.3 Statistics to Describe Flood Timing

Directional statistics have been used to express the mean date of occurrence of floods as an angle and their variability as a magnitude (Bayliss and Jones, 1993). Representing Julian dates as angular vectors helps to visualize flood timing at discrete sites or in fixed regions. Direct mapping of Julian flood dates using a GIS is preferable because it is spatially-explicit: it shows the occurrence of floods in time and space. Expressing flood timing and variability in days, which are readily understood, is also more intuitively appealing than angles and magnitudes.

Flood timing for the primary and secondary modes (or generating mechanisms) could be visualized separately based on a classification of each flood according to the nonparametric pdf. Finally, the variability of flood timing can also be mapped in three dimensions: in time (standard deviation) and in space (kriging variance, which may be anisotropic). The resulting map coverages can help to determine both the likely cause and the time of occurrence of floods at ungauged locations.

Such mapping assumes that the primary control on flood timing is local climate (as influenced by elevation and distance from large bodies of water) and that flood timing is a geostatistic whose mean and standard deviation can be transformed into continuous surfaces using kriging. A recent study has shown this assumption to be reasonable (Magiligan and Graber, 1997).

3.3 L-Moments for Regional Frequency Analysis

3.3.1 Estimating At-Site L-Moments

Definition: L-moments are linear combinations of order statistics which are robust to outliers and virtually unbiased for small samples. This makes them suitable for flood frequency analysis. A parallel theory of L-statistics exists to estimate the L-mean, L-

standard deviation, L-skewness and L-kurtosis; to identify parent distributions; and to estimate distribution parameters (Hosking, 1989; Hosking and Wallis, 1993).

The L-mean, λ_1, is a measure of central tendency and the L-standard deviation, λ_2, is a measure of dispersion. Their ratio: $\tau_2 = \lambda_2/\lambda_1$, is termed the L-coefficient of variation (L-CV). The third and fourth moments, λ_3 and λ_4, are analogous to conventional moments. The ratio: $\tau_3 = \lambda_3/\lambda_2$ is referred to as L-skewness while the ratio: $\tau_4 = \lambda_4/\lambda_2$ is the L-kurtosis (Maidment *et al.*, 1993).

L-moments can either be defined as linear combinations of probability weighted moments (PWM) or they can be estimated directly from a ranked dataset (Wang, 1996). The PWM can be estimated using either traditional but biased plotting-position estimators or using (virtually) "unbiased" estimators which are scale and skewness-invariant (Hosking and Wallis, 1995). Fill and Stedinger (1995) have shown that unbiased estimators are robust in the presence of autocorrelation in the observed data. They endorse the use of unbiased L-moments for distribution identification and parameter estimation – a position shared with Hosking and Wallis (1995), who state that "the use of plotting-position estimators should be discontinued".

Unbiased estimators b_r of the r^{th} order PWM, β_r, for any distribution can be obtained from (Vogel and Fennessey, 1993):

$$b_r = \frac{1}{n}\sum_{j=1}^{n-r}\left[\frac{\binom{n-j}{r}}{\binom{n-1}{r}}\right]x(j), \quad \text{or: } b_0 = \frac{1}{n}\sum_{j=1}^{n}x(j) \qquad \ldots\ldots\ldots\ldots\ldots\ldots\ldots\ldots (5)$$

$$b_1 = \sum_{j=1}^{n-1}\left[\frac{(n-j)}{n(n-1)}\right]x(j)$$

$$b_2 = \sum_{j=1}^{n-2}\left[\frac{(n-j)(n-j-1)}{n(n-1)(n-2)}\right]x(j)$$

$$b_3 = \sum_{j=1}^{n-3}\left[\frac{(n-j)(n-j-1)(n-j-2)}{n(n-1)(n-2)(n-3)}\right]x(j)$$

where x(j) is an ordered flood observation with the largest being x(1) and the smallest x(n). The first four unbiased L-moments can be obtained by substituting the first four unbiased PWM estimates into:

$$\lambda_{r+1} = \sum_{k=0}^{r} \beta_r (-1)^{r-k} \binom{r}{k} \binom{r+k}{k}, \text{ or: } \lambda_1 = \beta_0 \qquad \ldots\ldots\ldots\ldots\ldots\ldots\ldots\ldots (6)$$

$$\lambda_2 = 2\beta_1 - \beta_0$$

$$\lambda_3 = 6\beta_2 - 6\beta_1 + \beta_0$$

$$\lambda_4 = 20\beta_3 - 30\beta_2 + 12\beta_1 - \beta_0$$

Once the at site L-moment estimates are available, they can be used to identify the most suitable (parametric) probability distribution and to estimate its parameters. This can be done graphically by means of L-moment ratio diagrams or using the goodness-of-fit "Z-statistic" described in the next section.

L-moment Ratio Diagrams: Theoretical relationships have been derived between (τ_3 , τ_2) or (τ_4 , τ_3) for various two or three-parameter distributions, respectively (Hosking, 1990). A suitable distribution for single sites or regions can be selected based on the proximity of its moment ratios to a theoretical line or point as well as on the variability around the mean values. Vogel and Fennessey (1993) showed that L-moment diagrams are nearly unbiased for all combinations of sample size, L-CV and assumed distribution. They are therefore preferable to conventional moment diagrams for this purpose. The numerical version of this graphical method is called the Z statistic and is described in the next section.

A library of FORTRAN computer program is available for evaluating the unbiased L-moments of sample data; to diagnose regional datasets; perform goodness-of-fit tests for various distributions; and to estimate the parameters of these distributions using methods which are discussed in the following sections (Hosking and Wallis, 1996).

3.3.2 L-Moment Tests for Regions

A fundamental assumption of regional flood frequency analysis is that floods from each site in the region are hydrologically similar, e.g. that they have similar causes and characteristics. L-moment techniques are available for each step of regional analysis: a discordance measure (D) for screening site data; a heterogeneity measure (H) to diagnose candidate regions; and a goodness-of-fit statistic (Z) to choose the most appropriate probability distribution.

The H and Z statistics are obtained based on a comparison of the observed site statistics to those of an equivalent region, simulated numerically using a four-parameter Kappa distribution. The Kappa distribution is a flexible parent, having as special cases the Generalized Logistic (GLO), Generalized Pareto (GPA) and the Generalized Extreme Value (GEV) used herein (Hosking, 1988). In this study, 1000 equivalent regions have been simulated for each region.

Discordance Test for Site Data: If a single site's (τ_2, τ_3, τ_4) are too far removed from the centre of the cloud containing each site in the region, a discordance measure can be used to determine whether it should be removed. Let $\mathbf{u}_i = [\tau_{2i}, \tau_{3i}, \tau_{4i}]^T$ be a vector containing the L-moment ratios for site i (Hosking and Wallis, 1993). The unweighted group average $\mathbf{u}$, sample covariance matrix $\mathbf{S}$, and test statistic D, are defined as:

$$\bar{\mathbf{u}} = \frac{1}{N}\sum_{i=1}^{N}\mathbf{u}_i \qquad \ldots\ldots (7)$$

$$\mathbf{S} = \frac{1}{N-1}\sum_{i=1}^{N}(\mathbf{u}_i - \bar{\mathbf{u}})(\mathbf{u}_i - \bar{\mathbf{u}})^T \qquad \ldots\ldots (8)$$

$$D = \tfrac{1}{3}(\mathbf{u}_i - \bar{\mathbf{u}})^T(\mathbf{u}_i - \bar{\mathbf{u}}) \qquad \ldots\ldots (9)$$

where N is the total number of observations. Note that the average of D over all sites is 1. If a site's D statistic exceeds 3, its data is considered to be discordant from the rest

of the regional data and two possibilities must be investigated: there may be an error in the data or the data might properly belong to another nearby region. Hosking and Wallis (1993) state that the critical value, 3, would be exceeded by approximately 3% of sites if the cloud was multivariate normal. They advise that sites with the largest values of D be examined regardless of their magnitude.

Heterogeneity Test for Regions: The heterogeneity measure compares the region's observed sampling variability to that of an equivalent, simulated region under the assumption that all sites in a homogeneous region have the same population L-moments. It is obtained by fitting a four-parameter Kappa distribution to the regional data set, generating a series of 1000 equivalent regions' data by numerical simulation and comparing the variability of the L-statistics of the actual region to those of the simulated region.

Three heterogeneity statistics can be used to test the variability of three different L-statistics: H_1 for L-CV, H_2 for the combination of L-CV and L-skewness and H_3 for the combination of L-kurtosis and L-skewness. Each H statistic takes the form:

$$H = (V_{obs} - m_V)/s_V \quad \ldots\ldots (10)$$

where μ_V and σ_V are the mean and standard deviation of the simulated values of V while V_{obs} is calculated from the regional data and is based on a corresponding V statistic, defined as follows:

$$V_1 = \sum_{i=1}^{N}\left(n_i(\tau_{2i} - \bar{\tau}_2)^2\right)\Big/\sum_{i=1}^{N} n_i \quad \ldots\ldots (11a)$$

$$V_2 = \sum_{i=1}^{N}\left(n_i\sqrt{(\tau_{2i} - \bar{\tau}_2)^2 + \left(\tau_{3i} - \bar{\tau}_3\right)^2}\right)\Big/\sum_{i=1}^{N} n_i \quad \ldots\ldots (11b)$$

$$V_3 = \sum_{i=1}^{N}\left(n_i\sqrt{\left(\tau_{3i} - \bar{\tau}_3\right)^2 + \left(\tau_{4i} - \bar{\tau}_4\right)^2}\right)\Big/\sum_{i=1}^{N} n_i \quad \ldots\ldots (11c)$$

The H statistics indicate that the region under consideration is acceptably homogeneous when $H < 1$, possibly heterogeneous when $1 \leq H < 2$ and definitely

heterogeneous when $H \geq 2$ (Hosking and Wallis, 1993). A grouping of sites must therefore have $H < 2$ to be considered as a 'possibly homogeneous' region.

Based on simulation studies, Hosking and Wallis (1993) showed that sites in a region with $H = 1$ would have average flood estimation errors ranging from 20 to 40% less accurate than those estimated from the population values. For $H \geq 2$, a redefinition of the region should be considered. The authors of this study also noted that the assignment of sites to regions must be based on variables other than their L-moments (such as geography, pdf shape and timing) in order for the D and H statistics to have any significance.

Signal-to-Noise Ratio: Pilon *et al.* (1991b) proposed that the observed standard deviation of a flood parameter within a region, σ_{obs}, is composed of noise and signal components. The signal is the proportion of variance which can be explained systematically. Noise accounts for purely random variations, such as would be obtained by simulating equivalent regions, σ_{sim}. The signal to noise ratio, S/N, is expressed as the percentage:

$$S/N\ [\%] = 100\ (\sigma_{obs}^2 - \sigma_{sim}^2)\ /\ \sigma_{obs}^2 \qquad \text{(12)}$$

When the S/N ratio is high, it is reasonable to attempt to build a model to explain a portion of the observed variability. The ratio indicates the maximum proportion of variability which could be explained by such a model.

Goodness of Fit Test to Identify Parent Distributions: Once data within a region appears to be homogeneous and seems to belong to a single distribution, a goodness-of-fit criteria based on L-moments can be used to select the most likely (parametric) parent distribution (GEV, GPA, Wakeby, etc.) and to estimate its parameters. Floods with specific return periods are determined based on this "fitted" regional distribution. The goodness of fit criterion for each distribution is defined in terms of L-moments and is termed the Z statistic:

$$Z^{DIST} = \left(\tau_4^{DIST} - \bar{\tau}_4 + \varepsilon_4\right) / \sigma_4 \quad \ldots\ldots\ldots\ldots\ldots\ldots\ldots\ldots\ldots\ldots\ldots\ldots\ldots\ldots\ldots\ldots (13)$$

where DIST refers to a particular distribution while ε_4 and σ_4 are the bias and standard deviation of τ_4 (L-kurtosis), respectively, defined as:

$$\varepsilon_4 = \frac{1}{N_{sim}} \sum_{m=1}^{N_{sim}} \left(\bar{\tau}_{4_m} - \bar{\tau}_4\right) \quad \ldots\ldots\ldots\ldots\ldots\ldots\ldots\ldots\ldots\ldots\ldots\ldots\ldots\ldots\ldots\ldots (14)$$

$$\sigma_4 = \sqrt{\frac{1}{N_{sim} - 1} \sum_{m=1}^{N_{sim}} \left(\bar{\tau}_{4_m} - \bar{\tau}_4\right)^2 - N_{sim} \varepsilon_4{}^2} \quad \ldots\ldots\ldots\ldots\ldots\ldots\ldots\ldots\ldots\ldots\ldots\ldots\ldots\ldots (15)$$

where N_{sim} is the number of simulated regional datasets generated using a Kappa distribution in a similar way as for the heterogeneity statistic. Note that the subscript m denotes the m^{th} simulated region obtained in this manner.

The fit is deemed adequate when the criterion: $|Z^{DIST}| \leq 1.64$, for which the true distribution should be identified approximately 90% of the time. The performance of this statistic has been estimated based on simulation studies using uncorrelated i.i.d. normal distributions for Z^{DIST}, therefore it should be considered as a rough indicator of goodness of fit and not as a formal test (Hosking and Wallis, 1993).

3.4 GIS Techniques for Spatio-Temporal Datasets

3.4.1 Characterizing Spatial Associations

Spatial Correlation – an Analogy to Multivariate Statistics

Since spatial data are often auto-correlated, they rarely satisfy the assumptions required by multivariate correlation statistics, i.e. they are neither i.i.d. nor are they completely random. Such departures do not invalidate the use of these methods when the purpose is to explore – not explain – relationships between variables.

The association between two evidence maps can be quantified using a multivariate technique which is appropriate for the measurement scale (Bonham-Carter, 1994):

- Nominal: Use Chi-squared statistics, treating the area cross-tabulation results as a contingency table. As a special case, binary maps can be compared using conditional probability measures.
- Ordinal: Use Spearman's rank correlation coefficient.
- Interval: Use Pearson's correlation coefficient.

These methods require an area cross-tabulation of all map class combinations for the pair of evidence maps being compared. With the exception of conditional probability measures described below, the above correlation measures are in widespread use and their theoretical derivations are not given here. The details of their application for map comparisons are given in section 4.5.

Conditional Probability Relationships between Binary Map Pairs

For mapping and computational purposes, it is convenient to express probabilities, P, as odds, $O = P/(1-P)$. For the area under study, one evidence map's (B) dependence on another representing an explanatory variable (A) can be expressed in terms of conditional probability (Agterberg, 1992).

If it could be assumed that A causes B, then the conditional probability (expressed as odds) of B given A is (Bonham-Carter, 1994):

$$O(B|A) = P(B|A)/P(\overline{B}|A) \quad \ldots\ldots (16)$$

...where the denominator is the probability of "not B" given A. Since causative relationships are not necessarily one-way, a symmetrical measure called the odds ratio, O_r, is preferable when modelling with GIS:

$$O_R = \frac{O(B|A)}{O(B|\overline{A})} \equiv \frac{T_{AA}T_{BB}}{T_{AB}T_{BA}} \quad \ldots\ldots (17)$$

where T_{ij} refers to the area cross-tabulation totals for the two binary maps. The odds ratio is greater than one for positively associated map patterns, less than one for negatively associated patterns and one for independent patterns. Alternatively, the natural logarithm of the odds ratio, termed the contrast C_w, can be used. The contrast is zero for independent map patterns and positive or negative for corresponding associations between map patterns.

3.4.2 Measures of Spatial Contrast and Continuity

Measures of Spatial Contrast

Feature dilation or buffering is one of the operations of mathematical morphology. Within GIS, buffering techniques are used to measure distances from point, line or polygon features and to illustrate the change in properties of interest with distance. For polygonal regions, a measure of spatial contrast can be obtained by comparing the representative value within each successive buffer to that within the region.

This representative value can either be the class containing the regional average value (local) or the average of all area-weighted classes (global) for the region and/or buffer(s) considered. In the former case, the premise is that cells with the same class as the regional average are more likely to occur within a region than outside of it. This can

be tested rigorously using conditional probability measures for the occurrence of a given class given that its location is within (or within a certain distance of) a region of interest. The latter case, which uses the average class in successive buffers (often normalized by the average value in the region), is equivalent to evaluating the odds of each successive class and multiplying them by their class midpoint values. Both methods are used herein.

The use of conditional probability for measuring spatial contrast requires that both maps be reclassified as binary maps. The map, A, containing the L-statistic to be contrasted is reclassified as class 1 for the average value within the region and class zero elsewhere. The map, B, containing the region and buffers must be reclassified as follows:

1. To measure the likelihood that cells are average-valued within the region, space within the region must be assigned to class 1 and space outside of it class 0. This step compares odds or contrasts within the region to those for the entire study area.

2. To measure the likelihood that cells are average-valued within a certain distance of the region, the basemap must be redefined as the area within the specified distance. Areas within the region are assigned to class zero and those within the buffer as class 1. The process must be repeated for each successive buffer.

Once the odds ratio or contrast has been evaluated for cumulatively greater distances from the region's boundary, they can be normalized by the value within the region and plotted to provide a visual indication of the change in contrast with distance.

The width and number of buffers to use is a matter of judgement. Since regions vary in shape and area, it is desirable to express buffer width as a percentage, ζ, of the average of their major and minor axis dimensions:

$$\text{buffer width} = \zeta\,(\text{major axis} + \text{minor axis})/200 \qquad \ldots\ldots\ldots\ldots\ldots\ldots\ldots\ldots (18)$$

Based on the results of a pilot study (Daviau *et al.*, 1994), the value of ζ has been set to 10. This considered adequate to reveal distance-related trends. The spatial contrast measure described above is implemented in section 4.5.

Measures of Spatial Continuity

The complementary nature of contrast and continuity measures is best illustrated in terms of the dual questions asked by all spatial queries: "which value is likely to occur within a specific region in space?" and "within which region(s) do specific values occur?". Measures of contrast compare the values within and outside specific regions in space while continuity measures highlight the locations where specific values are equal (or less than or equal) to a value of interest.

The spatial continuity of regional phenomena can best be visualized (and quantified) using indicator maps (Srivastava *et al.*, 1993). These are obtained by reclassifying the evidence map to a series of binary maps using successively higher thresholds or quantiles. Each map highlights areas where specific values occur. For example, a series of ten maps showing only cells whose values are less than or equal to successively higher deciles can illustrate spatial continuity at each threshold. This is illustrated by map series C2 in Appendix C. Moving-window map measurements can also be used to simplify such maps by quantifying the occurrence of specific values within regular subdivisions of the study area.

3.4.3 Visualizing Data Quality and Global Variance

The coverage and accuracy of data in space and time can be visualized in two ways: by symbolization and by classification. Symbolization consists of assigning different symbols for data of each quality, such as circles for hydrometric sites in group A and squares for those in group B (see Figure 1 and Appendix A). The symbols' sizes can be set to increase in proportion to the number of years of record for each flow gauge. More complex methods have also been suggested (Ward and Zheng, 1991).

The variation in data quality throughout the study area can be illustrated by classifying maps showing the standard error of estimate (SEE) or the standard deviation of parameters. This can be done for both the primary (flood timing and magnitude) data's mean and L-CV and for the derived or output data (flood parameters and kriging variance). One useful method for comparing the results with their associated errors is

to display the output map as a 2.5D surface and to "drape" the prediction error map over it. On such surfaces, the elevation at each point represents the variable while the colour (or gray level) indicates the amount of uncertainty of the estimate.

If the performance of the model is expected to vary with direction, this composite 2.5D map can be rotated in various increments. To emphasize features in a given direction, the 2.5D "hills" can be shaded using a light source from a horizontally perpendicular direction. Different (vertical) sun angles and azimuths or vantage points can also be selected.

3.5 Geostatistical Methods for Spatially-Explicit Estimation

Geostatistical methods have only recently been introduced in hydrology (de Marsily and Delhomme, 1989). The formal integration of spatial statistics and GIS is also recent (Anselin and Getis, 1993). As mentioned in the literature review, these techniques have seldom been used in flood frequency analysis. For this reason, a summary derivation of the equations used in variogram estimation, kriging and co-kriging is given herein.

3.5.1 Variograms to Describe Spatial Autocorrelation

A variogram is a 2D (spatial) analogue to the time-domain autocorrelation function and is a pre-requisite for spatial estimation using kriging. Experimental variograms are simply plots of the autocorrelation function at various lags for a given direction (Isaaks and Srivastava, 1989; Srivastava, 1996). Since the available data is often sparse, the lags are often specified with tolerances for direction and distance. When the angular tolerance is omitted and only separation distance matters, the result is an omnidirectional variogram. The expression for the variogram or cross-variogram, γ, at lag h, for N pairs of observations v_i and u_j is:

$$\gamma(h) = \frac{1}{2Nh} \sum_{(i,j)|h_{ij} \approx h} (v_i - v_j)(u_i - u_j) \quad \ldots\ldots\ldots\ldots\ldots\ldots\ldots\ldots\ldots\ldots\ldots\ldots\ldots\ldots (19)$$

where v and u refer to the same variable for variograms and to different variables for cross-variograms. Variograms, being symmetric, have identical values in the +h and -h direction or axis. In cases where auto or cross-correlation is not isotropic, the variograms for several directions or axes (e.g. N-S, E-W, etc...) are computed and the two axes with the largest and smallest autocorrelation values are retained.

In order to guarantee a unique solution to kriging or co-kriging estimates, the variogram(s) or cross-variograms must be positive definite (Deutsch and Journel, 1992). This is achieved in practice by fitting one of several models to the experimental variogram which have this property. Such models or "transition functions" also provide values of $\gamma(h)$ for fractional lags which might not be obtained from the experimental variogram. Several least-squares variogram model fitting procedures have been suggested for this purpose (Gotway, 1991; Pannatier, 1992; Jian *et al.*, 1996).

The most common transition functions used to model experimental variograms are (in order of decreasing spatial continuity): the Gaussian, spherical and exponential functions shown as equations 20 to 22 below:

$$\gamma(h) = 1 - e^{-3h^2/a^2} \quad \ldots\ldots\ldots\ldots\ldots\ldots\ldots\ldots\ldots\ldots\ldots\ldots\ldots\ldots (20)$$

$$\gamma(h) = 1.5\frac{h}{a} - 0.5\left(\frac{h}{a}\right)^3 \text{ if } h \le a, \text{ 1 otherwise} \quad \ldots\ldots\ldots\ldots\ldots\ldots\ldots\ldots (21)$$

$$\gamma(h) = 1 - e^{-3h/a} \quad \ldots\ldots\ldots\ldots\ldots\ldots\ldots\ldots\ldots\ldots\ldots\ldots\ldots\ldots (22)$$

Due to the importance of variograms, model fitting has evolved into a parallel discipline in geostatistics. The properties of a typical variogram are summarized below and illustrated in Figure 3.2:

- **range, a**: distance at which the variogram reaches its average maximum value.
- **sill, C_0+C_1**: average maximum value reached by the variogram.

- **nugget effect, C_0**: discontinuity at the origin, named after the influence of gold veins or "nuggets" which result in vastly increased local ore grades. A pure nugget effect is a variogram which has a constant sill for any lag distance, i.e. no spatial autocorrelation.

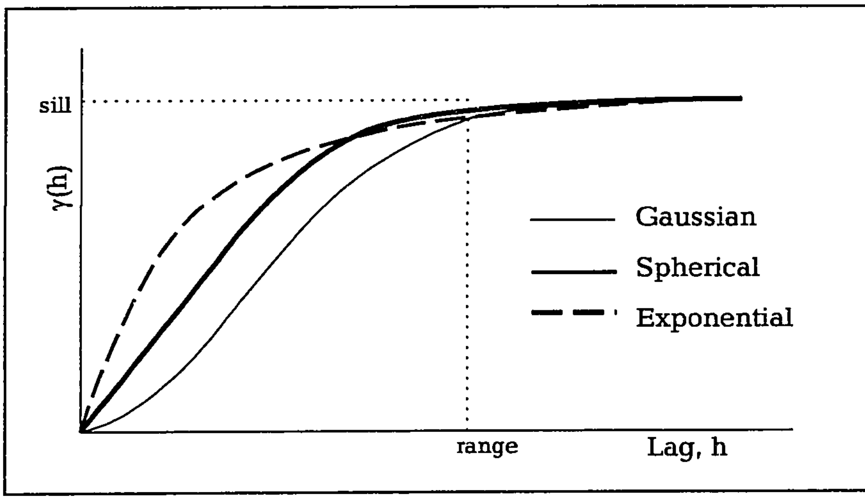

Figure 3.2:Three Common Variogram Models showing the Range and Sill (after Isaaks & Srivastava, 1989).

3.5.2 Kriging to Obtain Parameter Surfaces

Kriging is a best linear unbiased estimator (B.L.U.E.) method used to transform points to surfaces. This study uses two types: ordinary kriging (OK) and universal kriging (UK), which can incorporate a trend (see Gotway *et al.*, 1997, for an evaluation of different types of kriging). Only OK theory is reviewed herein, based on the derivation by (Isaaks & Srivastava, 1989). The method is based on the following random function model for the prediction error, $R(x_0)$, at the location where an estimate is required:

$$R(x_0) = \sum_{i=1}^{n} w_i \cdot V(x_i) - V(x_o) \qquad \text{(23)}$$

where each term is a random variable: w_i are the OK weights for values at each sample location, $V(x_i)$, and $V(x_o)$ is the unknown value at the point for which an estimate is required. The following assumptions are made (Isaaks & Srivastava, 1989):

1. Each random variable has the same probability distribution.
2. The expected value of the random variables at each location is E(V), i.e.: the random field and the random function describing it are stationary.
3. The expected value of the average error, $R(x_0)$, is zero (the estimator is unbiased).
4. The joint distribution of any pair of random variables depends only on their separation distance (not on their location).

In practice, assumptions 1, 2 and 4 can be approximately satisfied by an appropriate selection of the search window size. Since assumption 2 (stationarity) implies that $V(x_i)=V(x_0)$ and assumption 4 (unbiasedness) requires that $R(x_0) = 0$, a simple rearrangement of equation 23 indicates that the kriging weights must sum to unity. This suffices for the linear and unbiasedness properties, but the "best" in B.L.U.E. requires the minimization of estimation variance. This is done by formulating a random function model for the estimation variance, σ_k of a set of k estimates:

$$\mathrm{Var}\{R(x_0)\} = \tfrac{1}{k}\sum_{i=1}^{k}\left(R(x_i) - \overline{R}\right)^2 = \tfrac{1}{k}\sum_{i=1}^{k}\left(V(x_i) - V(x_0)\right)^2 \qquad \ldots\ldots\ldots\ldots\ldots (24)$$

where it has been assumed that the average prediction error is zero. An expression for the variance of a linear combination is substituted into 23, which rearranges to:

$$\mathrm{Var}\{R(x_0)\} = \hat{\sigma}^2 + \sum_{i=1}^{n}\sum_{j=1}^{n} w_i w_j \hat{C}_{ij} - 2\sum_{i=1}^{n} w_i \hat{C}_{i0} \qquad \ldots\ldots\ldots\ldots\ldots\ldots\ldots (25)$$

where the covariances C_{ij} are obtained from the fitted variogram models. The first term on the right hand side is the variance of the random variables which is assumed to be equal for each variable. After adding a Lagrangian parameter to account for the additional unknown due to the unbiasedness condition, the error variance $\mathrm{Var}\{R(x_0)\}$ is minimized by setting its partial derivatives with respect to the kriging weights to zero. This yields the OK system of equations $\mathbf{C} \cdot \mathbf{w} = \mathbf{D}$, or:

$$\begin{bmatrix} \hat{C}_{10} & \dots & \hat{C}_{1n} & 1 \\ \vdots & & \vdots & \vdots \\ \hat{C}_{n0} & \dots & \hat{C}_{nn} & 1 \\ 1 & \dots & 1 & 0 \end{bmatrix} \bullet \begin{bmatrix} w_1 \\ \vdots \\ w_n \\ \mu \end{bmatrix} = \begin{bmatrix} \hat{D}_1 \\ \vdots \\ \hat{D}_n \\ 1 \end{bmatrix} \quad \dots\dots\dots\dots\dots\dots\dots\dots\dots\dots\dots\dots (26)$$

The OK kriging system must be formulated and solved for each point x_0 where an estimate is required. This is necessary in order to obtain the covariance matrix, C (which accounts for spatial variability and clustering), and the distance matrix, D (which accounts for distances between the observations and the location where the estimate is required). Once the weights are found, the estimate for the parameter value, v_0, and for the error variance at this location is obtained from the observed values, v_i, using the equations:

$$\hat{v}_0 = \sum_{i=1}^{n} w_i v_i \quad \dots\dots\dots\dots\dots\dots\dots\dots\dots\dots\dots\dots\dots\dots\dots\dots\dots\dots\dots\dots\dots\dots\dots\dots (27)$$

$$\hat{\sigma}_R^2 = \hat{\sigma}^2 - \sum_{i=1}^{n} w_i \hat{C}_{i0} + \mu \approx (C_0 + C_1) - \sum_{i=1}^{n} w_i \hat{C}_{i0} + \mu \quad \dots\dots\dots\dots\dots\dots\dots\dots\dots\dots (28)$$

Note that in practice the first term on the right hand side of equation 28 is set equal to the variogram sill: $(C_o + C_1)$ since the covariance plateau is equivalent to the variance of the random field.

Public domain geostatistical software for spatial interpolation was reviewed by Varekamp *et al.* (1996). Widely-used packages include: GeoPACK (Yates, 1989), GeoEAS (Englund, 1990) and GSLIB (Deutsch and Journel, 1992). Various private software products are also available, such as VarioWIN (Pannatier, 1992) and SPANS™ GIS, which incorporates some statistical tools.

In order to avoid over-emphasising geostatistical techniques at the expense of FFA and GIS methods, derivations for the system of equations used to obtain kriging weights will not be given herein. Extensive literature and excellent texts already cover this material (Isaaks & Srivastava, 1989; Deutsch and Journel, 1992).

Chapter 4

4. RESULTS AND DISCUSSION

4.1 Introduction

The flood flows and other information used in this thesis are described in section 4.2. The results of statistical tests and screening procedures have been tabulated in Appendix A. Most of the maps have been printed in Appendix C. The algorithms developed or modified for this thesis are documented in Appendix B; which includes computer code in C^{++}, FORTRAN and in the SPANS™ GIS and QUATTRO™ macro languages.

The methodology used in this study is a hybrid of hierarchical FFA (see section 2.2.3) and of GIS and geostatistical studies (see sections 2.3.2 and 2.3.3). It is described in detail in section 4.7: "Spatial Considerations for Regional FFA". The intervening sections fulfil the principal objectives of this thesis. Spatially-continuous estimates of the L-moments of flood flow and timing are obtained in section 4.3. The global variance of these parameter estimates are also examined and quantified. The spatial variation of the principal flood-generating mechanisms and their associations with predictive variables, such as the new multimodality index, are described in section 4.4. A current procedure for the delineation of homogeneous regions is diagnosed using a new spatial contrast measure in section 4.5. The association of L-CV with snow precipitation is measured in section 4.6. Relationships with other independent variables are also considered.

4.2 Dataset Assembly, Testing and Screening

The study area data assembled within the SPANS™ GIS is essentially of two types: gauge data (points) and map data (rasters and polygons). Point data has to be transformed into maps in order to support spatial analysis (Appendix C). The metadata (origin, quality and transformations) for the flow gauge and map information are given in Appendices A and C, respectively.

Point or Gauge Data

Average daily maximum flow data is the dependent variable for the FFA, geostatistical and GIS models. It has therefore been subjected to a battery of tests to ensure that it conforms to the assumptions made by these analytical techniques. Nonparametric tests used to verify the 471 AM flood series' statistical properties include (Pilon *et al.*, 1993):

- The Spearman rank-order serial correlation coefficient test for independence.
- The Spearman rank-order correlation coefficient test for trend.
- The test of runs above and below the median for general randomness.
- The Mann-Whitney split sample test for homogeneity. This test can be used to detect differences in the mean over time or between seasons.

Flood data series failing any of the above tests at the 5% or 1% level of significance were identified in Table A.1. Gauges where recordings were not logged automatically or continuously were likewise flagged. The remaining 397 gauges, located in 272 third-order watersheds, are considered reliable (see Appendix A for a comparison with (Bobée, 1996a). Map postings showing each gauge's L-mean and L-CV (date) and L-skew and L-CV (flow) revealed extreme values whose spatial clustering was diagnosed in greater detail. A final set of 371 gauges were retained from the original 471.

No tests were required for the Julian flood dates of AM floods, which were used as indicators of flood generating mechanisms. A series of maps showing the number of observations within 5, 10 and 20-year periods was also produced (Appendix C). As a

result of an earlier NSERC (1993) study in which the author participated, physiographic and meteorologic data was available for 189 watersheds – roughly half of those used in the current study. The sparsity of this information, consisting primarily of point summaries of variables with a spatial extent, did not support map creation.

Map Data

The digital Canada Climate Normals (Environment Canada, 1992) were obtained and imported into the GIS study area. In all, six maps were converted: mean annual precipitation, rainfall and snowfall and mean annual minimum, average and maximum daily temperatures. Due to limitations in the source data, these maps have a somewhat lower resolution (300 m) than that available for other data (150 m).

Environment Canada also contributed a vegetation map and the boundaries of third-order watersheds. The latter were analysed with the GIS to extract their perimeter lengths and areas and to calculate their area to length or elongation ratio (A/L). The maps were simplified to show major patterns in drainage (second-order and continental divide), land cover types (plains, deciduous, conifers, tundra, ice) and major water bodies which could be expected to affect local climate and snowfall. The resulting watershed and water body maps were buffered to 300 km in 25 km increments.

The size of the SPANS GIS study area is 44° EW by 22° NS, divided approximately in thirds by its two standard parallels at 46° and 56° N latitude. It uses an Albers equal-area projection to allow for comparisons of neighbouring watersheds and homogeneous regions. The finest pixel size is 150 m and no map has less than a 300 m resolution. Errors introduced during map registration are less than a hundredth the size of the smallest third-order watershed area, which serve as the fundamental spatial units in this study, and/or less than 0.5% of the study area dimension for the worst map pair combination. These spatial errors are not significant in comparison to calculation errors.

Exploratory Data Analysis

Univariate and bivariate exploratory data analysis (EDA) was carried-out for each variable as shown in Table 4.1, which also defines them (summary statistics and histograms are provided in Appendix A). Map variables were sampled at the 371 gauge locations for this purpose. All variables have CV < 1 with the exception of L-mean and DA (the "unit flood" variable L-mean/DA has a CV < 1). They are also approximately normally distributed with the exception of MMI and NMODE which are both indicator variables. These properties are required for geostatistical analysis.

As shown in Table 4.1, no significant bivariate relationships exist between pairings of independent variables (LAT, LONG, DA, NY, DIST, P-snow, NMODE and MMI). Three proxy variables which also account for elevation (VEG, TEMP and P-rain) are associated with LAT and/or LONG. Details of the EDA for dependent variables are provided in the following sections where appropriate.

The weak relationships of P-snow and P-rain with LONG is a result of less precipitation in the "drier" W and more in the "wetter" E. Although the pattern repeats for P-rain and LAT (drier N), P-snow is too spatially variable to yield a linear relationship with LAT (r^2 = 0.03) – snow must therefore be modelled in a spatially-explicit manner. These directional tendencies are reflected in L-mean/DA, which is caused by precipitation. Since such moderate spatial trends do not impede geostatistical estimation, they were not removed.

The relationship between NMODE and MMI is discussed in section 4.4.1. The relationship between L-mean/DA and L-CV indicates that floods are heteroscedastic ($\sigma_t = f(\mu_t)$ with r^2 = 0.84). The impact on at-site (point) estimation can be minimized using the robust L-moment estimators and the flexible GEV distribution chosen for this study. Aside from the departure from normality, the implications for spatial estimation are discussed in section 4.3.

Weak linear relationships in one direction (LAT, LONG) may actually indicate strong associations between two spatial variables. This must be confirmed by map analysis.

Table 4.1: Multivariate EDA for Dependent and Independent Variables

	LAT	LONG	DA	NY	DIST	P-snow	NMODE	MMI	VEG	TEMP	P-rain	L-meanT	L-CV_T	L-skewT	L-kurtT	L-mean/DA	L-CV	L-SKEW	L-KURT
LAT	x	x																	
LONG	x	x																	
DA	.25	.00	x																
NY	.04	.00		x															
DIST	.09	.09	.03	.00	x														
P-SNOW	.03	.39				x													
NMODE	.00	.02	.01	.00			x												
MMI	.03	.00	.02	.02			.39	x											
VEG	.44	.03	.18	.01					x										
TEMP	.80	.03								x									
P-RAIN	.45	.45									x								
L-mean_T	.24	.05	.08	.00								x							
L-CV_T												.11	x						
L-skew_T												.01		x					
L-kurt_T												.18			x				
L-mean /DA	.23	.40	.09	.01				.01								x			
L-CV								.17								.84	x		
L-skew								.23								.05		x	
L-kurtosis								.09								.00			x

Variables are defined as drainage area DA [km^2], years of record NY, distance from water bodies DIST [km], mean annual precipitation P [mm], number of modes NMODES and multimodality index MMI for nonparametric pdf, vegetation VEG, mean annual temperature TEMP [°C] and the first four L-moments for flood timing _T and flow. Shown in some boxes is the linear regression coefficient, r^2. Italics are used for VEG, TEMP and P-rain since they can be used as proxy variables for LAT and/or LONG and elevation (elevation is not included in the table).

4.3 Spatially-Continuous Estimates of L-moments

To support map analysis in subsequent sections, spatially-continuous estimates of the at-site parameters were obtained using OK. The four steps of this procedure have been summarized below.

Description of Spatial Continuity using Variograms

Variograms are measures of spatial autocorrelation (or continuity) which are analogous to the correlograms used in time series analysis. Due to the possibility of anisotropic behaviour by the two-dimensional data, experimental variograms were calculated for twelve azimuths (directions). Two perpendicular directions were chosen as the anisotropy axes and used in estimation. Tolerances for lag distance and azimuth were chosen to minimize overlap while retaining an adequate number of pairs for each lag.

For the two anisotropic axes, the range and nugget parameters were identified from the variograms (with the help of three additional types of variograms which minimize the effect of outliers and data sparsity: rodograms, madograms and pairwise-relative variograms) (Isaaks and Srivastava, 1992). For many variables, changes in the range and sill with direction required the use of two nested variogram models to handle the resulting geometric and zonal anisotropy, respectively. The positive-definite variogram models fitted to each experimental variogram are shown in Figure 4.1.

The experimental variograms for flood timing (L-mean_T and L-CV_T) are well-behaved and exhibit only zonal anisotropy. Those for MMI and L-skew are very nearly pure nugget effects, indicating minimal spatial continuity for which only local averages are relevant (spatial noise). The MMI variogram is erratic, showing a discontinuity at lag zero and a periodic structure likely to result in very noisy estimates. Variograms for L-CV and L-mean/DA are well-behaved but exhibit both zonal and geometric anisotropy. This requires that nested variogram models be used but should nevertheless yield reliable estimates.

a) L-mean_T

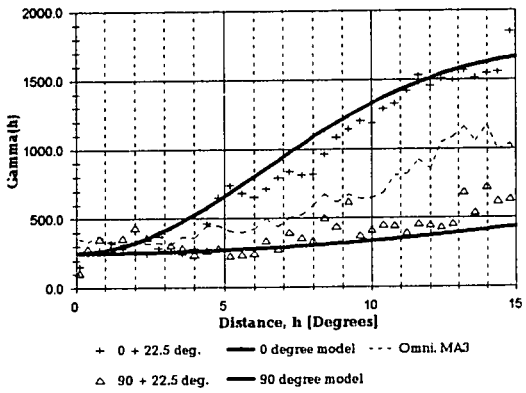

b) L-CV_T

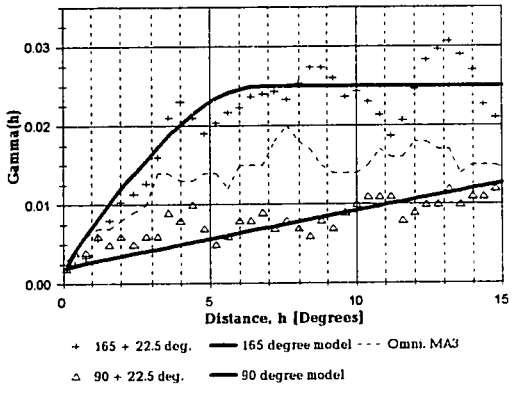

c) L-mean/DA

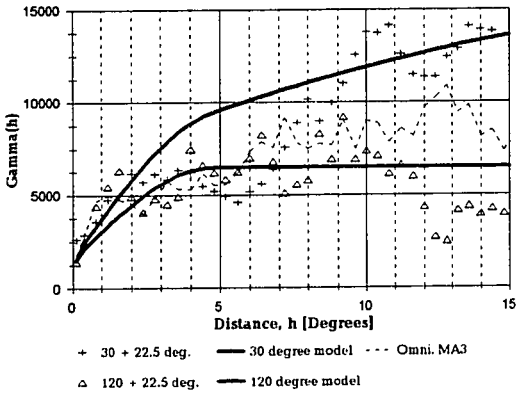

d) L-CV

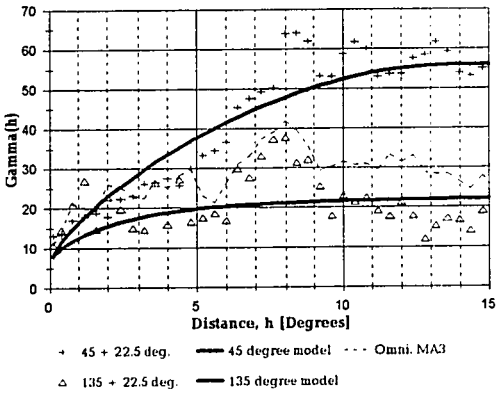

e) L-skew (isotropic)

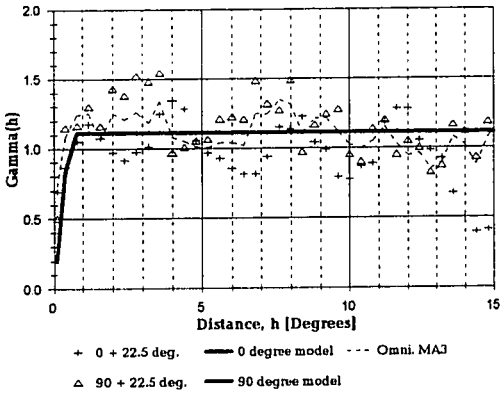

f) MMI and LRI

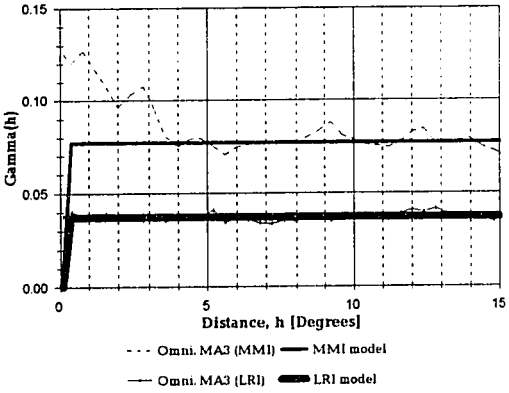

Figure 4.1: Variograms for Maximum and Minimum Spatial Continuity Axes

Parameter Estimates using Kriging

As discussed in section 4.2, the L-mean/DA parameter is heteroscedastic ($\sigma_t = f(\mu_t)$) and may also suffer from a "proportional effect" whereby ($\sigma_s = f(\mu_s)$). The impacts of such undesirable properties were kept to a minimum using a robust search strategy which restricts the effective range to less than half of the smallest dimension of the study area and which matches medium-scale variability using a minimum of 4 and a maximum of 12 neighbours for estimation. The resulting maps are of acceptable accuracy for the purposes of visualisation, evaluation of alternative regional models and investigations of the associations between variables which are discussed in sections 4.4 to 4.7.

Spatial OK estimates are based on 371 gauges, of which 275 gauges are of primary interest due to their location in the continental areas of Eastern Canada: Ontario, Quebec, Labrador and New-Brunswick. Figures 4.2 a and b show the estimated values μ_s and spatial standard deviation σ_s for L-mean/DA. Both equal-interval maps show the spatial distribution of estimates. The optimal number and width of map classes was selected iteratively in a manner analogous to histogram construction.

L-skew and L-CV parameter maps are discussed in sections 4.6 and 4.5, respectively. The apparent anisotropy for L-skew was too small to be differentiated from variogram noise, hence a single (omnidirectional) isotropic variogram was used to estimate this parameter. Use of nested anisotropic variograms did not result in appreciably different estimates, however the maps appeared noisy and exaggerated in the NS direction.

Global Mean and Variance of Spatial (Kriging) Estimates

The OK algorithm provides estimates of the global mean and variance of the estimates. Local means and variances, which can be used to construct confidence intervals for the parameter estimates, could have been obtained using block kriging and relative variograms but this would have greatly increased computing time. In cases where trends in local means were evident across the study area (e.g. L-mean_T), these were handled implicitly using OK with small search neighbourhoods which effectively re-scale the local means during estimation.

Figure 4.2 shows the OK estimates for the L-mean/DA (μ_s) and its spatial standard deviation of estimate (σ_s). Although the at-site estimates summarising the time dimension should coincide with the spatial estimates, the corresponding at-site L-CV incorporate σ_t, a measure of temporal variability which must not be confused with the spatial variability of the OK estimates, σ_s.

Cross-Validation of Spatial Estimation Procedures

Table 4.2 lists summary statistics for the original data and the cross-validated estimates. The ranges for the cross-validated estimates are smaller than for the original data values, indicating that the OK estimation procedures has behaved like a low-pass or smoothing filter. While the cross-validated CV values are correspondingly lower, the mean values are nearly identical to the original data.

Also shown are the Q_1 and Q_2 test statistics of the orthonormal residuals which are normally near 0 and 1, respectively. When a high nugget is used, OK estimates are closer to a local average. Based on the experimental variograms, some of the nugget values were reduced in order to minimize OK smoothing while keeping values of Q_2 to approximately 2.

Table 4.2: Comparison of Original and Cross-Validated Parameter Statistics

	L-mean/DA		L-CV		L-skew	
	original	x-validated	original	x-validated	original	x-validated
min	.0067	.0192	.0829	.1190	-.1573	-.0406
mean	.1564	.1577	.2403	.2422	.1783	.1805
max	.8317	.4870	.6562	.5603	.5614	.4328
range	.8250	.4678	.5733	.4413	.7187	.4734
CV	.75	.62	.43	.39	.68	.46
Q_1	–	0.03	–	0.06	–	0.03
Q_2	–	2.08	–	1.98	–	1.92

For the 371 estimates, test statistics for the orthonormal residuals should lie within the following intervals: $-0.10 < Q_1 < 0.10$ and $0.85 < Q_2 < 1.15$.

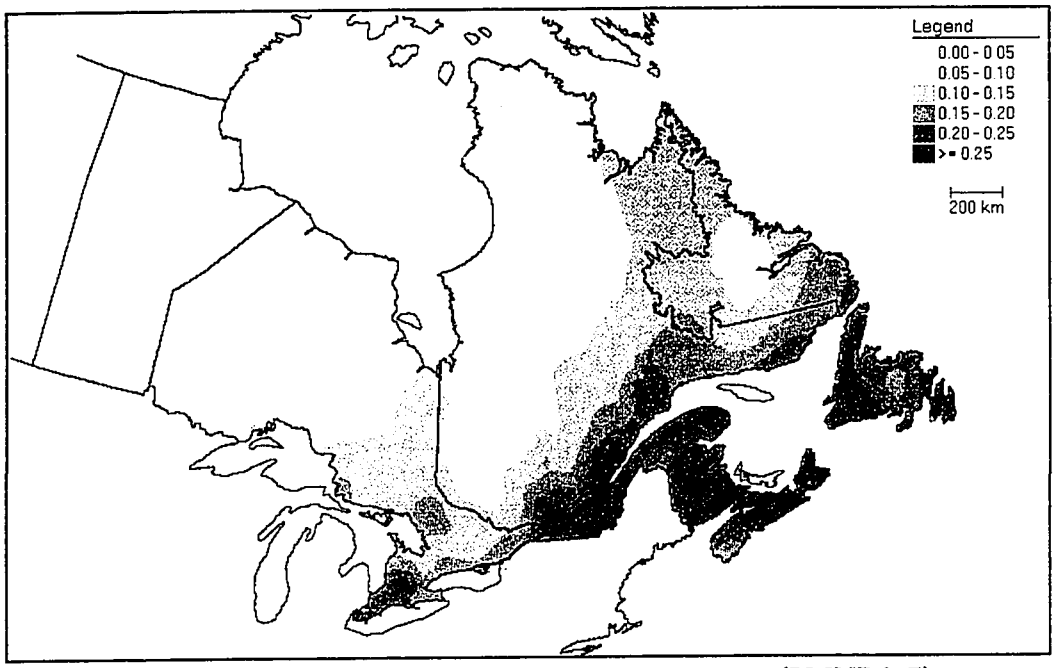

Figure 4.2 a: L-Mean of AM Flood Flow Normalised by Area (LMNDA-7)
Note the increase from the SE to the NW across the study area overall and from SW to NE near Nova Scotia and Newfoundland. SW Ontario also has high local values.

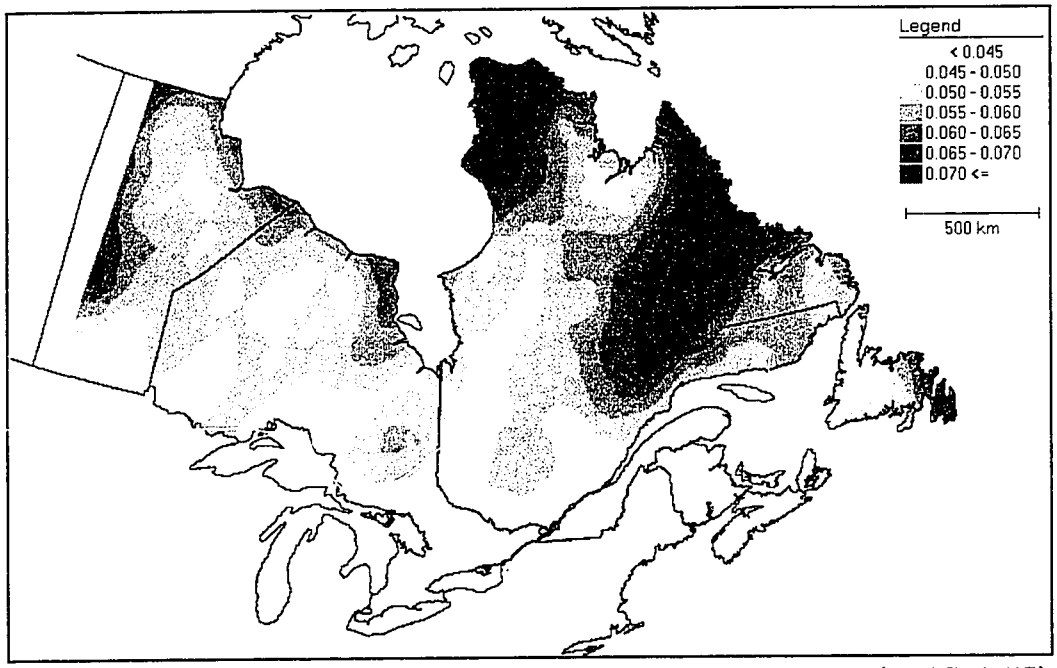

Figure 4.2 b: Spatial Standard Deviation for L-Mean of Flood Flows (LMNDA-7S)
Estimation uncertainty is greatest where the network of flow monitoring gauges is sparse, such as in northern Quebec and Labrador. Uncertainty also increases at the artificial boundaries where data were cut-off.

4.4 Characterization of Flood-Generating Mechanisms

4.4.1 Development of the Multimodality Index (MMI)

Due to the large number of sites considered in regional FFA, a numerical index summarizing the nonparametric PDF is essential for spatial estimation and mapping. Simple indices such as the number of significant modes, NMODE, or an assymmetry measure such as LRI cannot diagnose whether a site is unimodal (UM), heavy-tailed (HT) or multimodal (MM) – a new MMI combining their best features was therefore developed for this study in section 3.2.2 (the C^{++} computer code is provided in Appendix C). In this section, the practical usefulness of the MMI is diagnosed and the 371 at-site estimates are mapped to reveal spatial trends in flood-generating mechanisms.

The properties of the MMI are shown in Figure 4.3 a through e. Figure 4.1a shows four typical at-site pdf and their corresponding MMI value. In cases where there is a unique mode but a heavy right-hand tail, the MMI gives an indication of the influence of extreme floods on the overall distribution (site 02QC009). As the importance and number of secondary modes increases, the MMI also increases from 1.00 to 1.81 (or higher), as shown in the figure.

The MMI is weakly proportional to NMODE (part b of Figure 4.3) and only takes on values greater than two if the nonparametric PDF has more than one significant mode (part c of Figure 4.3). For NMODE = 1, it is also weakly proportional to L-CV and L-skew (parts d and e of Figure 4.3; Table 4.1) but it is independent of L-kurtosis. This supports the assumption, postulated in section 3.2.2, that sites with multiple flood-generating mechanisms tend to have larger values of L-CV and L-skew.

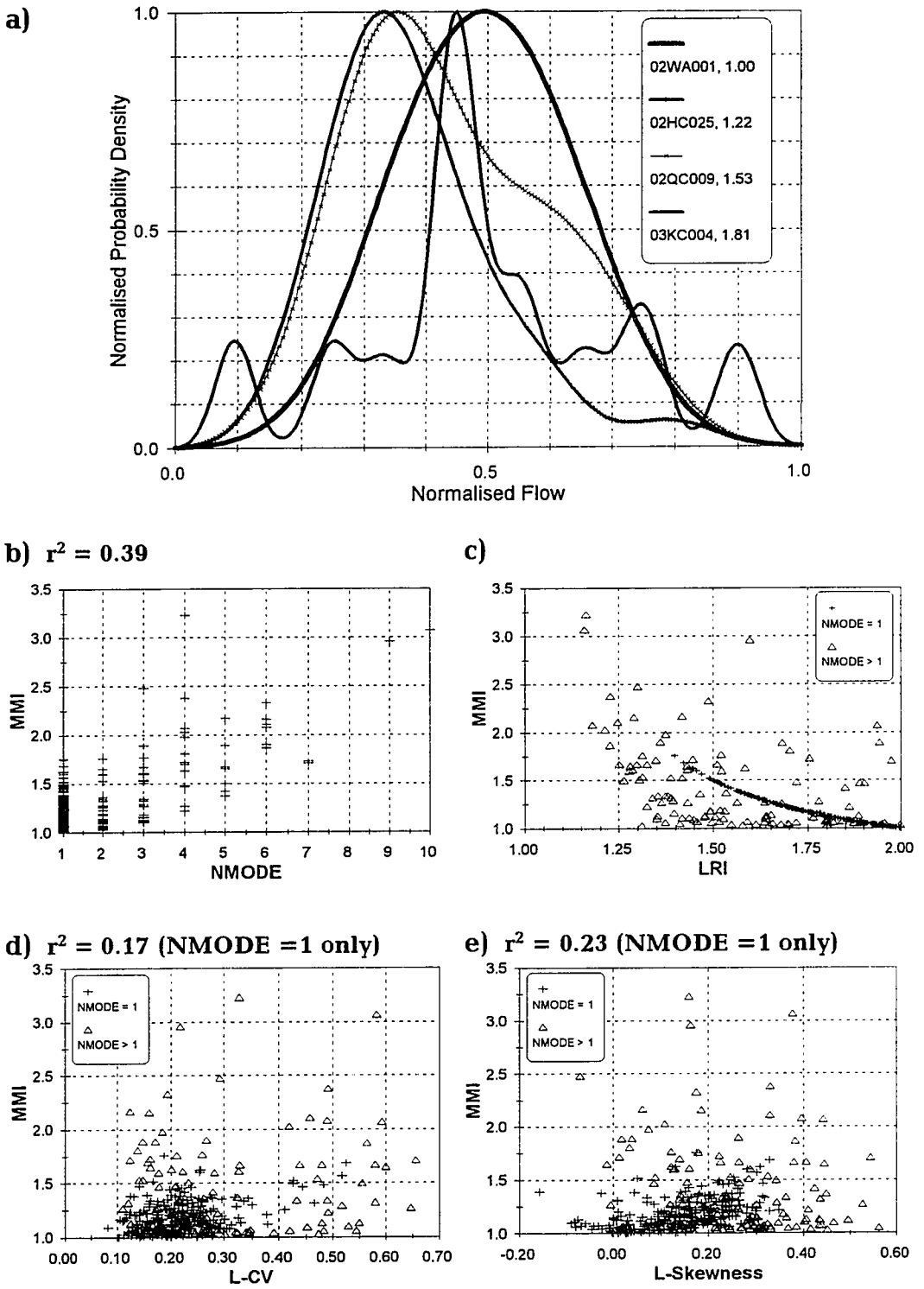

Figure 4.3: Diagnostic Plots for the Properties of the MMI

As shown in part c when NMODE = 1, the MMI increases more slowly and gradually than LRI from a perfectly unimodal PDF with equal areas in each tail (MMI = 1, LRI = 2) to a 2/3 to 1/3 PDF mass split (both indices 1.5); increasing faster than the LRI from then on. This desirable behaviour provides finer grades for nearly UM sites but spreads-out HT or MM sites' MMI ratings. The progression of MMI from 1 for UM to 2 or more for MM sites parallels the familiar NMODE index but also provides fractional values which could be used to classify UM sites as heavy-tailed (HT). This is more intuitive than LRI's corresponding decrease from 2 to 1.

When NMODE > 2, the MMI can take on different values depending on the number of significant modes and the probability density belonging to each – the LRI can only take a single value based on the asymmetry of the PDF (compare triangles and crosses in part c). This is an important property which allows MMI to distinguish symmetric but multimodal PDF such as site 03KC004 (part a) from a unimodal pdf such as site 02WA001, unlike the LRI.

Parts a and b of Figure 4.4 show how the spatial variation of LRI and MMI throughout the study area. While low values of MMI near Cape Breton reflect the predominance of late-fall floods in contrast to southern Nova Scotia, the LRI shows no such contrast. Similarly, MMI varies smoothly through the HT/MM range in the N Quebec region while the LRI gives no indication of MM sites since the PDF are "balanced" (like site 03KC004 in part a of Figure 4.3).

Overall, the LRI exhibits significant short-scale variation: areas of extreme high and low values alternate throughout the study area (Figure 4.4). No clear trends or "signals" can be distinguished and the map looks like spatially uncorrelated "noise" – this is supported by the experimental variogram for this variable which is a pure nugget effect (Figure 4.1 f).

While the experimental variogram for MMI is also very nearly a nugget effect, MMI varies smoothly throughout most of the study area with the exception of the mid-latitude regions where snowmelt and rainfall mechanisms mix. The MMI decreases from the SW towards the NE of Nova Scotia where late fall floods dominate (see Figure

4.5 a), resulting in UM populations with low variability (Figure 4.5 b) and, correspondingly, low MMI values. Higher MMI values are expected in the S portions of Nova-Scotia and New-Brunswick due to the presence of an additional flood-generating mechanism: hurricanes dissipating along their coast. The patterns resulting from the locations of high and low values of MMI have a physical interpretation and appear to be a spatial "signal".

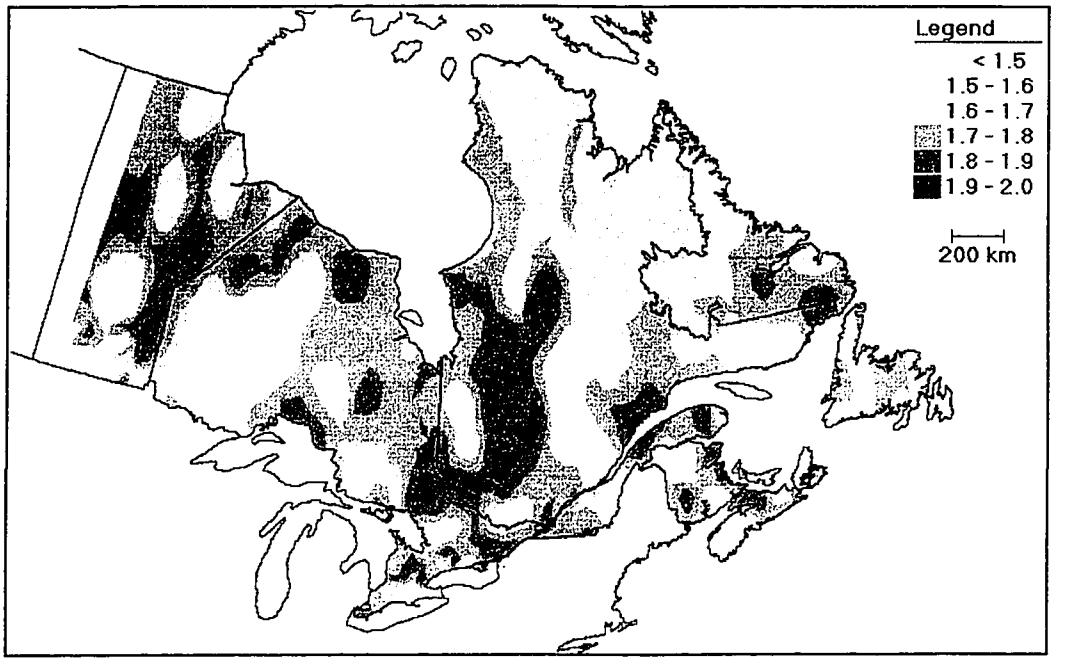

Figure 4.4 a: Simple Left-Right Index of PDF (LRI-5)
Note the lack of contrast from SW to NE Nova Scotia and the low values near Ungava Bay in N Quebec. Zones of high and low extremes alternate throughout the study area, indicating either highly variable data or "noise".

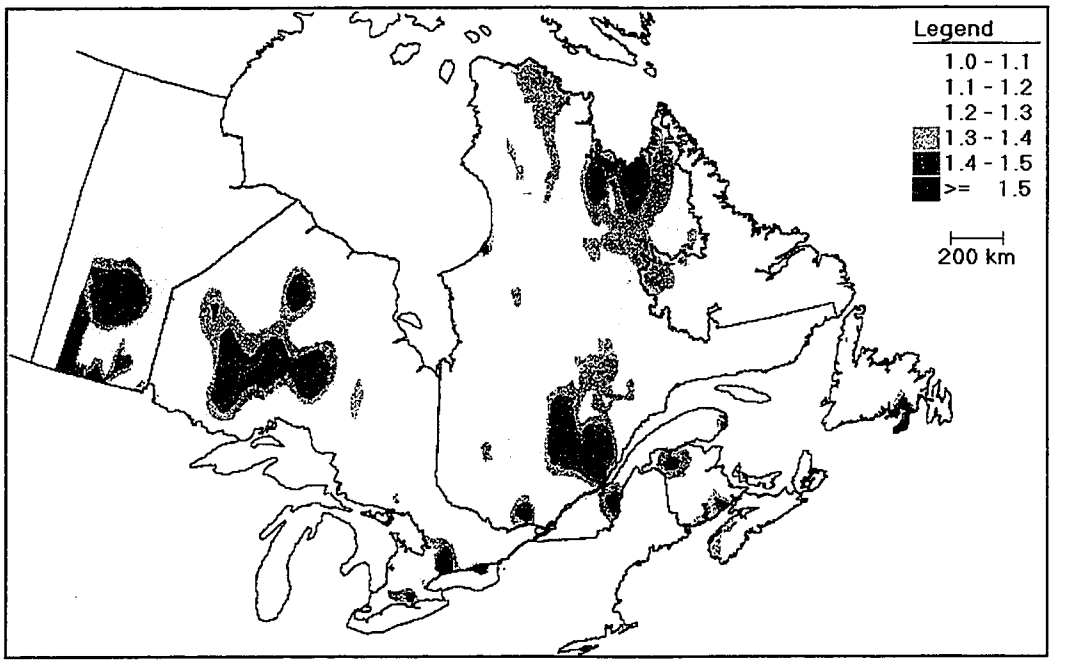

Figure 4.4 b: Multimodality Index (MMI-5)
Note the contrast in MMI from SW to NE Nova Scotia, where late rainfall floods predominate. High values of MMI occur at mid-latitudes where both the N snowmelt and S rainfall flood-generating mechanisms overlap. High values also occur near Toronto (urban) and in N Quebec (ice).

4.4.2 Spatial Variation of Flood-generating Mechanisms

The variation of L-mean/DA was described in section 4.3 and shown in Figure 4.2. The time of occurrence for floods expressed in Julian days (L-mean_T) and their temporal variability (L-CV_T), are shown in Figure 4.5. While the latest floods occur mainly due to snowmelt in N areas, fall floods can also occur in the S areas due to thunderstorms (SW Ontario) and/or dissipating tropical storms (Nova Scotia). Areas with greatest flood timing variability include SW Ontario and Nova-Scotia, both of which are subject to several types of rainfall flood-generating mechanisms in addition to snowmelt and (rarely) dissipating tropical cyclones or even hurricanes tracking north.

The map evidence generally confirm the flood-generating mechanisms identified in previous studies by others. Gingras' separation of New Brunswick into a northern area subject to snowmelt, a middle area experiencing rain and a southern area occasionally flooded due to dissipating hurricanes (also in Nova-Scotia) is confirmed by Figure 4.2 (L-mean/DA), 4.4 (MMI) and 4.5 (L-mean_T).

The mixture of snowmelt and rainfall identified by Waylen & Woo in 1982 for N Ontario is reflected by high values of MMI (Figure 4.4), as is the highly mixed UM, HT and MM populations reported by various investigators for the Saskatchewan-Nelson river basin (see SE Manitoba and W Ontario in Figure 4.4). The high values of L-skew and MMI in N Quebec may be attributed to ice jams and possibly to different flood times for tributaries to the principal watercourse.

Some of these large and medium-scale flood patterns were detected during the multivariate EDA in section 4.2 but the use of the GIS has greatly clarified their extents and possible causes. Should small-scale variability be investigated, such as variations in timing or mechanism in S Ontario or New-Brunswick, a GIS would become essential to organize and display the required information.

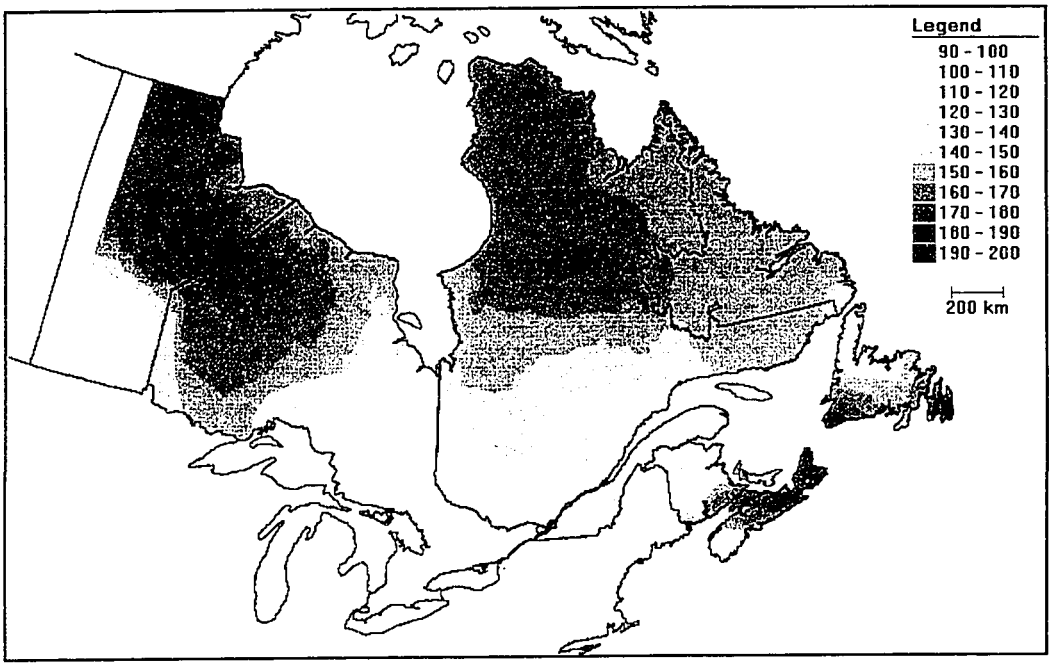

Figure 4.5 a: L-Mean of Julian Flood Date (LMNT-12)
The latest floods generally occur in northern inland areas due snowmelt while the earliest occur in the S due to rainfall. Late floods also occur in NE Nova Scotia and Cape Breton due to fall rains.

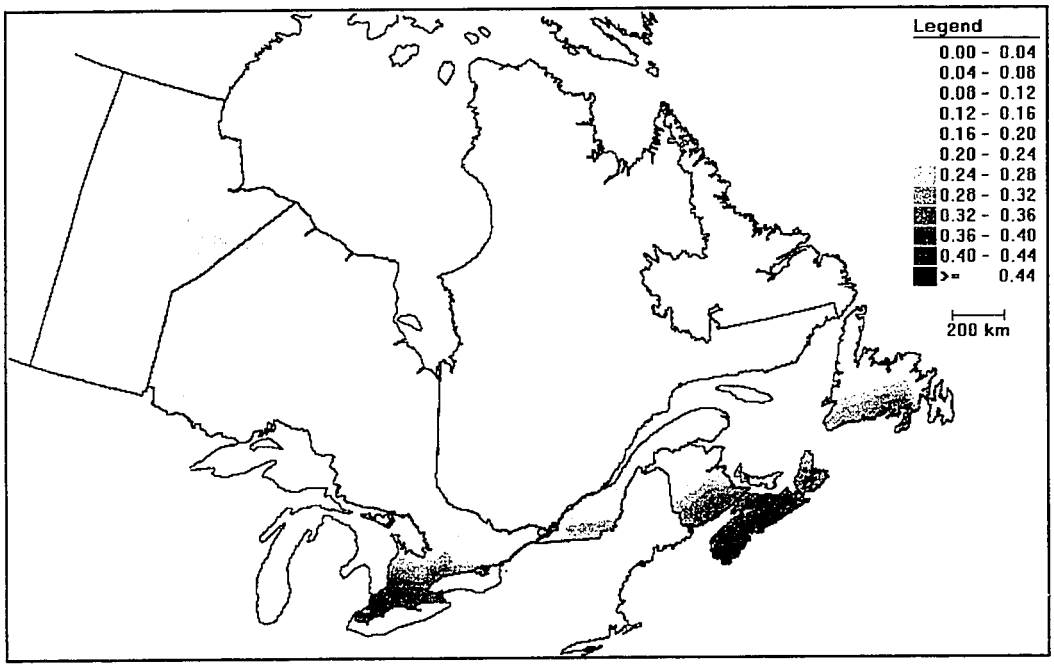

Figure 4.5b: L-CV of Julian Flood Date (LCVT-12)
Snowmelt-generated floods, which have the lowest temporal variability, occur to the N of the study area. Rainfall-generated floods, which have the highest temporal variability, occur to the S of the study area.

4.5 Homogeneous Region Delineation for L-Skewness

The homogeneous regions resulting from earlier studies within the present study area are assembled and rationalised. The resulting regions are diagnosed using both the traditional L-moment test statistics (section 3.3.2) and the new spatial contrast measure developed in section 3.4.2.

4.5.1 Homogeneous Region Delineation using L-moments

Implications of Spatial Variability for Hierarchical FFA

The use of hierarchical regionalisation methodology and the spatial treatment of floods by previous investigators were summarised in sections 2.2.2 and 2.2.3, respectively. The experimental variogram for L-skew shown in Figure 4.1 was poorly defined and any apparent anisotropy could not be differentiated from noise. The resulting isotropic variogram model had a very small range and was similar to a pure nugget effect. Consequently, the spatial standard deviation of the OK estimates increases rapidly with distance from local data clusters, as shown in Figure 4.6 b. The resulting OK estimates, mapped in Figure 4.6 a, approximately correspond to a short-scale moving average.

Due to the high spatial variability of L-skew, an average value is the most reliable measure which can be used for FFA. This average can be evaluated either for the entire study area or for smaller subdivisions within which it can be assumed to remain constant: homogeneous regions. Hierarchical regionalisation methodology suggests that lower-order L-moments, namely L-CV and L-mean/DA, should be estimated within these same regions or in subdivisions thereof.

In contrast to L-skew, the experimental variograms for L-CV were reasonably continuous and show clear anisotropy. The smoother and more predictable spatial variation of L-CV indicates that it can be modelled in a spatially-explicit manner either

across the entire study area or within each homogeneous region defined for L-skew. This topic is explored in section 4.6.

Delineation of Homogeneous Regions

In order to be amenable to testing using L-moment flow statistics, homogeneous regions must be delineated using other criteria such as physiography, meteorology, flood timing, etc... In this study, the earlier delineations based on physiography by Sangall and Kalio (1977) and by Gingras and Adamowski (1993) based on flood timing were used as a starting point. In addition to the L-mean and L-CV of the Julian flood date, the monthly and seasonal flood distribution were also mapped (see Appendix C). Maps showing MMI, vegetation and distance from major water bodies were also consulted.

The three objectives of the delineation process were to combine adjacent regions from previous studies wherever possible (e.g.: N New-Brunswick and E Quebec); to respect second-order drainage divide wherever possible; and to enclose contiguous areas of land wherever possible.

While lack of data in the NE USA and central Canada resulted in artificial regional boundaries, natural boundaries such as the Great Lakes, the Niagara escarpment and Hudson's and James' Bay served as natural regional boundaries. Peninsular areas such as Nova Scotia and islands such as PEI and Newfoundland were kept as individual regions, as recommended by previous studies. The 18 homogeneous regions shown in Figure 4.7 were grouped from the previous studies which were summarized earlier in Table 2.1 (section 2.2.2).

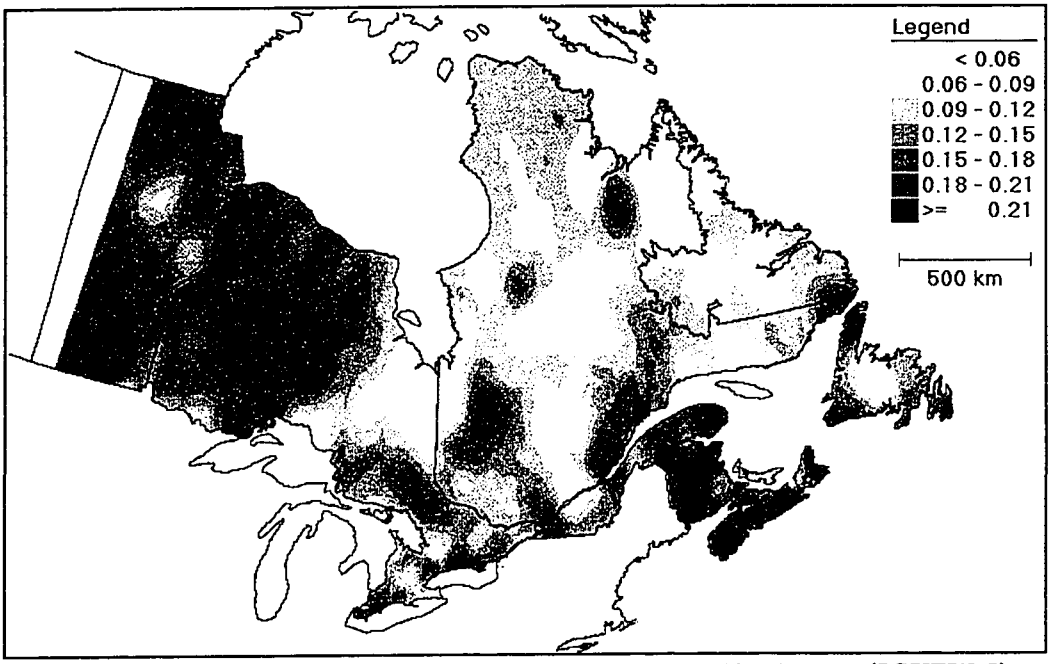

Figure 4.6 a: L-Skew of AM Flood Flow – Contours of OK Estimates (LSKEW-5)

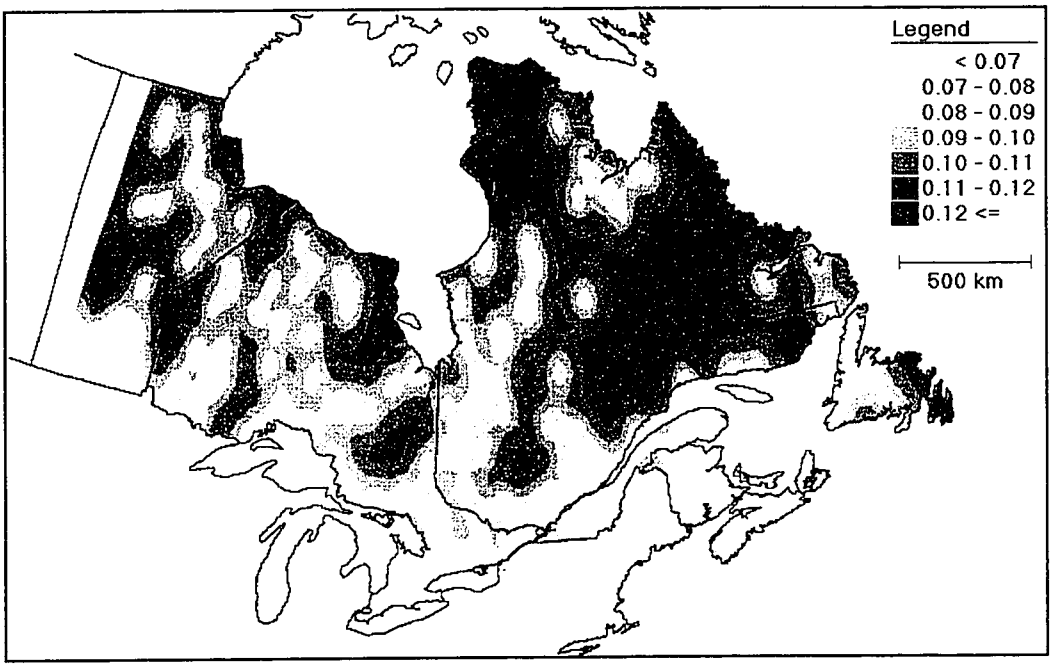

Figure 4.6 b: L-Skew of AM Flood Flow – Standard Deviation of OK Estimates (LSKEW-5S)

The tight, circular zones of increasing spatial variability about local gauge clusters indicate that a short-range and isotropic model of spatial continuity has been used (almost a pure nugget).

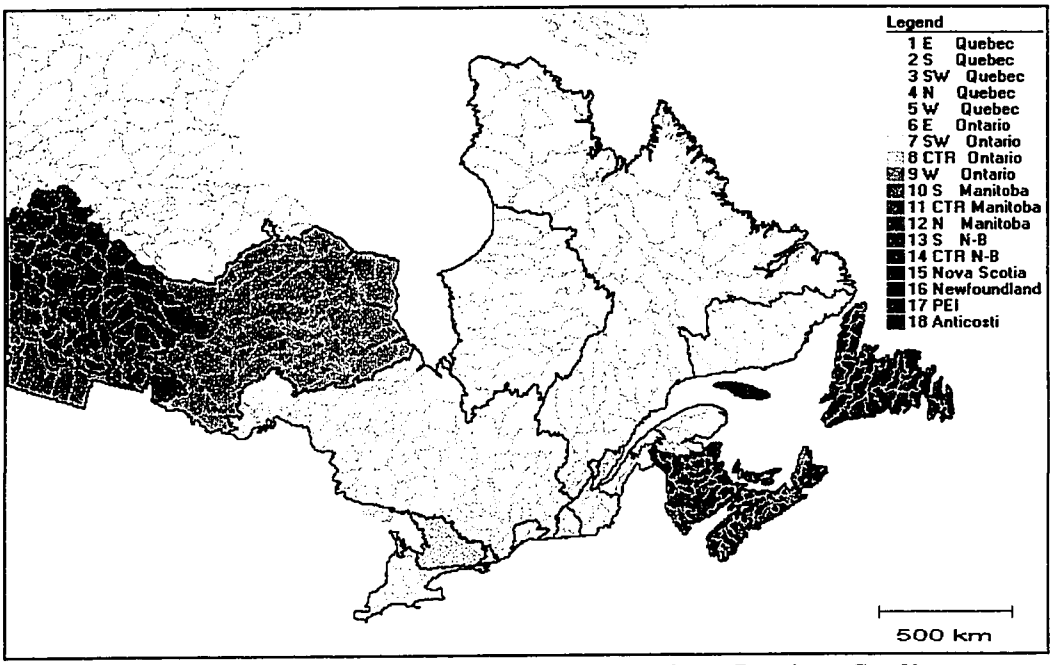

Figure 4.7: Sixteen Homogeneous Regions for FFA from Previous Studies
Also shown are the third-order drainage basins for the study area. Note that many of the smaller regions contain several small watersheds and gauges (not shown) – small regions can be defined accurately in densely sampled areas.

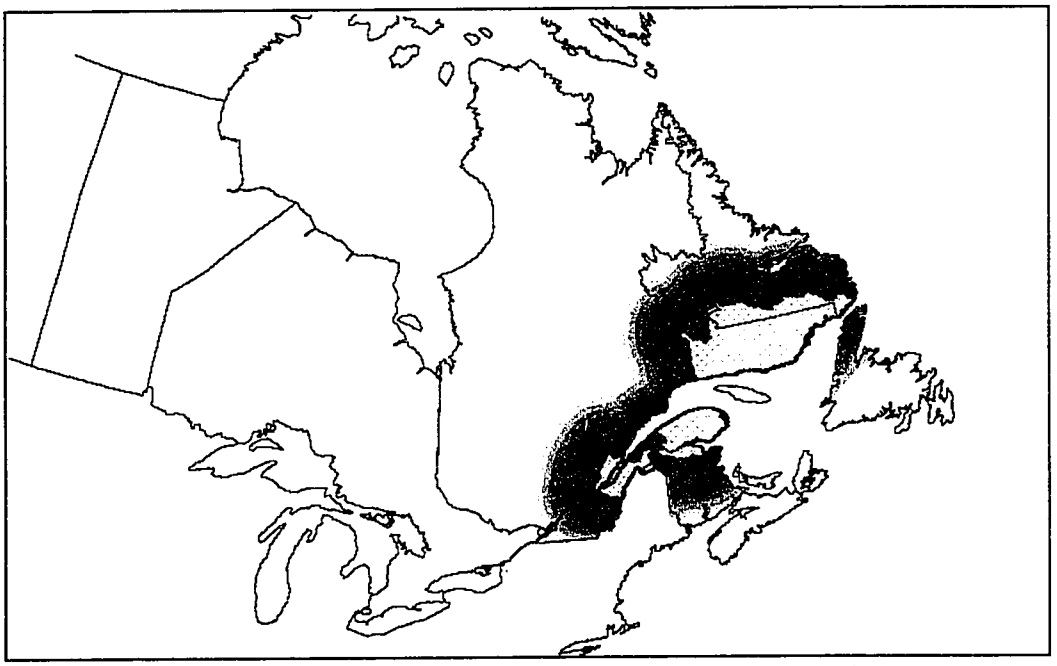

Figure 4.8: Definition Map for Calculation of the Spatial Contrast Measure
Example shown for region 1, which borders the St-Lawrence River in eastern Quebec. Values of L-CV (or any other suitable contrast measure) are cross-tabulated for each buffer away from (off-pattern, shown) and into (on-pattern, not shown) the region of interest.

Map Measurements of L-Moment Ratios

The fundamental assumption of L-moment is that L-moment ratios within a properly defined homogeneous region tend to the same (population) values and, therefore, that the observed variability should be the same as that resulting from numerical simulations of 1000 equivalent regions (i.e.: with the same number of sites and years of record). The L-CV and L-skew/L-CV ratios are used for the H_1 and H_2 test statistics, respectively. The spatial implication of this assumption is that values within a region should be significantly different than values outside the region if its boundaries have been delineated correctly.

Table 4.3 shows the non-spatial L-CV and L-skew average values for each region. These were obtained from both point (gauge) data and from a spatial average using GIS map measurements. Since there is reasonable agreement between the spatial and point values, map measurements can be considered reliable. It is possible that the map estimates are more accurate than point averages insofar as the observed spatial variation for each is statistically significant and not merely noise. The regional average values obtained from the map deviate from the non-spatial averages more for L-skew (9.8%) than for L-CV (2.5%), as expected, due to the high variability of the L-skew map.

Table 4.3 also shows the spatial average value of L-CV and L-skew outside the region within a distance equal to its average thickness. The L-moment ratios within several of the regions are not significantly different than those outside of them: average differences are of the order of 5 and 10% for L-skew and L-CV, respectively. This may indicate poorly-defined regions, or it may be the result of the smooth spatial variation of the parameter.

Simple measures of spatial contrast such as these bulk averages are not sufficient to diagnose many regions: the parameter values must be related to the distance from the region boundary. This is the rationale for the spatial contrast measure discussed in the next section.

Table 4.3: Comparison of Average Values of L-skew and L-CV for each Homogeneous Region and its Immediate Surroundings.

Region ID Number *	Number of Sites	L-Skewness			L-Coefficient of Variation		
		Point (inside)	Map (inside)	Map (outside)	Point (inside)	Map (inside)	Map (outside)
1	24	0.1774	0.1134	0.1102	0.1996	0.1788	0.1774
2	9	0.0780	0.1146	0.1186	0.1724	0.1815	0.2208
3	7	0.1002	0.1310	0.1165	0.2257	0.2041	0.1855
4	24	0.0719	0.0955	0.1207	0.1584	0.1566	0.1674
5	18	0.0936	0.0904	0.1168	0.1319	0.1345	0.1764
6	54	0.1432	0.1249	0.1439	0.1866	0.1841	0.2015
7	66	0.1635			0.2510		
8	16	0.1122			0.1916		
9	25	0.1700			0.2501		
10	8	0.4122			0.5851		
11	22	0.3078			0.4737		
12	18	0.2172			0.3592		
13	2	0.4440	n.a.	n.a.	0.2779	n.a.	n.a.
14 **	30	0.2533			0.2311		
15	27	0.2283			0.2058		
16	11	0.1546			0.1708		
17	12	0.1547			0.2026		
ALL	371	0.1784			0.2407		

* The spatial extent of the regions corresponding to the above ID numbers are shown in Figure 4.7.

** Includes the two sites from region 13 (SW New-Brunswick).

N.B: Region 18 was excluded from the table due to a lack of flow data.

a) Region 1: East Quebec

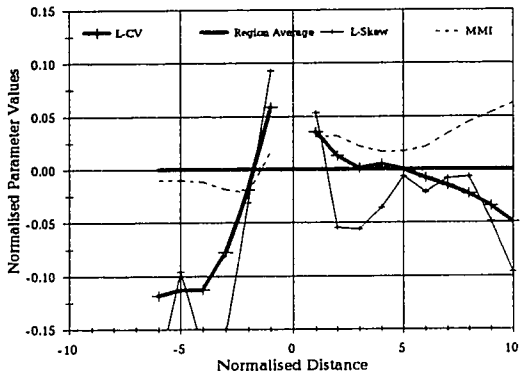

b) Region 2: South Quebec

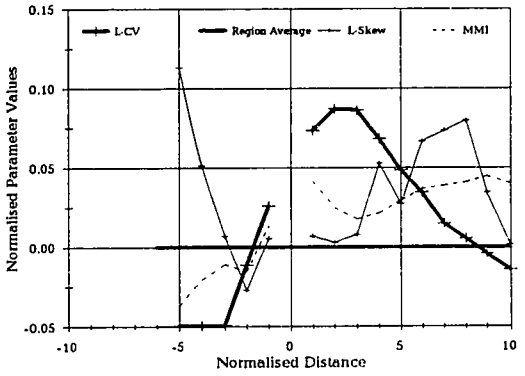

c) Region 3: SW Quebec

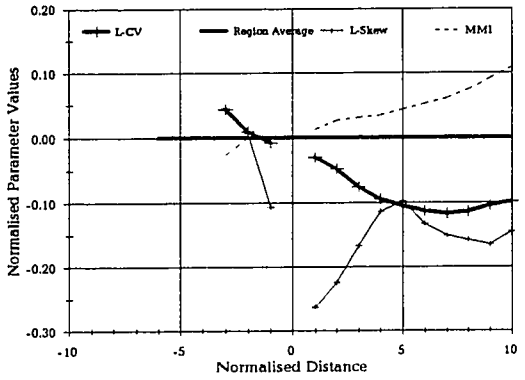

d) Region 4: North Quebec

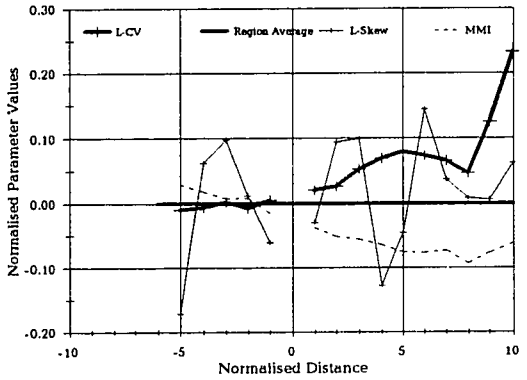

e) Region 5: West Quebec

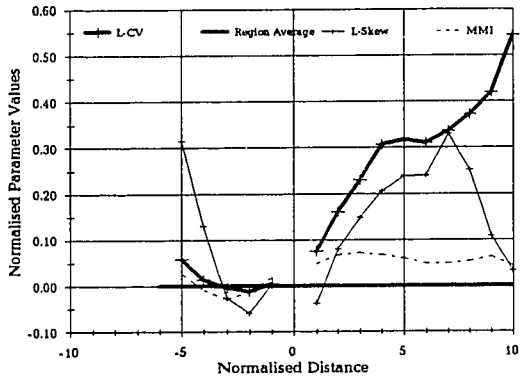

f) Region 6: East Ontario

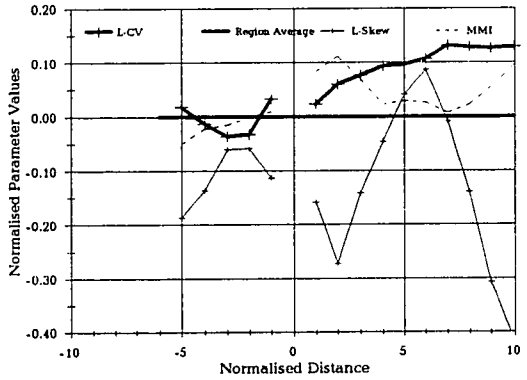

Figure 4.9: Spatial Contrast Measure for Homogeneous Regions

4.5.2 Spatial Contrast Measure to Optimize Regions' Shape and Size

The rationale underlying the development of the spatial contrast measure, SC, is that the average value of a given parameter within a homogeneous region should be differentiable from its value in the immediate vicinity. This differentiation can be expressed as the odds ratio (i.e. probability) of finding the average value within and outside the region, as discussed in section 3.4.2.

Calculation and Behaviour of the Spatial Contrast Measure

Figure 4.9 shows the map modelling operation used to calculate the spatial contrast measure. The measure was evaluated for each region using eight variables (see Appendix B), three of which are shown in the figure: L-CV, L-skew and MMI. The first two were chosen to illustrate the correspondence between spatial contrast and the H_1 and H_2 L-moment test statistics, respectively (additional detail being provided by SC).

Distances were buffered into (negative) and outward from the regional boundaries and normalised by the average thickness of each region, defined in section 3.4.2. Therefore, the spatial contrast measure is scale-independent. Some smaller regions have few negative distances but all regions have 10 external "steps". Similarly, the average value of the parameter of interest within each buffer was normalised by the average value within the homogeneous region (shown as a 0.0 line in Figure 4.9) to allow comparisons between neighbouring regions and/or between alternative regional boundary delineations.

A flat spatial contrast line indicates no change in the parameter with distance, as would be expected within a region for a smoothly varying parameter. Within each region shown in Figure 4.9, the SC for MMI is nearly horizontal and close to the regional average value (normalised to zero) – this confirms the assumption that MMI should be constant within a properly-defined homogeneous region. The SC for MMI is more variable outside the regions and appears to be a well-behaved and consistent indicator of regional homogeneity.

The slope of the spatial contrast measure represents the gradient of parameter vs distance. If the regional boundary is correctly situated, a change in sign and/or a significant discontinuity in the gradient can be expected. This clearly occurs for all three parameters for region 1 (Figure 4.9 a).

Furthermore, a smoothly varying parameter with good spatial continuity such as L-CV should have more gradual changes in slope than a more noisy variable such as L-skew – this is indeed the case for the corresponding SC measures for regions plotted in Figure 4.7. The greater usefulness of the L-CV SC parallels the standard practice of relying on the H_1 L-statistic over the H_2 statistic (corresponding to L-skew). The greater degree of continuity in the SC for L-CV also supports the hypothesis that it could be modelled in a spatially-explicit manner.

In cases where a highly variable parameter surface results in a spatial contrast line which oscillates above and below the regional average value, that particular parameter is considered too locally noisy and is not used to diagnose that particular region. This occurs with the L-skew SC for regions 4 and 6.

Use of Spatial Contrast to Diagnose Homogeneous Regions

Based on all three SC measures for region 1 (Figure 4.9 a), it appears to be well-defined and neither its size or shape should be modified. A sharp change in slope as well as discontinuities occurs at the region's boundary (at a normalised distance of zero).

Both MMI and (noisy) L-skew indicate that region 2 could be shrunk by 20% – moving the boundary to a location where the SC has a sudden change in slope. However, the L-CV SC also indicates that it could be grown 20%. Based on an inspection of Figure 4.7, a single third-order basin forming a small spur to the NE of this region might be removed to clarify the situation for this region. This region has only 9 sites.

Only the L-skew SC shows a discontinuity at the boundary of region 3. This region also has very few sites and both the L-skew and MMI SC indicate that it could be enlarged

from 50 to 70%, respectively. This would result in a merging of the two halves of region 3 as it is presently defined – a useful property for a homogeneous region – as well as increasing the number of sites in the region.

The L-skew SC for region 4 fluctuates about the normalised regional value (0.00) and is therefore non-informative. Both the L-CV and MMI SC measures indicate that this region could be enlarged by 50 to 80%, respectively (i.e. to the location of changes in the SC slope). Since its region 1 neighbour has been diagnosed to be correctly defined above, this would require region 4 to absorb significant portions of regions 5, 6 and possibly 2.

All three SC measures indicate that region 5 should be shrunk by 20 to 30%. This shows symmetry with the indication to grow region 4. As expected, the L-skew and L-CV SC measures indicate that region 6 should be shrunk by 20 to 30%. Results for the remaining regions were not available at press time due to computing time requirements.

Comparison with L-Moment Test Statistics

Three L-moment test statistics, obtained by simulating 1000 equivalent regions, were retained for comparison with the spatial contrast measures. The values of the H_1, H_2 and signal-to-noise (S/N) statistics defined in section 3.3.2 are shown in Table 4.4.

Screening of the original 497 flow gauges to the final 371 had negligible effect on the S/N ratio and H_1 but reduced the H_2 and H_3 statistics by half: from 30.5 to 15.4. When spatial screening was used to remove 22 sites from 393, the number of discordant sites was also reduced by 5. The resulting screened data set is therefore less heterogeneous and contains only 5% or 19 discordant sites – 14 if each region is considered separately. This is close to the 3% of discordant sites which can be expected due to random variations in large data sets (Hosking, 1996).

Table 4.4: Test L-Statistics for Homogeneous Region Candidates

Region ID	No. of Sites	No. Sites with D>3	S/N for L-CV	H_1	H_2	H_3
ALL	497	21	88.6%	54.7	30.5	16.3
ALL	393	24	89.2%	55.3	16.6	6.0
ALL	371	19	89.2%	55.0	15.4	5.2
1	24	1	40.2%	1.98	-0.37	-0.44
2	9	0	n.a.	2.42	0.62	0.52
3	7	0	n.a.	2.82	1.28	0.61
4	24	1	39.2%	1.85	-1.18	-1.77
5	18	0	30.7%	1.19	-1.05	-1.67
6	54	3	**59.3%**	**5.56**	0.05	-0.81
7	66	3	45.0%	**3.89**	1.58	1.51
8	16	0	**65.5%**	**3.80**	1.90	1.74
9	25	1	-0.7%	-0.03	-0.71	-0.91
10	8	0	n.a.	-0.53	-0.38	-0.09
11	22	1	35.0%	1.57	0.89	0.52
12	18	1	**75.4%**	**5.94**	**3.40**	1.35
13	2	0	n.a.	-0.69	-1.03	-1.07
14 *	30	2	9.0%	0.31	0.28	0.01
15	27	1	**78.1%**	**7.68**	1.59	0.56
16	11	0	**71.7%**	**3.97**	**2.75**	**2.02**
NE Man.	12	0	-0.7%	-0.03	-0.16	-0.53

* Includes the two sites from region 13 (SW New-Brunswick).

For most homogeneous region candidates, the S/N ratio is less than half that for the overall set of 371 sites. This indicates that a large proportion of the signal (i.e.: the explainable component of initial variability) can be explained using a set of step-wise increments in the average values within each homogeneous region. Peninsular and island provinces, which have not been subdivided, retain their high S/N ratio and so does region 12 for which data is missing due to its location at the edge of the study area. Neighbouring regions 6 and 8 still have moderate S/N values, indicating that further subdivision(s) may explain a greater proportion of the observed variability.

Similarly to the S/N ratio, values of the H statistics are reduced by an order of magnitude by the delineation of homogeneous regions. Regions 15, 16 and 12 once again retain high values, indicating that they should be considered to be heterogeneous and should perhaps be further subdivided. Regions 6 and 8 once again appear to remain "definitely heterogeneous" in L-CV (i.e.: $H_1 > 3$), as does region 7. The L-moment test statistics suggest that these should be re-examined. Regions 9, 10 and 14

are "probably homogeneous" in L-CV (i.e.: $H_1 < 1$) while remaining regions are "possibly homogeneous" in L-CV.

Note that while the lowest possible value of the H statistics are desirable, pragmatic objectives may partially overrule this criterion during adjustments to the region boundaries. For example, region 3 could be enlarged so as to become a single contiguous area even if the resulting region is "more heterogeneous".

4.6 Random Field Modelling for L-CV

Figures 4.10 a and b show the OK estimates of L-CV throughout the study area.

Spatial Association between L-CV and Support Variables

In previous sections, it has been shown that L-CV exhibits a significant degree of systematic spatial continuity. This is in contrast to L-skew which is nearly random and L-mean/DA whose variation is so gradual as to be largely explainable by regression against latitude and longitude. For this reason, the estimation of L-CV in a spatially-explicit manner seems likely to yield improved estimates.

To improve the ordinary kriging estimates of L-CV would require the use of support variables, ideally sampled more frequently than L-CV (especially where L-CV itself is sparsely sampled). A clear association between candidate support variable(s) and L-CV are also required for co-kriging. A summary exploration of such associations was therefore conducted using the GIS.

Spatial associations between L-CV and support variables were investigated based on the EDA (section 4.2). Table 4.5 shows the results of the map associations between L-CV and several other variables while Table 4.6 shows the associations with average monthly snow precipitation alone.

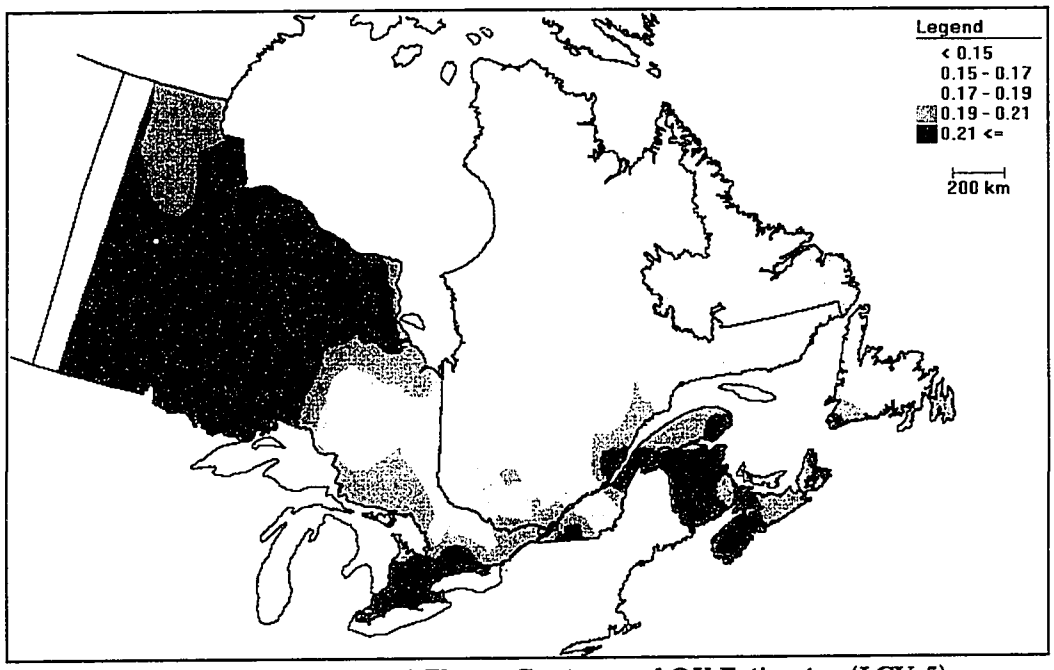

Figure 4.10a: L-CV of AM Flood Flow – Contours of OK Estimates (LCV-5)

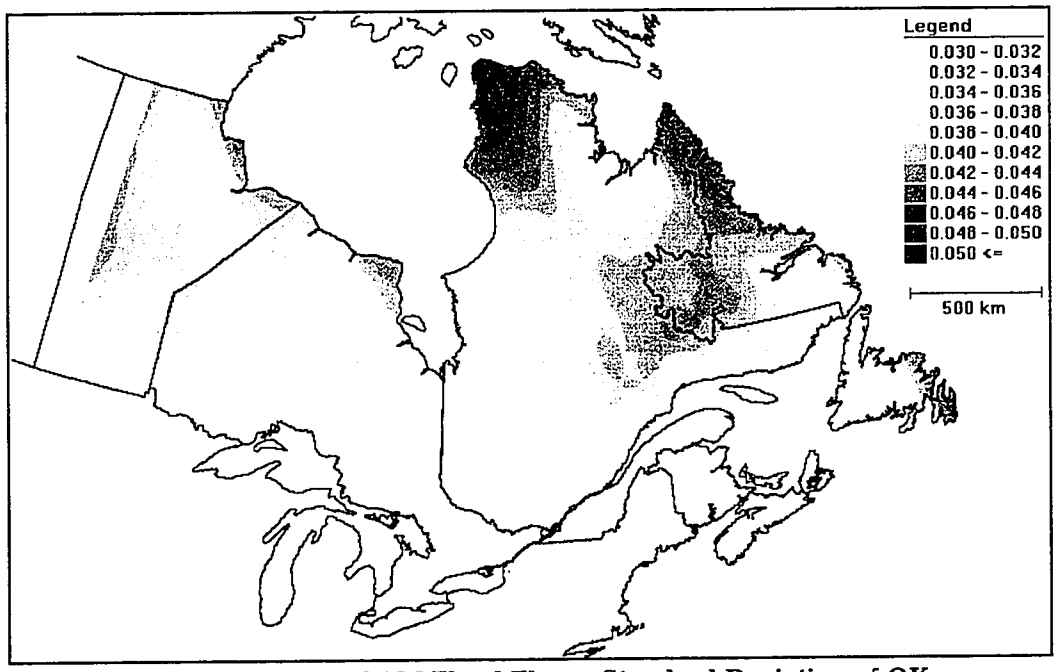

Figure 4.10b: L-CV of AM Flood Flow – Standard Deviation of OK Estimates (LCV-12S)

The gradual and slightly anisotropic spatial variation of the errors indicates precise estimation results. The resulting uncertainty is almost constant except in N Quebec due to sparse coverage.

Table 4.5: Map Associations between L-CV and Candidate Support Variables

Map Variable	Contingency Coefficient	Cramer's V	Comments
Flood Flow and Timing			
L-mean_T	0.6169	0.2363	
L-CV_T	0.6599	0.2648	
L-mean/DA	0.6927	0.3037	Second largest
L-skew	0.6760	0.2766	
Meteorologic and Physiographic Variables			
ANNMAXT	0.5734	0.2333	
ANNMEAN			
ANNMINT	0.5418	0.1943	
ANNPCPN	0.5749	0.2222	
ANNRAIN	0.5266	0.2341	
ANNSNOW	0.6977	0.3246	Largest. Better than monthly
DIST	0.4435	0.1492	Insignificant
VEG	0.5608	0.3029	Third largest
Monthly Snow Precipitation			
SNOW-NOV	0.6367	0.2611	
SNOW-DEC	0.6600	0.2778	Maximum monthly
SNOW-JAN	0.6298	0.2564	
SNOW-FEB	0.6138	0.2459	
SNOW-MAR	0.5949	0.2341	
SNOW-APR	0.5629	0.2154	

Other than the expected indication of a proportional effect between L-CV and L-Mean/DA, significant associations with the VEG and P-snow variables confirms that these variables might serve to support the estimation of L-CV (Cramer's V values greater than 0.3). Due to the weak dependence between the primary and support variables, it was decided to put-off further inquiry at this time.

4.7 Proposed Methodology for Flood Frequency Analysis

In order to account for the spatial autocorrelation and associations between flood parameters, a spatially-explicit flood frequency analysis methodology, as investigated in the present study, is proposed for future work. It relies heavily on an exploratory data analysis (EDA) or "data driven" approach and combines has the potential to unify existing regional flood frequency analysis approaches at a fundamental level. It is analogous to the Box-Jenkins time series analysis procedures, but with the application of geostatistical techniques to manage the spatial dimension (see Table 4.6).

The proposed methodology can be outlined as follows:

1) Define the study area's spatial and temporal limits and assemble the available data.

2) Evaluate diagnostic statistics for the entire study area.

   a) Size and shape measures (morphology)
   b) Univariate statistics and bivariate associations between map variables.
   c) L-moment S/N, D, H_1, H_2, H_3 test statistics.
   d) Spatial contrast (SC) measure with neighbouring areas, if possible.

3) Delineate homogeneous regions without using flow variables.

   ...group sites with similar:
   a) Physiography including land-use, soils and vegetation.
   b) Drainage based on continental divides, second and third-order basins.
   c) Meteorology including temperature and precipitation (rain and snow).
   d) Flood-generating mechanism "populations" such as MMI, flood timing, known ice effects, etc...
   e) Previous investigations by others.

   ...and screen-out individual sites using:
   f) L-moment D test statistic
   g) Data postings and visual inspection of MMI, flood timing.

4) Evaluate diagnostic statistics for each region

   a) Size and shape measures (morphology)
   b) Univariate statistics and bivariate associations between map variables.
   c) L-moment S/N, D, H_1, H_2, H_3 test statistics.
   d) Spatial contrast (SC) measure with neighbouring areas, if possible.

5) Examine S/N and SC measures for adjacent regions and redefine their shared boundaries accordingly:

   a) Gradual SC changes in slope without discontinuity at the boundary: consider spatially-explicit estimation techniques such as kriging.
   b) Gradual SC changes in slope with discontinuity at the boundary: consider growing or shrinking bordering regions.
   c) Discontinuous or "noisy" SC with or without discontinuity at the boundary: SC measure is non-informative for this regional boundary.

   ...if case b) occurs, repeat steps 3 to 5 until the smallest possible values of H statistics are attained while preserving reasonable SC properties for the regions.

Ideally, regions should be spatially contiguous and respect second-order drainage divides wherever possible. An examination of fourth-order drainage divides may be necessary in densely-sampled areas such as New Brunswick or SW Ontario.

Table 4.6: Issues Arising from Spatially-Explicit Modelling Methodology

	SELECT SAMPLE	CHARACTERIZE DATA			SELECT MODEL	USE MODEL
		Intensive Properties	Extensive Properties	Map Generation		
Regional FFA	• Study area covers area where flood estimates required.	• Flood timing. • PDF shapes. • L-moments & ratios. • Antecedent temp. and precipitation (API & ATI), MAP. • Watershed shape, elevation & physiography.	6) Define homogeneous regions: contiguous coverage. 7) Flood parameters regressed within each region based on signal to noise ratio.	• Minimal.	• Nonparametric method uses no model. • Parametric Z stat. for goodness of fit. • Mixed populations handled by bimodal pdf or classified to sub-populations.	• Estimate prob. distribution parameters using L-moments. • Estimate T-year floods.
Error Handling	• Test flow gauges' discordance and heterogeneity with D and H stats.	• Assess temporal coverage. • Simulation studies.	• Regional vs entire study area's SEE. • Simulated Kappa-distributed regions.			• Evaluation of SEE.
GIS Study	• Geographic region used as study area. • Specify spheroid, projection and extent of study area. • Register & geocode source maps. • Add non-spatial attribute data.	• As above.	• Variogram describes spatial autocorrelation of each variable determined. • Spatial trends noted. • Gauge & watershed topology (adjacency, containment). • Distances to features by buffering.	• As above, plus: • Each variable is transformed to an evidence map. • Spatial trends noted. • Variables represented as random fields or as average polygon values.	• As above, plus: • Kriging model for flood parameters (L-moments). • Co-kriging of L-ratios using support variables. • Crisp or fuzzy logical overlay models for L-mean.	• Flood parameters at a location used to fit a probability distribution. • Estimate T-year floods.
Error Handling	• As above.	• As above.	• Assess accuracy of continuous spatial coverages.	• Estimation error or variance is mapped.		• Evaluation of SEE. • Geostatistical simulation studies.

Chapter 5

GENERAL CONCLUSIONS AND RECOMMENDATIONS

General Conclusions

The following conclusions follow from the results of this study:

1. Previous regional FFA studies seldom considered the spatial dimension of the problem in detail (see Table 2.1). This study shows that EDA using nonparametric, L-moment and spatial visualization (GIS) methods helps to screen and to identify multiple populations in the data. The advantages of a spatially-explicit regional FFA methodology demonstrated herein are given in section 4.7 and in Table 4.6.

2. The use of normalised nonparametric pdf plots combined with maps of the new multimodality index (MMI) summarizing the number of significant populations revealed by these pdf aids in homogeneous region delineation. The index can be used to differentiate between UM, HT and MM data.

3. The direct mapping of floods' Julian flood date and of flood timing variability demonstrated in this study is superior to both tabular presentation showing monthly or seasonal flood frequencies and to circular statistics presently in vogue. This is because maps are more direct and intuitive data representations which can be related to other variables in a spatially-explicit and rigorous statistical framework.

4. The measures of spatial contrast developed herein, when combined with L-moment tests for regions, are useful in diagnosing and resizing homogeneous regions. This provides an objective methodology for re-shaping regions to achieve smaller values of the H test L-statistics, enabling investigators to respect the homogeneity assumption more closely. The proposed methodology allows step-wise refinements to heterogeneous regions while preserving those which are found acceptable.

5. It was hypothesized and verified that a spatially-explicit model using kriging or co-kriging methods might improve the estimates of the flood parameter, L-CV, compared with either at-site estimates or homogeneous region averages or relationships. Three possible variables were identified based on spatial associations measured with the GIS: annual snow precipitation (P-snow), at-site normalised mean (L-mean/DA) and vegetation (VEG).

6. The methodology for spatially-explicit (regional) flood frequency analysis developed and applied in this thesis results in an improved understanding of the flood-generating phenomena and, consequently, in a potential for improved regionalization. A key advantage is the built-in check for multimodal probability distribution function and flood timing variance.

Recommendations

1. The hierarchical, spatially-explicit flood frequency analysis advocated and tested in this study should be used in the future. Initial guidelines for the revised methodology has been provided in section 4.7 of this thesis. Regional average values of spatially-noisy L-skew can be estimated for homogeneous regions while L-CV and possibly L-mean/DA can be estimated in a spatially-continuous manner using kriging and co-kriging (either within regions or for the entire study area).

2. In future studies, geostatistical techniques for the simulation of random fields should be used to reproduce the full range of parameter values observed in the data since OK tends to smooth-out extreme values. Simulations should also be conducted to test the statistical properties of possible spatial models: whether for homogeneous region polygons or for spatially-continuous random fields representing L-CV.

3. This study' focus on the geographic and climatic causes of floods reinforces the findings of recent flood frequency studies. Future work should consider flood-generating mechanisms explicitly, perhaps using classified frequency analysis, combined with spatially-continuous models capable of relating flood parameters to climactic variables. Due to the growing importance of simulation, each parameter, input and output of the models should be amenable to it.

4. Nonparametric PDF can be classified as UM, HT or MM using Julian flood dates, NMODE and MMI. A temporal MMI could also be calculated and used for such determinations. Simulation studies would be required to determine specific values of MMI for which a PDF can be considered as being the result of a single population or flood-generating mechanism (UM, two or more populations (MM) or a mixture of a primary and a secondary flood-generating mechanism (HT). This may be accomplished by future investigators.

5. HT sites are common in Canada due to the overlapping areas of influence of the many possible causes of floods which include rainfall, snowmelt, ice break-up and large thunderstorms or dying hurricanes. Maps showing such areas of influence may prove useful for the delineation of homogeneous flood regions. These could be prepared by (or on behalf of) Environment Canada.

6. For each flood-generating mechanism, additional variables could be used in future studies to support the estimation of the L-skew, L-CV and L-mean parameters. For example, the L-skew of different types of rainfall can be used to support the estimation of L-skew for rainfall-generated floods (Rossi and Villani, 1994b); and the snow, L-mean and vegetation maps can help to estimate L-CV for snowmelt-generated floods. This process is analogous to multiple regression modelling.

7. The application of numerical simulation and co-kriging techniques to the inverse problem in flood frequency analysis should be considered: given the required accuracy for flood parameters, which locations and record lengths are optimal? The results could guide the rationalization of the hydrometric network by identifying areas where increased gauge densities and record lengths are most desirable. This is an ongoing problem for the Water Survey of Canada due to recent budget cuts.

Chapter 6

BIBLIOGRAPHY

[1] Adamowski, K. (1985): "**Nonparametric Kernel Estimation of Flood Frequencies**", Dept. of Civ. Eng., University of Ottawa, Water Resources Research, **21**(11), pp. 1585-1590.

[2] Adamowski, K. and Feluch, W. (1990): "**Nonparametric Flood Frequency with Historical Information**", J. Hydraulic Engineering, **116**(8), pp. 1035-1047.

[3] Agterberg, F.P. (1992): "**Estimating the Probability of Occurrence of Mineral Deposits from Multiple Map Patterns**", Geological Survey of Canada, in: "Use of Microcomputers in Geology", Ed. D.F. Merriam, Plenum Press, N.Y.

[4] Alila, Y. (1987): "**Nonparametric Flood Frequency Analysis with Historic Information and Hydroclimatically Defined Mixed Distributions**", M.A.Sc. Thesis, University of Ottawa, 140 pp.

[5] Alila, Y. (1993): "**A Regional Rainfall Distribution for Canada**", Ph.D. Thesis, University of Ottawa, 160 pp.

[6] Alila, Y., Adamowski, K., Pilon, P.J. and Kowalchuck, M.Z. (1993): "**A Regional Approach in the Identification, Estimation and Hypothesis Testing of Probability Distributions of Annual Maximum Flows**", Dept. Civ. Eng., University of Ottawa and Env. Canada, Proc. Waterloo Int. Hydrology Conf. in memory of T. Unny, Canada.

[7] Anselin, L. and Getis, A. (1993): "**Spatial Statistical Analysis and GIS**", Dept. of Geography, University of California, Proc. "GIS, Spatial Modelling and Policy Evaluation", pp. 35-49.

[8] Aronoff, S. (1989): "**Geographic Information Systems: A Management Perspective**", WDL Press, Ottawa, 294 pp.

[9] Ashkar, F. and Ouarda, T.B.M.J. (1996):"**On Some Methods of Fitting the Generalized Pareto Distribution**", Dept. of Mathematics, University of Moncton, J. Hydrology, **177**(1), 117-141.

[10] Bardsley, W.E. (1989): "**A Simple Parameter-Free Flood Magnitude Estimator**", Dept. of Earth Sciences, University of Waikato, Hydrological Sciences Journal, 34(2), pp. 129-137.

[11] Bayliss, A.C. and Jones, R.C. (1993): "**Peaks-Over-Threshold Flood Database – Summary Statistics and Seasonality**", Inst. of Hydraulics, Wallingford, Report No. 121.

[12] Beller, A. (1991): "**Spatial/Temporal Events in a GIS**", IBM Federal Sector Div., Proc. GIS/LIS '91, Vol. 2, pp. 766-775.

[13] Bobée, B., Cavadias, G., Ashkar, F., Bernier, J., Rasmussen, P. (1993): "**Towards a Systematic Approach to Comparing Distributions used in Flood Frequency Analysis**", J. Hydrology, **142**(1), pp. 121-136.

[14] Bobée B., Mathier L., Perron H., Trudel P., Rasmussen P.F., Cavadias G., Bernier J., Nguyen V.T.V., Pandey G., Ashkar F., Ouarda T.B.M.J., Adamowski K., Alila Y., Daviau J.L., Gingras D., Liang GC., Rousselle J., Birikundavyi S., Ribeirocorrea J., Roy R., Pilon PJ. (1996a): "**Presentation and Review of Some Methods for Regional Flood Frequency Analysis**", J. Hydrology, **186**(1), pp. 63-84.

[15] Bobée B., Mathier L., Perron H., Trudel P., Rasmussen P.F., Cavadias G., Bernier J., Nguyen V.T.V., Pandey G., Ashkar F., Ouarda T.B.M.J., Adamowski K., Alila Y., Daviau J.L., Gingras D., Liang GC., Rousselle J., Birikundavyi S., Ribeirocorrea J., Roy R., Pilon PJ. (1996b): "**Inter-Comparison of Regional Flood Frequency Procedures for Canadian Rivers**", J. Hydrology, **186**(1), pp. 85-103.

[16] Bonham-Carter, G. (1994): "**GIS for Geoscientists – Modelling with GIS**", Geological Dept., University of Ottawa, Pergamon Press, 415 pp.

[17] Brunsdon, C. (1995): "**Estimating Probability Surfaces for Geographical Point Data - An Adaptive Kernel Algorithm**", University of Newcastle upon Tyne, Computers & Geosciences, **21**(7), pp. 877-894.

[18] Burn, D.H.; Zrinji, Z.; Kowalchuck, M. (1997): "**Regionalization of Catchments for Regional Flood Frequency Analysis**", University of Manitoba, J. of Hydrologic Eng., **2**(2), pp. 76-82.

[19] Changnon D. (1996): "**Changing Temporal and Spatial Characteristics of Midwestern Hydrologic Droughts**", Dept. Geography, University of Illinois, Physical Geography, **17**(1), pp. 29-46.

[20] Chow, K.C. and Watt, W.E. (1990): "**Knowledge-Based Expert System for Flood Frequency Analysis**", Can. J. Civ. Eng., **17**(4), pp. 597-609.

[21] Cressie, N. (1993): "**Geostatistics: A Tool for Environmental Modelers**", Environmental Modeling with GIS, Ed. M.F. Goodchild, Ch. 41, pp. 414-421.

[22] Cromer, M V. (1996): "**Geostatistics for Environmental and Geotechnical Applications: A Technology Transferred**", ASTM Special Technical Publication No. 1283, pp. 3-12.

[23] Daniell, T.M. (1991): "**Neural Networks. Applications in Hydrology and Water Resources Engineering**", Proc. Challenges for Sustainable Development, **3**(91), pp. 797-802.

[24] Daviau, J.L., Gingras, D., Adamowski, K. (1994): "**Regional Analysis of Annual Maximum (AM) and of Partial Duration Series (PD) [Flood] Data by L-Moments**", Proc. AQTE, Montréal, pp. 514-519.

[25] de Marsily, G. and Delhomme, J.P. (1989): "**Geostatistics: From Mining to Hydrology**", Université de Paris IV, Proc. Natl. Conf. Hydraulic Eng., ASCE, pp. 659-666.

[26] Desbarats, A J. (1996): "**Modeling Spatial Variability using Geostatistical Simulation**", Geological Survey of Canada, ASTM Special Technical Publication No. 1283, pp. 32-48.

[27] Deutsch, C.V. and Journel, A.G. (1992): "**GSLIB – Geostatistical Software Library and User's Guide**", Oxford University Press, Toronto, 340 pp.

[28] Fill, H.D. and Stedinger, J.R. (1995): "**L-Moment and Probability Plot Correlation Coefficient Goodness-of-Fit Tests for the Gumbel Distribution and Impact of Autocorrelation**", Cornell University, Water Resources Research, **31**(1), pp. 225-229.

[29] Fortin V., Bernier J., Bobée B. (1997): "**Simulation, Bayes, and Bootstrap in Statistical Hydrology**", Water Resources Research, **33**(3), pp. 439-448.

[30] Garcia-Martino, A.R., Scatena, F.N., Warner, G.S. and Civco, D.L. (1996): "**Statistical Low Flow Estimation using GIS Analysis in Humid Montane Regions in Puerto Rico**", Water Resources Bulletin, **32**(6), pp. 1259-1271.

[31] Gingras, D. (1993): "**Regional Flood Frequency Analysis by Nonparametric Methods**", Ph.D. Thesis, University of Ottawa, 150 pp.

[32] Gingras, D. and Adamowski, K. (1992): "**Coupling of Nonparametric Frequency and L-Moment Analyses for Mixed Distribution Identification**", Water Resources Bull., **28**(2), pp. 263-272.

[33] Gingras, D. and Adamowski, K. (1993): "**Homogeneous Region Delineation based on Annual Flood Generation Mechanisms**", Hydrological Sci. J., **38**(2), 103-121.

[34] Gingras, D. and Adamowski, K. (1995): "**Impact of El Niño Southern Oscillation (ENSO) on Central Canadian Floods and Droughts**", Can. J. Civ. Eng., **22**, pp. 834-837.

[35] Gotway, C.A. (1991): "**Fitting Semivariogram Models by Weighted Least Squares**", Computers & Geosciences, **17**(1), pp. 171-172.

[36] Hosking, J.R.M. (1988): "**The 4-Parameter Kappa Distribution**", IBM Research Division, T.J. Watson Research Center, 17 pp.

[37] Hosking, J.R.M. (1989): "**L-moments: Analysis and Estimation of Distributions using Linear Combinations of Order Statistics**", IBM T.J. Watson Research Center, J. of the Royal Statistical Society, **51**(3).

[38] Hosking, J.R.M., Wallis, J.R. (1993): "**Some Statistics Useful in Regional Frequency Analysis**", IBM Research Division, Water Resources Research, **29**(2), pp. 271-281. See also 1995 correction in **31**(1), p. 251.

[39] Hosking, J.R.M., Wallis, J.R. (1995): "**A Comparison of Unbiased and Plotting-Position Estimators for L-Moments**", IBM Research Division, Water Resources Research, **31**(8), pp. 2019-2025.

[40] Hosking, J.R.M., Wallis, J.R. (1996): "**Regional Frequency Analysis of Floods in Central Appalachia**", IBM Research Report RC 2034.

[41] Hunter, G.J. and Goodchild, M.F. (1995): "**Dealing with Error in Spatial Databases - a Simple Case Study**", University of Melbourne, Photogrammetric Engineering & Remote Sensing, **61**(5), pp. 529-537.

[42] Isaaks, E.H. and Srivastava, R.M. (1989): "**An Introduction to Applied Geostatistics**", Oxford University Press Inc., Toronto, 561 pp.

[43] Jian, X.D., Olea, R.A. and Yu, Y.S. (1996): "**Semivariogram Modeling by Weighted Least Squares**", USGS, Computers & Geosciences, **22**(4), pp. 387-397.

[44] Journel, A G. (1986): "**Constrained Interpolation and Soft Kriging**", Stanford University, Proc. 19th Appl. of Computers and Operations Research in the Mineral Industry, pp. 15-30.

[45] Journel, A.G. (1996): "**Modelling Uncertainty and Spatial Dependence - Stochastic Imaging**", Stanford University, Int. J. of Geographical Information Systems, **10**(5), pp. 517-522.

[46] Kaden, S.O. (1993): "**GIS in Water-Related Environmental Planning and Management: Problems and Solutions**", Proc. HydroGIS'93, IAHS Publ. No. 211, pp. 385-397.

[47] Karim, M.A. and Chowdhury J.U. (1995): "**A Comparison of Four Distributions Used in Flood Frequency Analysis in Bangladesh**", Bangladesh University, Hydrological Sciences J., **40**(1), pp. 55-66.

[48] Kemp, K.K. (1993): "**Environmental Modelling and GIS: Dealing with Spatial Continuity**", University of California, Proc. HydroGIS '93, IAHS Publ. No. 211, pp. 107-115.

[49] Kite, J. (1977): "**Frequency and Risk Analysis in Hydrology**", Water Resources Publications, USA, 224 pp.

[50] Klemeš, V. (1993): "**Probability of Extreme Hydrometeorological Events – A Different Approach**", Proc. Extreme Hydrological Events: Precipitation, Floods and Droughts, Yokohama, IAHS publ. No. 213, pp. 167-176.

[51] Knapp, P.A. (1997): "**Spatial Characteristics of Regional Wildfire Frequencies in Intermountain West Grass-Dominated Communities**", Georgia State University, Prof. Geographer, 49(1), pp. 39-51.

[52] Kuczera, G. (1983): "**Effect of Sampling Uncertainty and Spatial Correlation on an Empirical Bayes Procedure for Combining Site and Regional Information**", Dept. Civ. Eng., University of Newcastle, J. Hydrology, **65**, pp. 373-398.

[53] Kuczera, G. (1996): "**Correlated Rating Curve Error in Flood Frequency Inference**", Dept. Civ. Eng., University of Newcastle, Water Resources Research, **32**(7), pp. 2119-2127.

[54] Liang, G.C., Gingras, D. and Adamowski, K. (1994): "**Regional Analysis of Annual Maximum (AM) and of Partial Duration (PD) Flood Series by Nonparametric Methods**", Proc. AQTE, Montréal, pp. 520-527.

[55] Magilligan, and Graber, (1997): "**Hydroclimatological and Geomorphic Controls on the Timing and Spatial Variability of Floods in New England**", Dept. Geography, Dartmouth College, J. Hydrology, 178(1), pp. 159-180.

[56] Maidment, D.R. *Ed.* (1993): "**Handbook of Hydrology**", McGraw-Hill Inc., Toronto, approx. 1000 pp.

[57] Mcdonnell, R.A. (1996): "**Including the Spatial Dimension - Using GIS in Hydrology**", Oxford University, Progress in Physical Geography, **20**(2), pp. 159-177.

[58] Mitasova, H., Mitas, L., Brown, W.M., Gerdes, D.P., Kosinovsky, I. and Baker, T. (1995): "**Modelling Spatially and Temporally Distributed Phenomena - New Methods and Tools for GRASS GIS**", Int. J. of Geographic Information Systems, **9**(4), pp. 433-446.

[59] National Research Council (NRC), (1988): "**Estimating Probabilities of Extreme Floods, Methods and Recommended Research**", Committee on Techniques for Estimating Probabilities of Extreme Floods, National Academy Press, Washington, D.C.

[60] Nebert, D.D. (1994): "**Interpreting the ASTM "Content Standard for Digital Geospatial Metadata**", ASTM Special Technical Publication No. 1279, pp. 127-130.

[61] Önöz, B. and Bayazit, M. (1995): "**Best-Fit Distributions of Largest Available Flood Samples**", Dept. Civ. Eng., Istanbul Tech. University, J. Hydrology, **167**, pp. 195-208.

[62] Ouarda, T.B.M.J., Ashkar, F. (1995): "**Bootstrap-Based Intercomparison of Regional Flood Estimation Procedures**", Proc. Int. Conf. on Hydropower – ASCE, volume 3, pp. 2466-2475.

[63] Pannatier, Y. (1992): "**Variowin version 2.2 – Software for Spatial Data Analysis in 2D**", University of Lausanne, Springer-Verlag, 104 pp.

[64] Pilon, P.J., Adamowski, K. and Alila, Y. (1991a): "**Regional Analysis of Annual Maxima Precipitation using L Moments**", Water Res. Branch, Env. Canada and Civ. Eng. Dept., University of Ottawa, Atmospheric Research, **27**, pp. 81-92.

[65] Pilon, P.J.; Alila, Y. and Adamowski, K. (1991b): "**Assessment of Risk of Flooding based on Regional Information**", Presented at the NATO ASI (Advanced Study Institute) on Risk and Reliability in Water Resources and Environmental Engineering, 18-28 May, Porto Carras, Greece.

[66] Pilon, P.J. and Adamowski, K. (1992): "**The Value of Regional Information to Flood Frequency Analysis using the Method of L-moments**", Water Res. Branch, Env. Canada and Dept. of Civ. Eng., University of Ottawa, Can. J. Civ. Eng., **19**, 137-147.

[67] Pilon, P.J. and Adamowski, K. (1993): "**Asymptotic Variance of Flood Quantile in Log Pearson Type III Distribution with Historical Information**", Water Res. Branch, Env. Canada and Dept. of Civ. Eng., University of Ottawa, J. Hydrology, **143**(3), 481-503.

[68] Pilon, P.J. and Harvey, D.K. (1994): "**Consolidated Frequency Analysis (CFA) – Version 3.1 Reference Manual**", Environment Canada, approx. 100 pp.

[69] Pitlick J. (1994): "**Relation between Peak Flows, Precipitation, and Physiography for Five Mountainous Regions in the Western USA**", University of Colorado, J. Hydrology, **158**(3), pp. 219-240.

[70] Rao, A.R., Hamed, K.H. (1994): "**Frequency Analysis of Upper Cauvery Flood Data by L-moments**", Water Res. Management, **8**(3), pp. 183-201.

[71] Ribeiro-Correa, J. and Rousselle, J. (1996): "**Robust Simple Scaling Analysis of Flood Peaks Series**", Can. J. Civ. Eng., **23**(6), pp. 1139-1145.

[72] Rossi, G. (1994): "**Historical Development of Flood Analysis Methods**", University of Catania, Proc. Coping with Floods, Ed. G. Rossi *et al.*, Kluwer Academic Publishers, pp. 11-34.

[73] Rossi, F., and Villani, P. (1994a): "**Regional Flood Estimation Methods**", University of Salerno, Proc. Coping with Floods, Ed. G. Rossi *et al.*, Kluwer Academic Publishers, pp. 135-169.

[74] Rossi, F., and Villani, P. (1994b): "**A Project for Regional Analysis of Floods in Italy**", University of Salerno, Proc. Coping with Floods, Ed. G. Rossi *et al.*, Kluwer Academic Publishers, pp. 193-217.

[75] Rouhani, S. (1996): "**Geostatistical Estimation: Kriging**", Georgia Inst. of Technology, ASTM Special Technical Publication No. 1283, pp. 20-31.

[76] Sangall, and Kallio, (1977): "**Magnitude and Frequency of Floods in Southern Ontario**", Technical Bulletin Series No. 99, Inland Waters Directorate, Fisheries and Environment Canada.

[77] Schultz, G.A. (1993): "**Application of GIS and Remote Sensing in Hydrology**", Proc. HydroGIS'93, IAHS Publ. No. 211, pp. 127-140.

[78] Silverman, B.W. (1986): "**Density Estimation for Statistics and Data Analysis**", School of Mathematics, University of Bath, Chapman and Hall Ltd.

[79] Singh, K.P. (1987): "**Development of a Versatile Flood Frequency Methodology and its Application to Flood Series from Different Countries**", in: "Hydrologic Frequency Modelling", V.P. Singh (ed.), D. Reidel Publishing Company, pp. 183-197.

[80] Srivastava, R M. (1996): "**Describing Spatial Variability using Geostatistical Analysis**", ASTM Special Technical Publication No. 1283, pp. 13-19.

[81] Streit, U. and Kleeberg, H. (1996): "**GIS-Based Regionalization in Hydrology: German Priority Programme on Spatial Transfer of Hydrological Information**",

University of Muenster, Proc. "Application of GIS in Hydrology and Water Res. Mgt.", IAHS Publ. No. 235, pp. 485-491.

[82] Tung, Y.K. and Mays, L.W. (1981): "**Reducing Hydrologic Parameter Uncertainty**", J. of the Water Res. Planning and Mgt. Div., ASCE, **107**, pp. 245-262.

[83] Turcotte, D.L. (1994): "**Fractal Theory and the Estimation of Extreme Floods**", Geological Dept., Cornell University, J. of Res. of the Int. Inst. on Standards & Technology, **99**(4), pp. 377-389.

[84] Veregin, H. (1994): "**Integration of Simulation Modeling and Error Propagation for the Buffer Operation in GIS**", University of Minnesota, Photogrammetric Engineering & Remote Sensing, **60**(4), pp. 427-434.

[85] Veregin, H. (1996): "**Error Propagation through the Buffer Operation for Probability Surfaces**", University of Minnesota, Photogrammetric Engineering & Remote Sensing, **62**(4), pp. 419-428.

[86] Vogel, R.M. and Fennessey, N.M. (1993): "**L-Moment Diagrams Should Replace Product Moment Diagrams**", Dept. Civ. and Env. Eng., Tufts University, Water Resources Research, **29**(6), pp. 1745-1752.

[87] Vogel, R.M., McMahon, T.A. and Chiew, F.H. S. (1993a): "**Flood Flow Frequency Model Selection in Australia**", Tufts University, J. Hydrology, **146**(1), pp. 421-449.

[88] Vogel, R.M., Thomas, W.O. Jr. and McMahon, T.A. (1993b): "**Flood Flow Frequency Model Selection in Southwestern United States**", Tufts University, J. of Water Res. Planning & Management, ASCE, **119**(3), pp. 353-366.

[89] Wallis, J.R. (1988): "**Catastrophes, Computing and Containment: Living with our Restless Habitat**", Speculation in Science and Technology, **11**(4), pp. 295-324.

[90] Wang, Q.J. (1996): "**Direct Sample Estimators of L-Moments**", Civil Eng. Dept., University of Melbourne, Water Resources Research, **32**(12), pp. 3617-3619.

[91] Ward, M.O. and Zheng, J. (1991): "**Visualization of Spatio-Temporal Data Quality**", Worcester Polytechnic Inst., Proc. GIS/LIS '91, Vol. 2, pp. 727-737.

[92] Watt, W.E. *et al.* (1989): "**Hydrology of Floods in Canada – A Guide to Planning and Design**", Associate Committee on Hydrology, National Research Council Canada, Ministry of Supply and Services Press, 245 pp.

[93] Waylen, P.R. and Woo, M.K. (1984): "**Areal Prediction of Annual Floods Generated by Two Distinct Processes**" for Northern Ontario, Hydrological Sciences J., **29**(1), pp. 75-88.

[94] Zrinji, Z. and Burn, D.H. (1996): "**Regional Flood Frequency with Hierarchical Region of Influence**", J. of Water Res. Planning & Mgt., ASCE, **122**(4), pp. 245-252.

APPENDIX A

DATA & STATISTICAL TEST RESULTS

A.1 Introduction

The information used in this study consists of two complementary formats: gauge (point) and map data. Sources for the latter are discussed in Appendix C. This appendix provides a general description of the sources, statistical tests and screening procedures used for the flow and meteorological gauge data.

A.2 Flow Data

The flow data used in this study was obtained from the HYDAT CD-ROM (Environment Canada, 1992). Flows are measured and recorded at a number of gauges by the Water Survey of Canada (WSC) or the Ministère de l'Environnement du Québec. Wherever possible, only flood observations resulting from observations recorded automatically and over the entire water year were used in this thesis. Since instantaneous flow-recording gauges are rare, average daily maximum flows were used herein. These can be related to instantaneous flows using standard techniques.

Water level observations were not used in this thesis – although many gauges' flows are derived from water levels measurements using a hydraulic rating curve. It is acknowledged that such rating curves often do not extend far enough to include the

larger flows considered in FFA, and that alternative FFA procedures have recently been suggested to account for the effect of correlated rating curve error (Klemeš, 1997). Due to the large number of gauges used herein, the effect of rating curves was not investigated.

The sub-continental scale of this study excluded flows on islands such as Newfoundland or P.E.I. and required that an arbitrary western limit be selected. The 99° W longitude, west of Lake Superior, was selected since it provided enough overlap beyond Ontario. Any study beyond this limit would have to consider flows measured in the USA, which were not available.

Nonparametric Tests

Since flow data is the dependent variable in the statistical, geostatistical and GIS models developed and used in this thesis, it has been subjected to numerous statistical tests to ensure that it conforms to the assumptions made by these analytical techniques. The results of these nonparametric tests, performed using the CFA software package (Pilon *et al.*, 1993), have been summarized in Table A1. The complete listing of test statistics and critical values for each test is available for inspection.

Non-Spatial Data Screening Procedures

The reliability of observations at each site was classified based on the following hydrometric criteria (see Table A.1):

CLASS I:

i) Within the geographical extents of the study area: $40 < {}^{\circ}N\ LAT < 63$ and $55 < {}^{\circ}W\ LON < 99$. Drainage area upstream of flow gauge is greater than 10 km^2.
ii) With at least 20 years of observations (as reported by HYDAT).
iii) Based on continuous hourly or daily flow measurements recorded automatically and over the entire water year.
iv) Unaffected by river regulation or by large storages such as lakes or reservoirs.

CLASS II:
As for class I, but:
iii) may be based on manually recorded observations which may be seasonal.
iv) may be affected by regulation (but have 20 or more natural observations prior to regulation).

CLASS III:
As for class II, but
iii) may be based on manually recorded observations at miscellaneous intervals.
iv) may be significantly affected by watershed storage (lake effect).

Stations are sorted by class (I to III) and assigned a star rating: one star (*) if the gauge failed at least one test at the 5% level of significance and two stars (**) if the gauge failed at least one test at the 1% level of significance. It is interesting to note that roughly 18% of all gauges get a single star rating while 24%, 39% and 29% get two stars for classes I, II and II, respectively. Based on the foregoing, each flow gauge is assigned to one of the following three groups:

GROUP A: Data is reliable and can be used by all analytical methods.
GROUP B: Data is reliable but of lower quality – to be used to augment coverage.
GROUP C: Data may be unreliable and should be used with caution.

Group B sites may have from 16 to 20 years of data (accounting for missing AM flood observations). Of the 33 class I sites with 16 to 20 years of observations, 15 are the only available results for their respective third-order basins. These and other group B sites will be used to augment spatial coverage for the L-CV geostatistic.

Of the 55 group C gauges, 27 represent the only available flood information for a third-order basin – with most located in sparsely-covered northern areas. Following closer inspection, 18 of these sites were upgraded to group B (these are shown in bold face in Table A.1). Many such sites had multimodal PDF or high outliers which, once identified, allowed the flood record to pass the diagnostic tests at the 5% significance level.

Of the 434 sites reported by HYDAT to have 20 years of data, 212 have been classified as group A, 185 as group B and 37 as group C. Due to the presence of multiple gauges in some basins, 147 third-order watersheds have one or more group A gauge, 125 have at least a group B gauge while 28 only have a group C gauge. Consequently, 272 watersheds have at least a single group B gauge (there are 434 watersheds in the entire study area).

The 179 gauges used in an earlier NSERC study form a subset of the present dataset, as shown in Table A.1 (Bobée *et al.*, 1996a). While most are class I, 13 are class II (due to seasonal or manual observations) and 10 are class III (due to their location at the outlet of lakes). Thirty (30) of the 179 sites got a single star rating and 11 got two stars. These were included in the previous NSERC study after a general discussion of additional diagnostic plots and of their hydrometric history. They will also be used herein.

Spatial Screening Techniques

After initial screening, the resulting data set consists of 393 gauges. From the Figure A2 shows a diagnostic posting of the extreme 5% values of MMI for two categories of data with observations above or below NY = 20. With the exception of the Toronto area, the map shows that both low and high extremes are evenly distributed throughout the study area. This is confirmed by the accompanying exhaustive posting of data values (for which more detailed views of S Ontario and the maritimes are also provided). Local patterns in the variable vary gradually and appear normal.

This graphical diagnostic procedure was repeated for each of the variables considered in this study. It was found that 22 more sites were problematic due to tight local clustering and/or contradictions with local neighbours – these sites were removed from consideration. Histograms for the principal variables are shown in Figure A1. It appears that many variables are approximately normally-distributed, a useful property for geostatistical estimation techniques.

A.3 Physiographic Data

As a result of the NSERC study, physiographic information was compiled for 189 third-order watershed in Ontario and Quebec (Bobée *et al.*, 1996a). This information has been extracted and is available for inspection, however it was not used due to time limitations and to its sparse spatial coverage of the large study area. More exhaustive information would be required to support spatial analysis. The physiographic variables are as follows:

LAKES	Area covered by lakes and marshes upstream of the flow gauge.
STORAGE	Area affected by significant storage within the basin.
FORESTS	Area covered by forests upstream of the flow gauge.
ELEVATION	Average elevation of watershed tributary to the gauge.
LENGTH	Length of the main channel.
AOVERL	Area divided by length – a measure of watershed elongation.
AZIMUTH	Average angle (from due north) faced by the watershed slopes.
BASIN_S	Average basin slope.
STREAM_S	Average slope of the principal channel.

A.4 Meteorological Data

As a result of the NSERC study, meteorologic information was compiled for 189 third-order watershed in Ontario and Quebec (Bobée *et al.*, 1996a). This information has been extracted and is available for inspection, however it was not used due to time limitations and to its sparse spatial coverage of the large study area. More exhaustive information from hundreds of meteorological stations would be required to support spatial analysis. The meteorologic variables are as follows:

MAXATI_#	Average of the average maximum daily temperatures 1, 3 or 5 (#) days preceding the annual maximum flood.

MEANATI_#	Average of the average mean daily temperatures 1, 3 or 5 (#) days preceding the annual maximum flood.
R_API_#	Average of total rainfall 5 or 10 (#) days preceding the annual flood.
P_API_#	Average of total precipitation 5 or 10 (#) days preceding the annual flood.
S_API_#	Average of total snowfall 1, 3, 5 (#) days preceding the annual flood. Also, for the last available reading before the flood (L).
MAP	Mean annual (total) precipitation for the watershed upstream of the flow gauge.

Similar statistics are available for the median API and ATI. Instead of the above summary values available only at gauge locations, the Canada Climate Normals were used in this study. The relevant variables are shown as maps in Appendix C.

TABLE A.1: CRITERIA USED IN ASSIGNING FLOW DATA TO TWO GROUPS

Station ID	Class hydrometric	CFA tests?	NSERC incl. set	Years of record	Other gauges in basin?	Area km^2	GROUP	Independence		Trend		Randomness		Homogeneity	
								Serial Cor.? 5%	1%	Trend? 5%	1%	Not Random? 5%	1%	Homogeneous? 5%	1%
01AG002	I					199.0	A								
01AJ003	I				Y	1210.0	A								
01AJ004	I				Y	484.0	A								
01AJ010	I			19	Y	350.0	B								
01AJ011	I			19	Y	156.0	B								
01AK001	I				Y	234.0	A								
01AK005	I				Y	26.9	A								
01AK006	I				Y	5.7	A								
01AK007	I				Y	240.0	A								
01AL002	I				Y	1450.0	A								
01AL004	I				Y	3.9	A								
01AN001	I					34.4	A								
01AP002	I				Y	668.0	A								
01AP004	I				Y	1100.0	A								
01AQ001	I					239.0	A								
01BC001	I					3160.0	A								
01BD002	I		Y			2760.0	A								
01BE001	I					2270.0	A								
01BF001	I		Y			1140.0	A								
01BG001	I			19		1390.0	B								
01BH001	I		Y		Y	748.0	A								
01BJ001	I				Y	363.0	A								
01BJ003	I				Y	510.0	A								
01BJ007	I				Y	7740.0	A								
01BL001	I				Y	175.0	A								
01BO001	I				Y	5050.0	A								
01BO002	I				Y	611.0	A								
01BO003	I				Y	484.0	A								
01BP001	I					1340.0	A								
01BS001	I					166.0	A								
01BU002	I				Y	391.0	A								
01BU003	I				Y	129.0	A								
01BU004	I			19	Y	34.2	B								
01BV006	I					130.0	A								
01DD004	I					8.8	A								
01DG003	I					96.9	A								
01DH003	I					10.1	A								
01DN004	I					298.0	A								
01DO001	I					249.0	A								
01DP004	I					92.2	A								
01EC001	I					495.0	A								
01ED007	I				Y	295.0	A								
01EF001	I					1250.0	A								
01EG002	I					370.0	A								
01EH003	I					26.9	A								
01EJ001	I					146.0	A								
01EN002	I					389.0	A								
01EO001	I					1350.0	A								
01FB001	I				Y	368.0	A								
01FB003	I				Y	357.0	A								
01FJ001	I					199.0	A								
02AB008	I		Y		Y	187.0	A								
02AB014	I				Y	111.0	A								
02AD010	I					650.0	A								
02BA002	I		Y		Y	1190.0	A								
02BA003	I				Y	1320.0	A								
02BB002	I		Y		Y	1980.0	A								
02BB003	I		Y		Y	4270.0	A								
02BD003	I		Y			1930.0	A								

Station ID	Class hydrometric	CFA tests?	NSERC incl. set	Years of record	Other gauges in basin?	Area km^2	GROUP	Independence Serial Cor.? 5%	Independence Serial Cor.? 1%	Trend Trend? 5%	Trend Trend? 1%	Randomness Not Random? 5%	Randomness Not Random? 1%	Homogeneity Homogeneous? 5%	Homogeneity Homogeneous? 1%
02BF001	I		Y		Y	1190.0	A								
02BF002	I		Y		Y	1160.0	A								
02CA002	I		Y			108.0	A								
02CD001	I		Y		Y	1350.0	A								
02CD006	I				Y	157.0	A								
02CF007	I		Y		Y	243.0	A								
02CF008	I			17	Y	179.0	B								
02CF011	I				Y	704.0	A								
02DD008	I		Y		Y	90.4	A								
02DD012	I				Y	741.0	A								
02EA005	I		Y		Y	321.0	A								
02EA010	I		Y		Y	149.0	A								
02EB013	I			19		593.0	B								
02EC002	I		Y		Y	1520.0	A								
02EC009	I		Y		Y	181.0	A								
02EC010	I		Y		Y	42.9	A								
02EC011	I		Y		Y	282.0	A								
02ED003	I		Y		Y	1180.0	A								
02ED007	I		Y		Y	177.0	A								
02ED009	I				Y	94.8	A								
02ED014	I				Y	195.0	A								
02ED102	I			18	Y	211.0	B								
02FA001	I		Y			927.0	A								
02FB007	I		Y			181.0	A								
02FC001	I		Y		Y	3960.0	A								
02FC002	I		Y		Y	2150.0	A								
02FC015	I				Y	663.0	A								
02FF002	I		Y		Y	865.0	A								
02FF007	I		Y		Y	466.0	A								
02FF008	I				Y	110.0	A								
02GA017	I		Y		Y	324.0	A								
02GB009	I		Y		Y	91.9	A								
02GC002	I		Y		Y	329.0	A								
02GC010	I		Y		Y	342.0	A								
02GC018	I		Y		Y	287.0	A								
02GD010	I		Y		Y	150.0	A								
02GD013	I			19	Y	38.9	B								
02GD019	I		Y		Y	36.0	A								
02GD020	I		Y		Y	108.0	A								
02GG002	I		Y		Y	730.0	A								
02GG004	I		Y		Y	609.0	A								
02GG005	I		Y		Y	172.0	A								
02GG006	I		Y		Y	267.0	A								
02GH001	I			18	Y	14.2	B								
02GH002	I				Y	125.0	A								
02HA006	I		Y		Y	293.0	A								
02HB004	I		Y		Y	199.0	A								
02HB012	I		Y		Y	82.6	A								
02HC023	I		Y		Y	62.2	A								
02HC025	I		Y		Y	303.0	A								
02HC027	I		Y		Y	58.0	A								
02HC028	I		Y		Y	77.7	A								
02HC029	I		Y		Y	130.0	A								
02HC030	I		Y		Y	204.0	A								
02HC032	I		Y		Y	94.8	A								
02HC033	I		Y		Y	70.6	A								
02HD006	I		Y		Y	82.9	A								
02HD008	I		Y		Y	95.8	A								
02HD009	I		Y		Y	82.6	A								
02HE001	I		Y			13.9	A								

Station ID	Class hydrometric	CFA tests?	NSERC incl. set	Years of record	Other gauges in basin?	Area km^2	GROUP	Independence Serial Cor.? 5%	Independence Serial Cor.? 1%	Trend Trend? 5%	Trend Trend? 1%	Randomness Not Random? 5%	Randomness Not Random? 1%	Homogeneity Homogeneous? 5%	Homogeneity Homogeneous? 1%
02HL004	I		Y		Y	712.0	A								
02HL005	I		Y		Y	308.0	A								
02HM004	I		Y		Y	112.0	A								
02HM005	I		Y		Y	155.0	A								
02JB013	I		Y		Y	2590.0	A								
02KA004	I				Y	0.9	A								
02KA005	I			19	Y	3.6	B								
02KA006	I				Y	0.8	A								
02KJ003	I		Y		Y	2110.0	A								
02KJ007	I		Y		Y	2110.0	A								
02LB006	I		Y		Y	433.0	A								
02LC043	I		Y			39.9	A								
02LH004	I		Y		Y	1290.0	A								
02MC001	I		Y			404.0	A								
02OA030	I			18	Y	18.9	B								
02OA057	I			17	Y	686.0	B								
02OD003	I					1540.0	A								
02OE018	I		Y		Y	220.0	A								
02OE027	I		Y		Y	642.0	A								
02OG026	I		Y		Y	342.0	A								
02OJ007	I		Y		Y	22000.0	A								
02PA007	I		Y			4480.0	A								
02PB006	I		Y			642.0	A								
02PC009	I		Y			355.0	A								
02PD002	I				Y	1100.0	A								
02PD014	I		Y		Y	1.2	A								
02PD015	I				Y	3.6	A								
02PE009	I		Y		Y	865.0	A								
02PE014	I			16	Y	30.0	B								
02PJ007	I		Y		Y	709.0	A								
02PJ030	I		Y		Y	691.0	A								
02PL005	I		Y		Y	919.0	A								
02PL007	I				Y	2330.0	A								
02QA002	I		Y			1610.0	A								
02QC001	I		Y		Y	1200.0	A								
02RD002	I		Y		Y	9320.0	A								
02RD003	I		Y		Y	9870.0	A								
02RF001	I		Y		Y	15300.0	A								
02RF002	I		Y		Y	11100.0	A								
02RF006	I		Y		Y	4330.0	A								
02RH027	I			18	Y	495.0	B								
02RH035	I				Y	1110.0	A								
02SC002	I			17		2010.0	B								
02VA001	I		Y			684.0	A								
02VC001	I		Y			13000.0	A								
02WA001	I		Y		Y	2060.0	A								
02WA002	I			19	Y	5590.0	B								
02XC001	I		Y			6630.0	A								
02YA001	I					306.0	A								
02YC001	I					624.0	A								
02YD001	I			19		237.0	B								
02YJ001	I					640.0	A								
02YK005	I				Y	391.0	A								
02YL001	I					2110.0	A								
02YM001	I					974.0	A								
02ZB001	I					205.0	A								
02ZD002	I			15		1340.0	B								
02ZE001	I					2640.0	A								
03AB002	I		Y		Y	31900.0	A								
03AB003	I			19	Y	18700.0	B								

Station ID	Class hydrometric	CFA passes tests?	NSERC incl. set	Years of record	Other gauges in basin?	Area km^2	GROUP	Independence Serial Cor.? 5%	Independence Serial Cor.? 1%	Trend Trend? 5%	Trend Trend? 1%	Randomness Not Random? 5%	Randomness Not Random? 1%	Homogeneity Homogeneous? 5%	Homogeneity Homogeneous? 1%
03AC002	I		Y		Y	8310.0	A								
03AC004	I		Y		Y	22200.0	A								
03AD001	I		Y			57500.0	A								
03BA003	I		Y			7280.0	A								
03BB002	I		Y			18100.0	A								
03BD002	I			17		9820.0	B								
03BE001	I		Y			17100.0	A								
03CB003	I			17	Y	1870.0	B								
03CE001	I			18		3390.0	B								
03DD002	I		Y		Y	13200.0	A								
03DF001	I			18		96600.0	B								
03EC001	I		Y			4660.0	A								
03ED001	I		Y		Y	36300.0	A								
03ED004	I		Y		Y	7280.0	A								
03FC008	I		Y		Y	10400.0	A								
03HA001	I		Y		Y	26900.0	A								
03HA009	I			16	Y	4120.0	B								
03JB001	I		Y			41700.0	A								
03KA001	I		Y			8830.0	A								
03KC004	I		Y			42700.0	A								
03MB001	I			16	Y	2140.0	B								
03MB002	I		Y		Y	29800.0	A								
03MC001	I			18		3680.0	B								
03ME002	I			13		35200.0	C								
03QC001	I					10900.0	A								
04AC007	I				Y	14000.0	A								
04AD002	I			18		65500.0	B								
04CA003	I		Y		Y	619.0	A								
04CB001	I		Y			10800.0	A								
04CC001	I					94300.0	A								
04DA001	I		Y			5960.0	A								
04DC001	I		Y		Y	50000.0	A								
04EA001	I		Y			10400.0	A								
04FA003	I		Y			4900.0	A								
04GB005	I			16	Y	1170.0	B								
04JA002	I		Y			3780.0	A								
04JC002	I		Y		Y	2410.0	A								
04JD005	I		Y			2020.0	A								
04JF001	I		Y			5360.0	A								
04KA001	I					4250.0	A								
04LJ001	I		Y			8940.0	A								
04LM001	I					22900.0	A								
04MF001	I		Y			6680.0	A								
04NA001	I		Y		Y	3680.0	A								
04NB001	I			18		11200.0	B								
05OB016	I				Y	981.0	A								
05OB031	I				Y	149.0	A								
05OD001	I				Y	5260.0	A								
05OD031	I				Y	455.0	A								
05OD032	I				Y	197.0	A								
05OE004	I				Y	398.0	A								
05PB014	I		Y		Y	4870.0	A								
05PB015	I			11	Y	443.0	C								
05PH003	I				Y	3750.0	A								
05QA002	I				Y	6230.0	A								
05QA004	I		Y		Y	4450.0	A								
05QC003	I		Y			2370.0	A								
05SA002	I				Y	1610.0	A								
05SD003	I				Y	1720.0	A								
05TD001	I					15400.0	A								

Station ID	Class hydrometric	CFA pass tests?	NSERC incl. set	Years of record	Other gauges in basin?	Area km^2	GROUP	Independence Serial Cor.? 5%	Independence Serial Cor.? 1%	Trend Trend? 5%	Trend Trend? 1%	Randomness Not Random? 5%	Randomness Not Random? 1%	Homogeneity Homogeneous? 5%	Homogeneity Homogeneous? 1%
05TG002	I					883.0	A								
05UA003	I			16		4610.0	B								
06FC001	I					5810.0	A								
06GA001	I					13000.0	A								
06GD001	I					48100.0	A								
01AD002	I	*			Y	14700.0	B					fail			
01AL003	I	*			Y	6.5	B							fail	
01AM001	I	*				557.0	B							fail	
01BH002	I	*	Y		Y	1010.0	B			fail					
01BH007	I	*		17	Y	534.0	B							fail	
01BL002	I	*			Y	173.0	B							fail	
01BQ001	I	*				948.0	B	fail							
01BR001	I	*				177.0	B							fail	
01DR001	I	*				177.0	B			fail					
01ER001	I	*				45.1	B							fail	
01FA001	I	*				193.0	B							fail	
01FD001	I	*				31.0	B							fail	
01FH001	I	*				120.0	B			fail				fail	
02AA001	I	*				1550.0	B							fail	
02AC001	I	*	Y			736.0	B			fail				fail	
02ED010	I	*			Y	127.0	B			fail				fail	
02FC011	I	*	Y		Y	163.0	B							fail	
02FE008	I	*	Y		Y	648.0	B	fail						fail	
02FE009	I	*	Y		Y	376.0	B	fail							
02GA018	I	*	Y		Y	552.0	B							fail	
02GA037	I	*			Y	25.1	B			fail					
02GA038	I	*			Y	326.0	B							fail	
02HB015	I	*			Y	63.5	B							fail	
02HC009	I	*	Y		Y	197.0	B							fail	
02HC018	I	*	Y		Y	106.0	B							fail	
02HC019	I	*	Y		Y	93.5	B			fail				fail	
02HC031	I	*	Y		Y	148.0	B			fail				fail	
02HD002	I	*	Y		Y	262.0	B			fail					
02HD007	I	*	Y		Y	77.7	B			fail				fail	
02JC008	I	*	Y			1780.0	B							fail	
02KA007	I	*			Y	0.2	B	fail							
02LB007	I	*	Y		Y	246.0	B			fail					
02LB008	I	*	Y		Y	440.0	B	fail						fail	
02LD005	I	*	Y		Y	1330.0	B			fail					
02NF003	I	*				1390.0	B			fail				fail	
02OG007	I	*			Y	153.0	B			fail					
02PD012	I	*	Y		Y	3.9	B							fail	
02PD013	I	*	Y		Y	9.2	B							fail	
02PG004	I	*	Y			500.0	B							fail	
02QB011	I	*	Y			721.0	B	fail							
02QC009	I	*		18	Y	774.0	B	fail							
02RG005	I	*		14		2280.0	B							fail	
02YK004	I	*			Y	529.0	B							fail	
02ZG001	I	*				205.0	B	fail							
03CB001	I	*		19	Y	27700.0	B							fail	
03CC001	I	*	Y			44300.0	B			fail				fail	
03DD003	I	*	Y		Y	19100.0	B							fail	
03LD004	I	*		19		8990.0	B			fail				fail	
04AC005	I	*			Y	25900.0	B	fail		fail		fail			
04DB001	I	*	Y			7950.0	B			fail					
04FC001	I	*	Y			36000.0	B			fail				fail	
04GB004	I	*			Y	11200.0	B							fail	
04JC003	I	*	Y		Y	3290.0	B							fail	
05OD030	I	*			Y	4150.0	B	fail							
05UG001	I	*				3290.0	B							fail	

Station ID	Class hydrometric	CFA pass tests?	NSERC incl. set	Years of record	Other gauges in basin?	Area km^2	GROUP	Independence: Serial Cor.? 5%	Independence: Serial Cor.? 1%	Trend: Trend? 5%	Trend: Trend? 1%	Randomness: Not Random? 5%	Randomness: Not Random? 1%	Homogeneity: Homogeneous? 5%	Homogeneity: Homogeneous? 1%
06FB002	I	*				4250.0	B							fail	
01BH005	I	**	Y		Y	645.0	B	fail	fail					fail	fail
01BL003	I	**			Y	383.0	C							fail	fail
01DL001	I	**				63.2	**B**							fail	fail
02FF004	I	**			Y	41.4	C	fail	fail	fail				fail	fail
02GB007	I	**	Y		Y	360.0	B					fail	fail		
02HC013	I	**	Y		Y	86.2	B			fail				fail	fail
02HJ001	I	**	Y			110.0	B			fail	fail			fail	
02KF011	I	**				269.0	**C**			fail	fail			fail	
02LA007	I	**				559.0	**C**	fail		fail	fail			fail	fail
02NE011	I	**	Y		Y	1570.0	B			fail	fail			fail	fail
02OJ024	I	**		18	Y	287.0	C	fail		fail				fail	fail
02UC002	I	**	Y			19000.0	B	fail	fail	fail	fail			fail	fail
02YK002	I	**			Y	470.0	C	fail	fail	fail	fail			fail	fail
02ZF001	I	**				1170.0	**C**			fail	fail			fail	fail
03DC002	I	**	Y			37000.0	B	fail	fail	fail				fail	
03LF002	I	**	Y			86800.0	B			fail	fail			fail	fail
04AB001	I	**		11		103000.0	**C**	fail	fail	fail	fail			fail	fail
05QA001	I	**	Y		Y	13900.0	B			fail	fail			fail	
05RA001	I	**			Y	1830.0	**B**	fail	fail					fail	
05RA002	I	**			Y	712.0	**C**			fail	fail			fail	fail
05UF004	I	**				1090.0	**B**	fail	fail	fail				fail	fail
01DC003	II					107.0	B								
01EK001	II					650.0	B								
01FC002	II				Y	190.0	B								
02FC004	II		Y		Y	249.0	B								
02GA010	II		Y		Y	1030.0	B								
02GA023	II				Y	118.0	B								
02GB001	II				Y	5210.0	B								
02GD001	II				Y	1340.0	B								
02GD003	II				Y	1450.0	B								
02GD008	II				Y	200.0	B								
02GE002	II				Y	3110.0	B								
02GE005	II		Y		Y	146.0	B								
02HC004	II			18	Y	119.0	B								
02JB003	II		Y		Y	1680.0	B								
02LB012	II			19	Y	76.7	B								
02LD001	II		Y		Y	1990.0	B								
02LD002	II		Y		Y	1300.0	B								
02LH002	II		Y		Y	1780.0	B								
02NE007	II		Y		Y	1850.0	B								
02OJ001	II		Y		Y	22000.0	B								
04NA002	II			18	Y	3680.0	B								
05OB006	II				Y	135.0	B								
05OB010	II				Y	398.0	B								
05OC016	II				Y	919.0	B								
05OC022	II				Y	204.0	B								
05OC024	II				Y	68.4	B								
05OE001	II				Y	1340.0	B								
05OE006	II				Y	496.0	B								
05OE007	II				Y	329.0	B								
05OE009	II				Y	219.0	B								
05OE010	II				Y	393.0	B								
05OF010	II				Y	274.0	B								
05OF011	II				Y	574.0	B								
05OF020	II				Y	2120.0	B								
05OG001	II					1820.0	B								
05OJ007	II				Y	187.0	B								
05OJ008	II				Y	645.0	B								
05OJ009	II				Y	287.0	B								

Station ID	Class hydrometric	CFA tests?	NSERC incl. set	Years of record	Other gauges in basin?	Area km^2	GROUP	Independence Serial Cor.? 5%	Independence Serial Cor.? 1%	Trend Trend? 5%	Trend Trend? 1%	Randomness Not Random? 5%	Randomness Not Random? 1%	Homogeneity Homogeneous? 5%	Homogeneity Homogeneous? 1%
05OJ016	II				Y	239.0	B								
05OJ017	II				Y	471.0	B								
05PC011	II		Y		Y	461.0	B								
05PC016	II				Y	274.0	B								
05PD022	II				Y	0.6	B								
05PH001	II			17	Y	3760.0	B								
05SA001	II			16	Y	1540.0	B								
05SB002	II					253.0	B								
05SC002	II					1270.0	B								
05SD004	II				Y	390.0	B								
02HC005	II	*			Y	88.1	B			fail				fail	
02HD010	II	*			Y	64.8	B							fail	
02PL001	II	*	Y		Y	1410.0	B							fail	
03AC001	II	*	Y		Y	2010.0	B			fail					
05LL007	II	*			Y	635.0	B							fail	
05LL015	II	*			Y	1070.0	B							fail	
05OC019	II	*			Y	776.0	B			fail					
05OD004	II	*			Y	4390.0	B							fail	
05OD028	II	*			Y	240.0	B							fail	
05OD029	II	*			Y	23.8	B							fail	
05OF017	II	*			Y	76.9	B			fail					
05OH007	II	*			Y	566.0	B			fail					
05OJ002	II	*			Y	674.0	B							fail	
05OJ006	II	*			Y	0.0	C			fail				fail	
05SA004	II	*			Y	857.0	B			fail				fail	
01DB002	II	**				193.0	B	fail	fail						
01FE002	II	**				125.0	C	fail		fail	fail			fail	fail
02GD006	II	**		10	Y	554.0	C	fail	fail	fail	fail				
02HA003	II	**			Y	686000.0	C	fail	fail	fail	fail	fail	fail	fail	fail
02OJ003	II	**			Y	22700.0	C	fail	fail	fail	fail				
03OE001	II	**				92500.0	B	fail	fail	fail				fail	
04GA001	II	**			Y	0.0	C	fail	fail	fail	fail	fail	fail	fail	fail
05LM001	II	**				79900.0	C	fail	fail			fail			
05MH008	II	**				277.0	B			fail				fail	fail
05OF009	II	**			Y	149.0	C			fail				fail	fail
05OF014	II	**			Y	649.0	C							fail	fail
05OF015	II	**			Y	165.0	C			fail				fail	fail
05OF018	II	**			Y	174.0	C			fail	fail			fail	fail
05OH006	II	**			Y	0.0	C			fail	fail			fail	
05PC010	II	**	Y		Y	168.0	B	fail	fail						
05QE006	II	**			Y	26400.0	C	fail	fail	fail	fail	fail	fail	fail	fail
01AD003	III				Y	1350.0	C								
01AR012	III					0.0	B								
01ED005	III				Y	723.0	C								
01FC001	III			19	Y	49.2	C								
02JB004	III		Y		Y	984.0	B								
02KA003	III				Y	7.3	C								
02OA035	III				Y	146000.0	C								
03BC002	III		Y			40900.0	B								
03FC007	III				Y	10400.0	C								
04CA002	III				Y	36500.0	C								
04CA004	III			18	Y	0.0	C								
04CD002	III					4270.0	B								
04DC002	III		Y		Y	4710.0	B								
04FB001	III		Y			24200.0	B								
04GA002	III		Y		Y	5390.0	B								
04GF001	III			14		1890.0	B								
05LN002	III					334.0	B								
05PD017	III				Y	1.7	C								
05PD019	III				Y	0.5	C								

Station ID	Class hydro-metric	CFA pass tests?	NSERC incl. set	Years of record	Other gauges in basin?	Area km^2	GROUP	Independence		Trend		Randomness		Homogeneity	
								Serial Cor.?		Trend?		Not Random?		Homogeneous?	
								5%	1%	5%	1%	5%	1%	5%	1%
05PD023	III				Y	3.9	C								
05QE008	III		Y		Y	1690.0	B								
05RD007	III				Y	0.0	B								
05RD008	III				Y	0.0	B								
05RE001	III					6850.0	B								
04CE002	III	*	Y			4350.0	B	fail		fail					
05PA006	III	*	Y			13400.0	B			fail				fail	
05PD014	III	*			Y	0.6	C							fail	
05PD015	III	*			Y	7.3	C							fail	
05QE009	III	*	Y		Y	1530.0	B			fail				fail	
06GB001	III	*				18400.0	B			fail				fail	
03DA002	III	**		19		12800.0	B			fail				fail	fail
03EA001	III	**	Y			21000.0	B	fail		fail				fail	fail
05PJ001	III	**				1040.0	C			fail	fail			fail	fail
05QD008	III	**				0.3	B			fail	fail			fail	

N.B: CFA column contains a single star (*) if the gauge fails at least one test at a 5% level of significance and two stars(**) if it fails at least one test at the 1% level of significance.

N.B.B: Stations shown in bold type have been re-classified manually to increase spatial coverage

APPENDIX B

COMPUTER PROGRAMS

This appendix summarizes every program developed or modified by the author during the course of this study. Each program is listed in Table B.1 and described in the following sections. Only a partial listing of the source code showing modifications or improvements has been provided for software published previously or obtained from the public domain. References cited herein are listed in the main body of the report.

Table B.1: Programs Developed or Modified for use in this Study

Name	Language	Purpose	Author(s)
MER_2	C++	nonparametric regional FFA	Denis Gingras & Jean-Luc Daviau [1]
MER_4	C++	parametric regional FFA using L-moment methods	Adapted from Hosking and Wallis by Paul Pilon & Jean-Luc Daviau [1]
XFIT, XTEST	FORTRAN	L-moment software, revision 3	Hosking & Wallis
TIME	QUATTRO	computes flood timing	Jean-Luc Daviau
PDF	QUATTRO	plots nonparametric pdf	Jean-Luc Daviau
MMI	C++	counts number of modes and evaluates multimodality index from a nonparametric pdf	Jean-Luc Daviau
VARIOUS (GSLIB)	FORTRAN	variograms, kriging & co-kriging	Stanford University
CONTRAST	SPANS	buffers regions & measures contrast	Jean-Luc Daviau

[1] Assisted by Andrew Widlak for the conversion from FORTRAN to C++.

B.1 Description of MER_2 Class

The descriptions for the MER_2 and MER_4 classes (subroutines) and of their methods and functions are extracted from an appendix previously written by the author and included in (Adamowski *et al.*, 1994): "Regional Flood Frequency Analysis by Nonparametric and L-Moment Methods for Ontario and Quebec – Report to NSERC Strategic Grant". Please refer to this report for a description of the MER (parent) class and of the INTER main program (Bobée *et al.*, 1996a; Bobée *et al.*, 1996b).

MER_2 stands for "Méthode d'Estimation Régionale 2" or regional (flood) estimation method number 2. This class and its methods and functions evaluate the at-site nonparametric probability density function and calculate a number of descriptive statistics. If enough sites are available, the T-year flood quantiles are regressed against drainage area to establish a regional equation. The parent class for MER_2 is the class: MER, which operates within the main line program INTER.

The methods and functions used by MER_2 are as follows:

mer2::calcul_XT	Calculates return periods of floods.
mer2::ols_regression	Regional log-regression of flow vs area.
mer2::sample_sufficient	Checks whether enough data is available.
mer2::sort_data	Sorts data in descending order.
mer2::calc_H	Calculates smoothing parameter h.
mer2::Pn_H	Cross-validation.
mer2::SdMoment	Calculates standard variation of data.
mer2::mean	Calculates mean of data.
mer2::GaussDistribution	Gauss distribution at a point (Gaussian kernel).
mer2::calc_flood	Computes flow for a given return period, T.
mer2::Pn	Computes probability given the flood magnitude.
mer2::OLS	Ordinary Least Squares Regression of log(flow) vs log(drainage area)

The TRS_1 parameter in MER.CPP can be modified to change the minimum number of years required for at-site analysis to proceed (default 20). The TRS_2 parameter is the minimum number of sites required for a meaningful regional regression equation (default 5). The program has been tested against a previously-compiled FORTRAN version contained in CFA, version 3 and found to provide accurate results.

B.2 Description of MER_4 Class

MER_4 stands for "Méthode d'Estimation Régionale 4" or regional (flood) estimation method number 4. This class and its methods and functions use the L-moment method (Hosking and Wallis, 1993) and the GEV distribution to estimate floods with given return periods based on regional observations. The nonparametric method is used to count the number of modes to ensure that the majority of sites within the homogeneous region are not multimodal (a number of descriptive statistics are also computed).

Each region is also submitted to a battery of tests: discordant sites are not used and heterogeneous regions are rejected. If enough sites are available and the region is somewhat or wholly heterogeneous (H>1), the L-CV and L-skew parameters are regressed against physiographic and/or meteorological variables in order to explain any apparent systematic variations within the region.

The parent class for MER_2 is the class: MER, which operates within the main line program INTER. To the best of the author's knowledge, the code is ANSI C^{++} and has been compiled under DOS and UNIX. The methods and functions used by MER_4 are as follows:

mer4::calcul_XT	Calculates return periods of floods.
mer4::ols	Regional log-regression of flow vs area (Ordinary Least Squares).
mer4::stations_to_process	Identifies each station with enough years of at-site data.
mer4::stations_multimodal	Counts the number of multi modal stations in a region.
mer4::sort_data	Sorts data in descending order.
mer4::calc_H	Calculates smoothing parameter h.
mer4::Pn_H	Cross-validation.
mer4::SdMoment	Calculates standard variation of data.
mer4::mean	Calculates mean of data.
mer4::calculate_flood	Computes flow for a given return period, T.
mer4::calc_L_mom	Computes L-moments and ratios (after Hosking and Wallis).
mer4::L-moments	Computes L-moments.
mer4::calc_averages	Computes L-moment averages weighted by NY
mer4::L_discordancy_test	Checks whether a region has too many discordant sites.
mer4::L_discordancy	Calculates L-discordance measure for a region.
mer4::estimate_first_L_mom	Calculates L-mean.
mer4::heterogeneity	Calculates H statistics for a region by L-moments.
mer4::best_regression	Regression for L-parameters vs physio or meteo variables
mer4::get_num_modes	Counts the number of modes on a nonparametric pdf estimate.
mer4::pdf_modes	Manages nonparametric pdf estimation, mode counts, MMI, etc...
mer4::store_pdf	Stores nonparametric pdf if required.

mer4::normal	Computes ordinate for the normal distribution (Gaussian kernel).
mer4::gammlm	Computes the log of a gamma value.
mer4::stats	Computes mean, standard deviation and coefficient of variation.
mer4::calc_hetero_stats	Computes heterogeneity statistics and variance based on simulations.
mer4::kappa_GLO_simulation	Simulates Kappa or GLO-distributed worlds based on regional data.
mer4::simulation	Numerical simulation and comparison loop.
mer4::pelkap	Parameter estimation for the Kappa distribution.
mer4::pelGLO	Parameter estimation for the GLO distribution.
mer4::durand	Provides random numbers for the simulations.
mer4::quakap	Quantile estimation for the Kappa distribution.
mer4::dlgama	Double-precision gamma function for a given input (GEV parameters).
mer4::digamd	Double-precision digamma function for a given input.

The parameters controlling the execution of MER4 are described below:

```
 1 : 20 # yrs for at-site information to be useful for computing L-moments
 2 : 5    number of stations required to perform a meaningful regional analysis
 3 : 20   min. # yrs to est. at-site L-moments and ratios
 4 : 20   min. # yrs to est. at-site L-discordance measure
 5 : 51   number of yrs for using target site estimate of LAMBDA_1
 6 : 100  acceptable % of bimodal pdfs in unimodal pop'n (if 100, skip test)
 7 : 0    if one, stop calculating the pdf at cutoff.
 8 : 10   % of pdf's upper tail to ignore when counting modes (CUTOFF)
 9 : 640  number of increments in the cdf and pdf
10 : 0    min. # of non-discordant sites req'd to calc. floods. If zero, only
11 : 100  acceptable % of discordant sites in a homogeneous region (D_PERCENT)
12 : 9    number of different physiographic variables
13 : 1    number of different meteorological variables
14 : 10   min. # of sites required to perform regression
15 : 50   # of regions simulated in heterogeneity subroutine
16 : 0.65 min. R2 for a meaningful regression equation
17 : 1    if 1 store pdf, if 0 do not store pdf
18 : 1    if 1, do full reporting.  If 0 (zero), only normal reporting.
19 : 5    % of minimum difference between PDF min and max when counting modes
```

The core routines in this program have been tested against a previously-compiled FORTRAN version, version 3, and found to provide accurate results.

B.3 Modifications to MER_4 to Calculate MMI

The following partial listing shows the algorithm for the evaluation of the multimodality index developed in this thesis. The MER_4 class and the INTER program were previously documented by (Bobée *et al.*, 1996a; Bobée *et al.*, 1996b).

```
mer4::get_num_modes() : Calculate PDF and determine number of its modes
Input :     donnees : Sorted observations
              h       : Smoothing factor
              ny      : Number of years
Output:     pdf     : Pointer to the PDF
```

```
int get_num_modes( Tmatrice& donnees, FLOAT h, int ny )
{
      FLOAT       beginning= 0, ending   = 0,  delta_x= 0,   hny = 0;
      FLOAT       locate   = 0, prob_ne  = 0,       z  = 0,  dpdf = 0;
      FLOAT       max_abs  = 0, MIN_DIF  = 0,       MMI= 0,  area = 0;
      FLOAT       alpha_MMI= 1, beta_MMI = 1, LHS_area= 0,    dl = 0;
      FLOAT       left_min = 0, right_min= 0, dr=0, t_max=0, nrm = 0;
      FLOAT       area_sum = 0, global_max=0, global_max_area = 0;
      Tmatrice    pdf, extremum, ext_area, npeak, adj_area;
      register int m, j, k, sign = 0, ext_num=0, num_modes = 0,
                  second_last=0;
      register int      outlier  = 0, max_npeak= 0;
      double      norm_y;
      //BLOCK BELOW TO CREATE PDF FILES
      char  file_name[12];
      static      int STATION_ID = 1;
      FILE    *pdf_file,*MMI_out;
      MMI_out = fopen( "MMI_out.OUT", "at" );   // append to ASCII file
      sprintf( file_name, "%d.PDF", STATION_ID++ );
      if ( STATION_ID < 500 )
            { pdf_file = fopen(file_name,"wt");    // open up to 500 }
      // END OF BLOCK
      pdf.taille( STEPS_2 + 2 );      // taille is French for size
      extremum.taille( 40 );          // ample allowance for max & mins
      ext_area.taille( 40 );          // ample allowance maxima's area
      npeak.taille( 40 );         // store NET PEAKS after precomputed
      adj_area.taille(  40);      // adjusted area for each mode (eg: max)
      beginning = (FLOAT) donnees( 0 + 1 )    - 3 * h;
      ending = (FLOAT) donnees( ny - 1 + 1 ) + 3 * h;
      delta_x = ( ending - beginning ) / STEPS_2;
      MIN_DIF = (FLOAT) PMODE_2 / 100.0;
      outlier  = STEPS_2;                    // last pdf coordinates to use
      outlier *= (100 - CUTOFF_2);           // (used to cut-off RHT "noise"
      outlier /= 100;
      if( WHOLE_PDF_2 == 0 )
            outlier = STEPS_2;            //  and is usually not used)
      hny = h * ny;
      // LOOP TO EVALUATE PROBABILITY DENSITY ORDINATE FOR EACH ABCISSA
      for( j = (0+1); j <= (outlier+1); j++ )
      {
            locate   = beginning + (j-1) * delta_x;
            prob_ne  = 0.0;
            pdf( j ) = 0.0;
            for( k = 0; k < ny; k++ )
            {
                  if ( h == 0.0 )
                  { printf("int get_num_modes( Tmatrice& donnees, FLOAT h,
                   int ny )   h = 0"); exit(1); }
                  z = (  locate - (FLOAT) donnees( k + 1 ) ) / h;
```

```
                nrm = normal( z );
                prob_ne += nrm; // probability of non-exceedance
            }                   // for a given observation, k+1.
// CALCULATE PDF VALUE & MANIPULATE IT
            pdf( j ) = prob_ne / hny;
            if( j == (0+1) )              // assign first minimum
            {     ext_num++;
                  extremum( ext_num ) = pdf( j );     }
// differentiate the pdf & cumulate area under pdf curve
            if( j > (0+1) )   // for every pdf ordinate but the first
            {                       // (pdf(0) undefined)
                  dpdf      = ( pdf( j ) - pdf( j - 1 ) ) / delta_x;
                  area     += ( pdf( j ) + pdf( j - 1 ) ) / 2 * delta_x;
                  area_sum += ( pdf( j ) + pdf( j - 1 ) ) / 2 * delta_x;
                  // check for sign changes (local max or min)
                  if( dpdf < 0 && sign == 0 )   // pos to neg slope (max)
                  {     ext_num++;
                        extremum( ext_num ) = pdf(j-1);
                        if( pdf(j-1) > max_abs)  { // if this is largest
                        max_abs   = pdf(j-1);}  // retain max pdf value
                  // store area on the rising limb, minus current segment.
                        LHS_area = area-(pdf(j)+pdf(j-1))/2 * delta_x;
                        sign = 1;   // change current slope to neg (1)
                  }
                  if( dpdf > 0 && sign == 1 )   // neg to pos slope (min)
                  {     ext_num++;                // incr. extrema counter
                        extremum( ext_num ) = pdf(j-1);
                        area -= (pdf(j) + pdf(j-1))/2 * delta_x;
                                          // substract upward segment
                        ext_area( ext_num - 1 ) = area;
                                          // assign area to prior max
                        ext_area( ext_num ) = (area-LHS_area);
                                          // area on falling limb
                  // reset zero for next max but add current panel.
                        area  = (pdf(j) + pdf(j-1))/2 * delta_x;
                        sign = 0;      // change current slope to pos (0)
                  }
            }
      }
      ext_num++;                                  // account for last min.
      extremum( ext_num ) = pdf( outlier + 1 );   // set last "minimum"
      ext_area( ext_num - 1 ) = area;     // assign area to last maximum
      ext_area( ext_num ) = (area-LHS_area);
                                  // " area on falling limb to last min
// PRINT-OUT (X,Y) and (X,Y)_NORMALIZED
      for( j = (0+1); j <= (outlier+1); j++ )
      {     locate  = beginning + (j-1) * delta_x;
            norm_y      = (double) (pdf( j ) / max_abs);
            fprintf(pdf_file, "%10.3lf, %12.7lf, %5.3lf, %12.7lf\n", locate,
```

```
            pdf( j ), (locate-beginning)/(ending-beginning), norm_y );  }
      flushall();
// LOOP OVER ALL MAXIMA TO COUNT MODES AND RE-ASSIGN INSIGNIFICANT MODES' AREA
      second_last = ext_num - 2;          // prepare for next loop.
// COUNT MODES AND FLAG INSIGNIFICANT MODES.
      for( m = 1; m <= second_last; m += 2 )  // for each maxima
      {                                       // nb: loops by minima
            left_min = extremum( m - 1 + 1 ); // eg: current ext. = min
            t_max = extremum( m + 1 );        //     next ext. = max
            right_min= extremum( m + 1 + 1 );
            dl = t_max - left_min;            // L and R relative rise
            dr = t_max - right_min;

            // new mode iff both L & R risers are significant
            if( dl / max_abs > MIN_DIF && dr / max_abs > MIN_DIF )
            {     num_modes++;      }
            else                          // insignificant mode
            {
      fprintf(pdf_file, "\nInsignificant mode detected,  max = ,%12.7lf,"
              " Area = %12.7lf.", extremum(m+1), ext_area(m+1));
            }
      }
      if  ( STATION_ID < 500 )
      {
      fprintf(pdf_file, "\nabcissa (x), ordinate (y), norm (x), norm(y)\n");
      fprintf(pdf_file, "\n%10.3lf = h, %3d = no. steps,%10.3lf = start,"
                        " %10.3lf = end, %8.2lf = DX\n\n", h, outlier,
                        beginning, ending, delta_x );
      fprintf(MMI_out, "%10.3lf,%3d,%10.3lf,%10.3lf,%8.2lf,", h, outlier,
                        beginning, ending, delta_x );
            }
      flushall();
      global_max_area = 0;
      global_max = 0;
// LOOP OVER ALL MAXIMA TO CALCULATE NET PEAKS (npeak) AND
      for( m = 1; m <= second_last; m += 2 )  // for each minima
      {
            left_min  = extremum( m - 1 + 1 );
            t_max     = extremum( m + 1 );
            right_min = extremum( m + 1 + 1 );
            npeak(m+1)= t_max - (left_min + right_min)/2;
            if (npeak(m+1) > global_max )
            {
            global_max = npeak(m+1);      // update global_max net peak value
            max_npeak  = (m + 1);         // store index value for max npeak
            }
      }
// LOOP OVER ALL MAXIMA TO CALCULATE AREA TO THE L OF GLOBAL MAXIMUM.
      LHS_area = 0;
```

```
      for( m = 1; m <= max_npeak; m += 2 )        // for each minima up to big max
      {
            LHS_area +=  ext_area(m+1);                // add whole mode's area
      }
      LHS_area -= ext_area(max_npeak+1);         // subtract falling limb of max
// PROCESS MAXIMA L TO GLOBAL MAX AND COMPUTE ADJUSTED AREAS (L-R pass)
      // n.b: from L to R, L = (m-1) and R=(m+3) for max, (m) and (m+2) for min.
      if( ext_num > 3 ) {          // if more than one mode exists
      if ( max_npeak != 2 ) { // do L-R pass only if global max not first max
      for( m = 1; m <= (max_npeak-3); m += 2 )// for each mode up to that
      {                                          // to the L of the global max
      adj_area(m+1) = ext_area(m+1);        // initialize adj_area for current max
// ADJUST AREA UNDER CURRENT MODE DEPENDING ON R &/or L NEIGHBOURS
      // Three cases: i and ii in L-R pass; iii and ii in R-L pass.
      // Case i: current max is the first maximum (only R neighbour exists)
      if( m == 1 )
      {
//          CASE 3 - Current mode gives up area to R (no L side)
            if( npeak(m+1) < npeak(m+3) )
            {
            adj_area(m+1) -= pow(alpha_MMI ,(1- npeak(m+1) /  npeak (m+3)))*
                              pow( beta_MMI ,(extremum(m+2) /extremum(m+1)))*
                               ext_area(m+1);
      }
//          CASE 4 - Current mode takes from R side (no L side)
            if( npeak(m+1) >= npeak(m+3) )
            { adj_area(m+1) += (1 - npeak(m+3)/ npeak(m+1)  ) * alpha_MMI *
             (extremum(m+2) /extremum(m+3)) * beta_MMI  * ext_area(m+3); }
      }
            // Case ii: current max between first and glcbal max (two neighbours)
            if( m > 1 && m <= (max_npeak-3) )
            {
//          CASE 1 - Current mode gives up area to both R and L neighbours
            if( npeak(m+1) < npeak(m+3) && npeak(m+1) < npeak(m-1) )
            {
            if( npeak(m+3) > npeak (m-1) ) // R mode > L mode
            {                                 // Give area to largest mode first
            adj_area(m+1) -= (1-npeak(m+1) / npeak(m+3)  ) * alpha_MMI *
                              (extremum(m+2)/extremum(m+1)) * beta_MMI  *
                               ext_area(m+1);
            adj_area(m+1) -= (1-npeak(m+1) / npeak(m-1)  ) * alpha_MMI *
                              (extremum(m)  /extremum(m+1)) * beta_MMI  *
                               ext_area(m+1);
            if( adj_area(m+1) < 0 ) adj_area(m+1) = 0;  // set to zero if neg.
                  }
            else                                       // L mode > R mode
                  {                             // Give area to largest mode first
            adj_area(m+1) -= (1-npeak(m+1) / npeak(m-1)  ) * alpha_MMI *
                   (extremum(m)  /extremum(m+1)) * beta_MMI  * ext_area(m+1);
```

```
            adj_area(m+1) -= (1-npeak(m+1) / npeak(m+3)  ) * alpha_MMI *
                   (extremum(m+2)/extremum(m+1)) * beta_MMI  * ext_area(m+1);
            if( adj_area(m+1) < 0 ) adj_area(m+1) = 0;  // set to zero if neg.
            }
            }
//                CASE 2 - Current mode takes area from both R and L neighbours
            if( npeak(m+1) >= npeak(m+3) && npeak(m+1) >= npeak(m-1) )
            { adj_area(m+1) += ((1-npeak(m+3) / npeak(m+1)  ) * alpha_MMI *
              (extremum(m+2)/extremum(m+3)) * beta_MMI  *   ext_area(m+3) +
              (1-npeak(m-1) / npeak(m+1)  ) * alpha_MMI *
              (extremum(m)  /extremum(m-1)) * beta_MMI  *
               ext_area(m-1)); }
//          CASE 3 - Current mode gives up area to R but takes from L side
            if( npeak(m+1) < npeak(m+3) && npeak(m+1) >= npeak(m-1) )
            { adj_area(m+1) -= ((1-npeak(m+1) / npeak(m+3)  ) * alpha_MMI *
              (extremum(m+2)/extremum(m+1)) * beta_MMI  * ext_area(m+1) -
              (1-npeak(m-1) / npeak(m+1)  ) * alpha_MMI *
              (extremum(m)  /extremum(m-1)) * beta_MMI  * ext_area(m-1)); }
//          CASE 4 - Current mode takes from R side but gives up area to L side
            if( npeak(m+1) >= npeak(m+3) && npeak(m+1) < npeak(m-1) )
            { adj_area(m+1) += ((1-npeak(m+3) /npeak(m+1)   ) * alpha_MMI *
              (extremum(m+2)/extremum(m+3)) * beta_MMI  * ext_area(m+3) -
              (1-npeak(m+1) /npeak(m-1)   ) * alpha_MMI *
              (extremum(m)  /extremum(m+1)) * beta_MMI  * ext_area(m+1)); }
            }
      }}} // end of L to R pass
// PROCESS MAXIMA R TO GLOBAL MAX AND COMPUTE ADJUSTED AREAS (R-L pass)
// n.b: from R to L, R = (m+1) and L=(m-1) for max, (m) and (m-2) for min.
      if( ext_num > 3 ) {           // do R-L pass only if more than one mode
      if(max_npeak != (ext_num-1)){// do R-L pass only if global max not last max
      for( m=(ext_num-2); m>=(max_npeak+1); m -= 2 )// for each mode up to that
      {                                              // to the R of the global max
            adj_area(m+1) = ext_area(m+1);// initialize adj_area for current max
      // ADJUST AREA UNDER CURRENT MODE DEPENDING ON R &/or L NEIGHBOURS
      // Three cases: i and ii in L-R pass; iii and ii in R-L pass.
      // Case iii: current is the last maximum (only L neighbour)
      if( m == (ext_num-2) )
      {
//    CASE 3 - Current max gives up area to L (no R side)
      if( npeak(m+1) < npeak(m-1) )
      { adj_area(m+1) -= (1-npeak(m+1)/   npeak(m-1)) * alpha_MMI *
       (extremum(m) /extremum(m+1)) * beta_MMI  *  ext_area(m+1); }
//    CASE 4 - Current max takes from L side (no R side)
      if( npeak(m+1) >= npeak(m-1) )
      { adj_area(m+1) += (1-npeak(m-1)/   npeak(m+1)) * alpha_MMI *
       (extremum(m) /extremum(m-1)) * beta_MMI  * ext_area(m-1); }
      }
      // Case ii: current max between 2nd last & global max (two neighbours)
      if( m < second_last && m >= (max_npeak+1) )
```

```
      {
//    CASE 1 - Current mode gives up area to both R and L neighbours
      if( npeak(m+1) < npeak(m+3) && npeak(m+1) < npeak(m-1) )
      {
            if( npeak(m+3) > npeak (m-1) ) // R mode > L mode
            {                              // Give area to largest mode first
            adj_area(m+1) -= (1-npeak(m+1) / npeak(m+3)  ) * alpha_MMI *
                   (extremum(m+2)/extremum(m+1)) * beta_MMI  * ext_area(m+1);
            adj_area(m+1) -= (1-npeak(m+1) / npeak(m-1)  ) * alpha_MMI *
                  (extremum(m)  /extremum(m+1)) * beta_MMI  * ext_area(m+1);
            if( adj_area(m+1) < 0 ) adj_area(m+1) = 0;  // set to zero if neg.
            }
            else                           // L mode > R mode
            {                         // Give area to largest mode first
            adj_area(m+1) -= (1-npeak(m+1) / npeak(m-1)  ) * alpha_MMI *
                   (extremum(m)  /extremum(m+1)) * beta_MMI  * ext_area(m+1);
            adj_area(m+1) -= (1-npeak(m+1) / npeak(m+3)  ) * alpha_MMI *
                  (extremum(m+2)/extremum(m+1)) * beta_MMI  * ext_area(m+1);
            if( adj_area(m+1) < 0 ) adj_area(m+1) = 0;  // set to zero if neg.
            }
      }
//    CASE 2 - Current mode takes area from both R and L neighbours
      if( npeak(m+1) >= npeak(m+3) && npeak(m+1) >= npeak(m-1) )
            { adj_area(m+1) += ((1-npeak(m+3) / npeak(m+1)  ) * alpha_MMI *
              (extremum(m+2)/extremum(m+3)) * beta_MMI  * ext_area(m+3) +
              (1-npeak(m-1) / npeak(m+1)  ) * alpha_MMI
            * (extremum(m)  /extremum(m-1)) * beta_MMI  * ext_area(m-1)); }
//    CASE 3 - Current mode gives up area to R but takes from L side
      if( npeak(m+1) < npeak(m+3) && npeak(m+1) >= npeak(m-1) )
            { adj_area(m+1) -= ((1-npeak(m+1) / npeak(m+3)  ) * alpha_MMI *
            (extremum(m+2)/extremum(m+1)) * beta_MMI  * ext_area(m+1) -
              (1-npeak(m-1) / npeak(m+1)  ) * alpha_MMI *
              (extremum(m)  /extremum(m-1)) * beta_MMI  * ext_area(m-1)); }
//    CASE 4 - Current mode takes from R side but gives up area to L side
            if( npeak(m+1) >= npeak(m+3) && npeak(m+1) < npeak(m-1) )
            { adj_area(m+1) += ((1-npeak(m+3) /npeak(m+1)   ) * alpha_MMI *
              (extremum(m+2)/extremum(m+3)) * beta_MMI  * ext_area(m+3) -
              (1-npeak(m+1) /npeak(m-1)   ) * alpha_MMI *
              (extremum(m)  /extremum(m+1)) * beta_MMI  * ext_area(m+1)); }
      }
      }}}   // end of R to L pass
      // NOW ADJUST THE AREA OF THE GLOBAL MAX (ALWAYS TAKES FROM BOTH SIDES)
      // Three cases: Global max is first max, last max or between other maxima
      m = (max_npeak - 1);
      if ( m == 1 && ext_num > 3 )          // global max is also L-most local max
      {                               // and there are more than one maxima
      adj_area(m+1)  = ext_area(m+1);      // initialize adj_area for global max
      adj_area(m+1) += (1 - npeak(m+3) / npeak(m+1)  )* alpha_MMI *
                     (extremum(m+2) /extremum(m+3))* beta_MMI  * ext_area(m+3);
```

```
}     // (takes from R (& only) neighbour).
if ( m == (ext_num-2) && ext_num>3 )// global max is also R-most local max
{                                  // and there are more than one maxima
adj_area(m+1)  = ext_area(m+1);      // initialize adj_area for global max
adj_area(m+1) += (1- npeak(m-1)/   npeak(m+1) ) * alpha_MMI *
            (extremum(m) /extremum(m-1) ) * beta_MMI  * ext_area(m-1);
}     // (takes from L (& only) neighbour).
if ( ext_num > 6 )       // global max has two or more neighbours
{ if( m != 1 && m != (ext_num - 2) )
{
adj_area(m+1)  = ext_area(m+1);      // initialize adj_area for global max
adj_area(m+1) += ((1-npeak(m+3) / npeak(m+1)  ) * alpha_MMI *
               (extremum(m+2)/extremum(m+3)) * beta_MMI  * ext_area(m+3) +
               (1-npeak(m-1) / npeak(m+1)  ) * alpha_MMI *
               (extremum(m)  /extremum(m-1)) * beta_MMI  * ext_area(m-1));
                           // (takes area from L and R neighbours).
}}
if ( ext_num == 3 )                  // global max is only max (unimodal)
{ adj_area(m+1)  = ext_area(m+1);}   // initialize adj_area for global max
for( m = 2; m < ext_num; m += 2 )    // Print each mode's stats
{ fprintf(pdf_file, "\n%2d %12.7lf = min,%34.6lf = area (falling limb)",
                    (m-1), extremum(m-1), ext_area(m-1) );
 fprintf(pdf_file, "\n%2d %12.7lf = max,%10.7lf = net peak %12.6lf = area,"
                    "%12.6lf = adjusted area", m, extremum(m), npeak(m),
                    ext_area( m ), adj_area( m ) );
if ( m == max_npeak ) fprintf(pdf_file," **");
global_max_area += adj_area( m );
if(m==(ext_num-1))
{fprintf(pdf_file, "\n%2d %12.7lf = min,%34.6lf = area (falling limb)",
                    (m+1), extremum(m+1), ext_area(m+1) ); }}
fprintf(pdf_file, "\n\n%42.6lf, total area", area_sum);
fprintf(pdf_file, "\n%42.6lf, total area (adjusted)", global_max_area);
if( (global_max_area - area_sum) < 0.000001 ) {
fprintf(pdf_file, "\n%42.2lf, percent difference is effectively zero.");}
else {
fprintf(pdf_file, "\n%42.2lf, percent difference.",
                          (global_max_area-area_sum)/area_sum*100 ); }
// CALCULATE MMI
fprintf(pdf_file,"\n\n%8.6lf = LHS_area\n%8.6lf = RHS_area\n%4.2lf area"
                    " in RHS tail.", LHS_area, (area_sum-LHS_area),
                    area_sum/(area_sum-LHS_area) );
fprintf(MMI_out, "%10.7lf,%10.7lf,%4.2lf,",LHS_area,(area_sum-LHS_area),
                    area_sum/(area_sum-LHS_area)*100 );
flushall();
if ( ext_num > 3 )
{ MMI = area_sum / adj_area(max_npeak); }
else
{ if(LHS_area < (area_sum-LHS_area)) { LHS_area = (area_sum-LHS_area);}
  MMI = area_sum / LHS_area; }
```

```
        fprintf(pdf_file, "\n\n%6d = ID no. for this station", STATION_ID);
        fprintf(pdf_file, "\n%6d = No. of modes for this station", num_modes);
        fprintf(pdf_file, "\n%6.2lf = MMI for this station", MMI);
        fprintf(MMI_out,  "%6d,%6d,%6.2lf,",STATION_ID,num_modes,MMI);
        // Print each mode's stats
        for( m = 2; m < ext_num; m += 2 )
        {fprintf(MMI_out,"%2d,%12.7lf,%12.6lf,",(m-1),extremum(m-1),ext_area(m-1));
         fprintf(MMI_out,"%2d,%12.7lf,%12.6lf,%10.7lf,",m,extremum(m),ext_area(m),
                         npeak(m),adj_area(m));
        if(m==(ext_num-1)) {
        fprintf(MMI_out,"%2d,%12.7lf,%12.6lf\n",(m+1),extremum(m+1),ext_area(m+1));
        }}
        flushall(); fclose(pdf_file); fclose(MMI_out);  // clean-up
        return num_modes;
}
```

B.4 SPANS GIS Script to Evaluate Spatial Contrast

The following listing shows a script used to perform repetitive GIS tasks. The CONTRAST macro runs in just over seven hours on a 486 DX4-100 PC and is typical of the more than 15 such scripts used in this study for buffering, mapping temporal coverage, etc.

```
::::::::::::
:: REGION 1
::::::::::::
: RECLASSIFICATIONS BELOW EDITED MANUALLY FOR EACH REGION 1
:reclcreat  f =r01on-1 m =reg-alt1
:reclcreat  f =r01off1 m =reg-alt1
:
: CREATE NEW BASEMAPS FOR ON- AND OFF-REGION AREAS
:setbase  b =b-land
:reclass  m =reg-alt1 o =r01on-1 w =00 b =n s =y f =r01on-1 q =15
:reclass  m =reg-alt1 o =r01off1 w =00 b =n s =y f =r01off1 q =15
:: SET BASEMAP TO "ON-" REGION & MEASURE ON-PATTERN VARIABLES
:setbase  b =r01on-1
:area2  m =buf-0101 n =lskew12  w =00 r =r01skw1a s =n p =n
:area2  m =buf-0101 n =l-cv-12  w =00 r =r01cv-1a s =n p =n
:area2  m =buf-0101 n =lmnda12  w =00 r =r01mn-1a s =n p =n
:area2  m =buf-0101 n =lcvt-12  w =00 r =r01cvt1a s =n p =n
:area2  m =buf-0101 n =lmnt-12  w =00 r =r01mnt1a s =n p =n
:area2  m =buf-0101 n =buf-lak5 w =00 r =r01dis1a s =n p =n
:area2  m =buf-0101 n =VEG      w =00 r =r01veg1a s =n p =n
:area2  m =buf-0101 n =mmi-12   w =00 r =r01mmi1a s =n p =n
:
:
:
```

```
: SET BASEMAP TO "OFF" REGION & MEASURE OFF-PATTERN VARIABLES
:setbase  b =r01off1
:area2  m =buf-0101 n =lskew12  w =00 r =r01skw1b s =n p =n
:area2  m =buf-0101 n =l-cv-12  w =00 r =r01cv-1b s =n p =n
:area2  m =buf-0101 n =lmnda12  w =00 r =r01mn-1b s =n p =n
:area2  m =buf-0101 n =lcvt-12  w =00 r =r01cvt1b s =n p =n
:area2  m =buf-0101 n =lmnt-12  w =00 r =r01mnt1b s =n p =n
:area2  m =buf-0101 n =buf-lak5 w =00 r =r01dis1b s =n p =n
:area2  m =buf-0101 n =VEG      w =00 r =r01veg1b s =n p =n
:area2  m =buf-0101 n =mmi-12   w =00 r =r01mmi1b s =n p =n
```

...repeats for 16 regions and two alternatives. Total run time approximately 16 hours.

APPENDIX C

OUTPUT MAPS AND TABLES - A Flood Frequency Atlas for Central and Eastern Canada

This appendix documents all source and derived maps used in this study. It loosely follows the ASTM (1996) guidelines for digital spatial metadata and covers the specification of the study universe; the origin of source data or maps; the principal data transformations; and the accuracy of each resulting evidence map used in the study. Representative maps have been printed for quick reference and in order to make this document as self-contained as possible.

Specification of the Study Universe

In SPANS™ GIS terminology, the spheroid, projection and extent of the area mapped in a study is called the study universe. The Clarke 1866 spheroid was selected due to its widespread use in North America. The Albers equal area projection was selected since the primary variable, stream flow, is supplied as point data and since point pattern analysis is the central objective of the study. The extents were selected so as to position Ontario and Quebec near the centre of the study area and to support a minimum pixel dimensions of 150 m (at quad level 15). This resulted in an area approximately bounded by: $55 < {}^{\circ}W\ LON < 110$ and $42 < {}^{\circ}N\ LAT < 63$.

Source Maps

Source maps are the result of mapping primary information without transformations. Each source map used in this study is listed in Table C.1, which gives the origin, accuracy and versions for each map. Due to the large number of maps, numbering well over a hundred, produced in this study, the most detailed version of each source map are available for inspection upon request.

Table C.1: Metadata for Source Maps

Name	Origin	Quality	Versions
ANN_____	Canada Climate Normals (in map form)	300 m resolution and few classes – general patterns.	7 to 9 classes
B-LAND	Environment Canada	300 m resolution	islands or no islands
B-LAKE	Environment Canada	Mosaic	all lakes, large lakes, great lakes
B-PROV	Environment Canada	Mosaic	also vectors
COV-____	HYDAT flow gauges	Daily temporal coverage	5, 10, 20 year spans, monthly & seasonal.
PHYSLAND	Environment Canada	300 m resolution	12 or 6 classes
WSHD-0_	Environment Canada	Mosaic	3rd, 2nd and 1st order drainage divides

N.B: Underscore is a wildcard used to represent any letter or number.

The term: "mosaic" indicates that this map was itself assembled from three source maps brought into spatial register within the study area: Canada (300 m resolution), Ontario and Quebec (both at 150 m resolution. This was done to ensure the highest possible location accuracy within the central portions of the study area for drainage basin divide and water body features.

Derived Maps

The first task in a GIS study is to visualize the temporal and spatial coverage for the study area. Spatial coverage is displayed by assigning the entire area to Thiessen polygons for each data type, e.g. flows or meteorological data, and adding the gauge locations as symbols whose dimension increases with record length. Temporal coverage is displayed by creating a series of maps, each representing a fixed time-span, and colour-coding each polygon according to completeness of coverage within each span. These maps are provided for 10-year time spans.

Some of the source maps were buffered to support distance-to-feature measurements (BUF-). Some of the maps were obtained by transforming point data to surfaces (or contour maps) using kriging. The most detailed version of each derived map has been provided at the end of this appendix and listed in Table C.2.

Table C.2: Metadata for Derived Maps

Name	Origin	Transformation(s)	Versions
BUF-LAKE	B-LAND and B-LAKE source maps	Buffering to 300 km in 25 km increments.	Small and great lakes, oceans & all (4 maps)
BUF-####	WSHD- source maps	Buffering to average homo. region size in 10 increments.	Two times 16 maps (on and off-pattern)
COV-###	Flow gauge points	Voronoi polygons combined with point buffering to 150 km every 25 km	50 to 150 m "radius of influence" (5 maps). Time coverage (31) and frequency (16 maps).
L-_____	HYDAT Flow Data	Geostatistical estimation on a 1o grid followed by import, interpolation	10 and 5 equal-interval classes for measurement and visualisation
REG-####	WSHD-3 map	Reclassification	16 regions and two alternatives (32 maps)
VEG	PHYSLAND	Simplification	
WSHD-#	WATER-0 source map	Simplification	3rd, 2nd and 1st order drainage divides

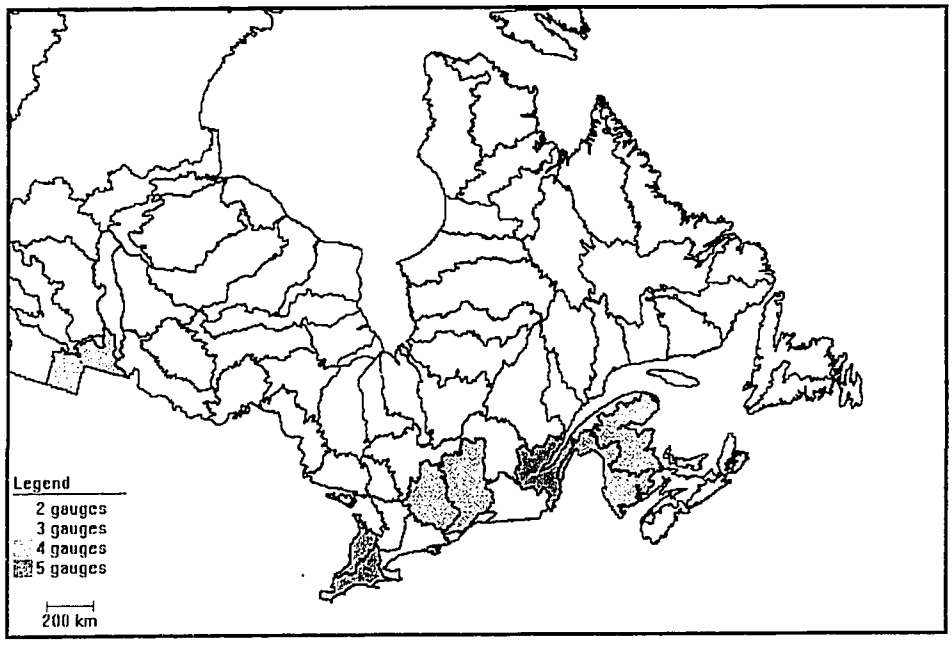

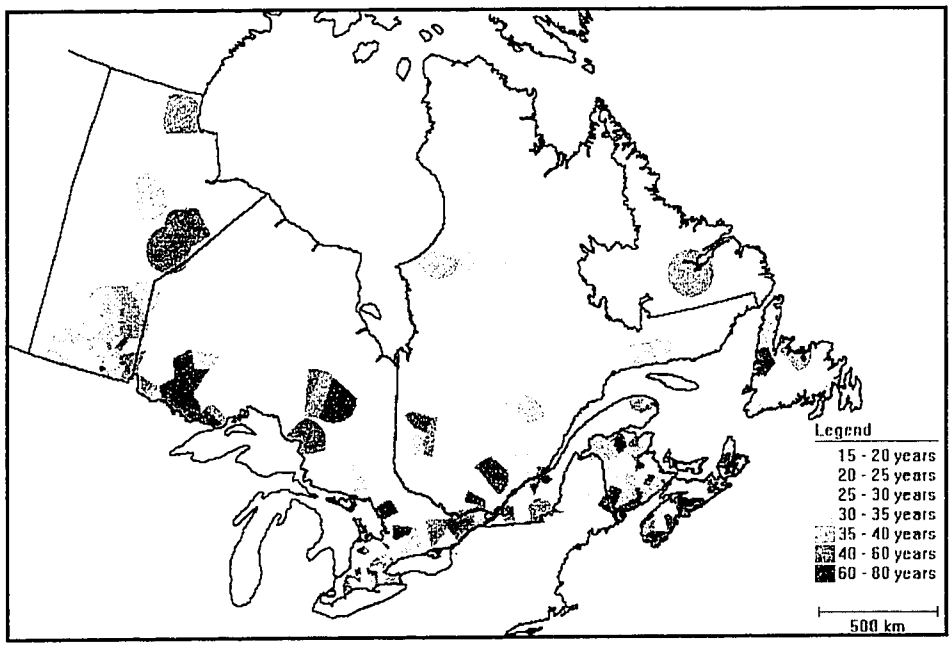

Gauge Density and Years of Record

Figure C1: Spatial and Temporal Coverage of Flow Gauges

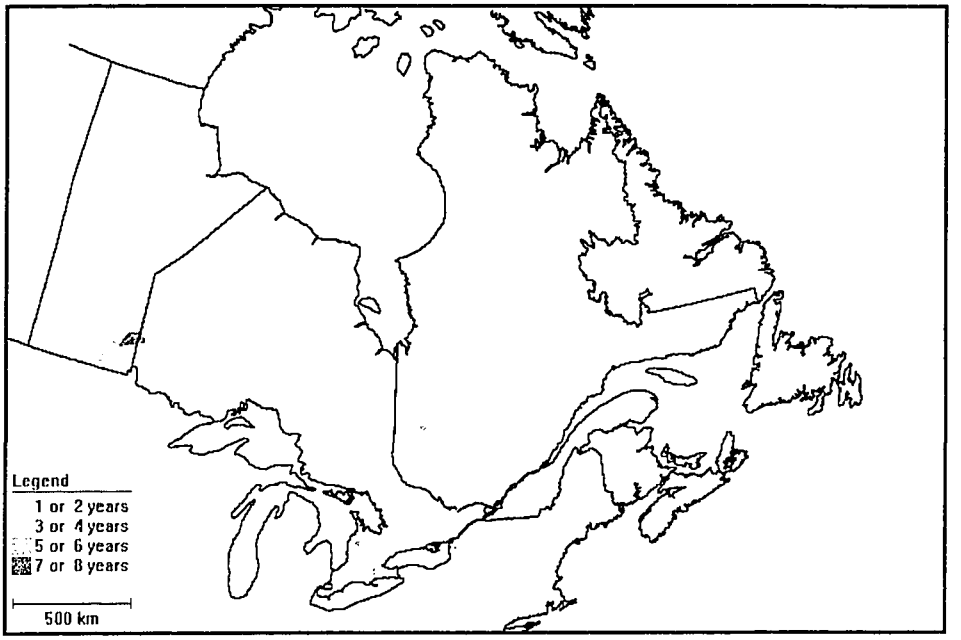

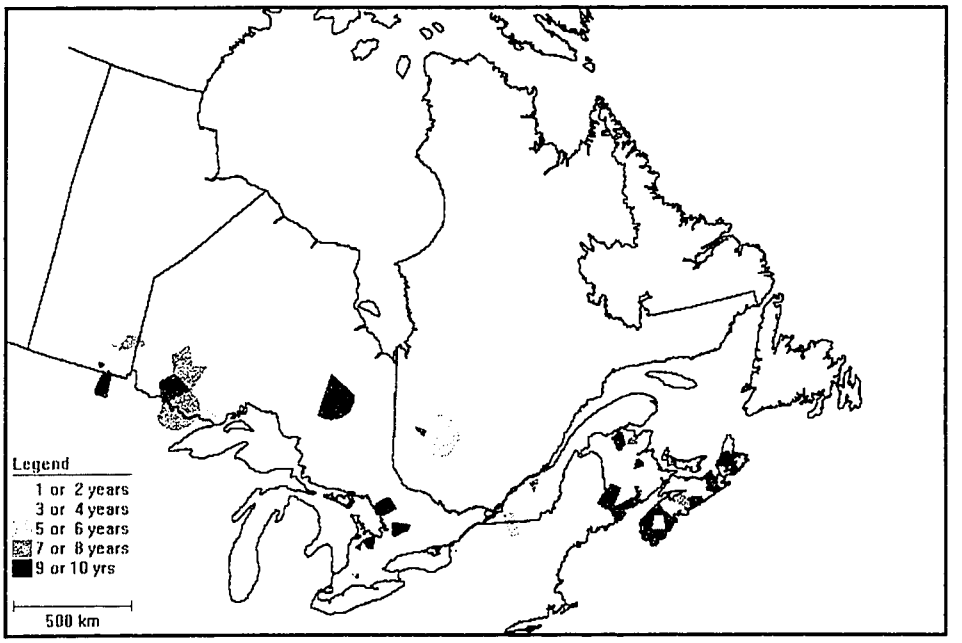

1910 to 1920 and 1920 to 1930

Figure C2: Years of Record for Gauged Areas

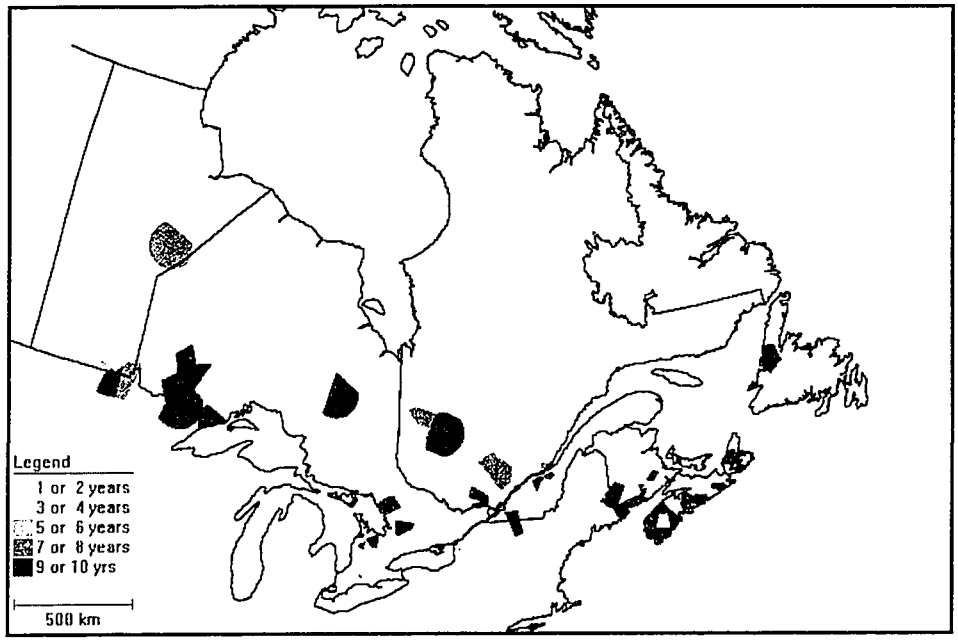

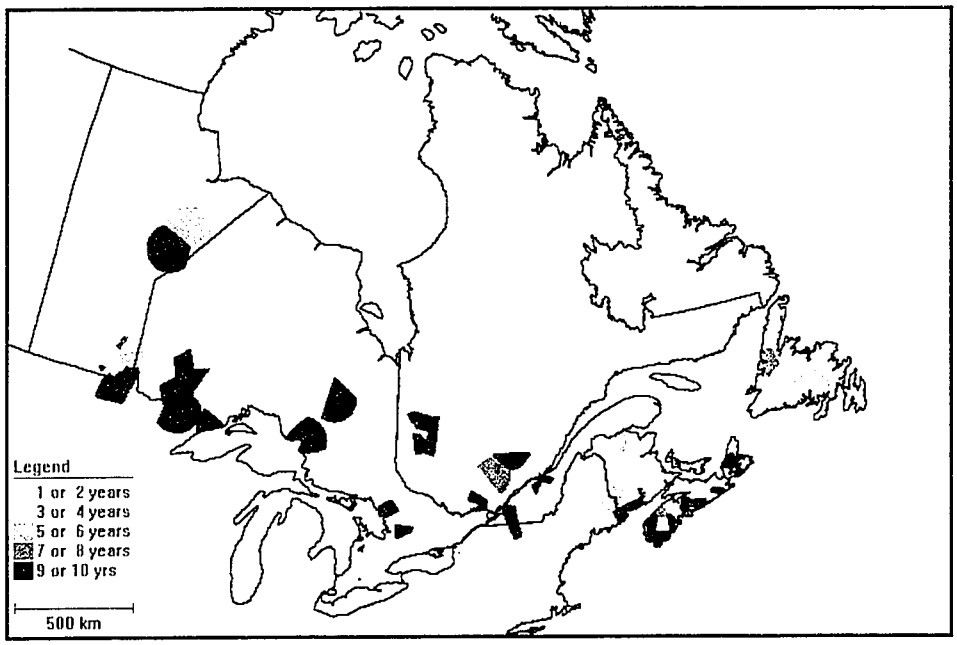

1930 to 1940 and 1940 to 1950

Figure C2: Years of Record for Gauged Areas

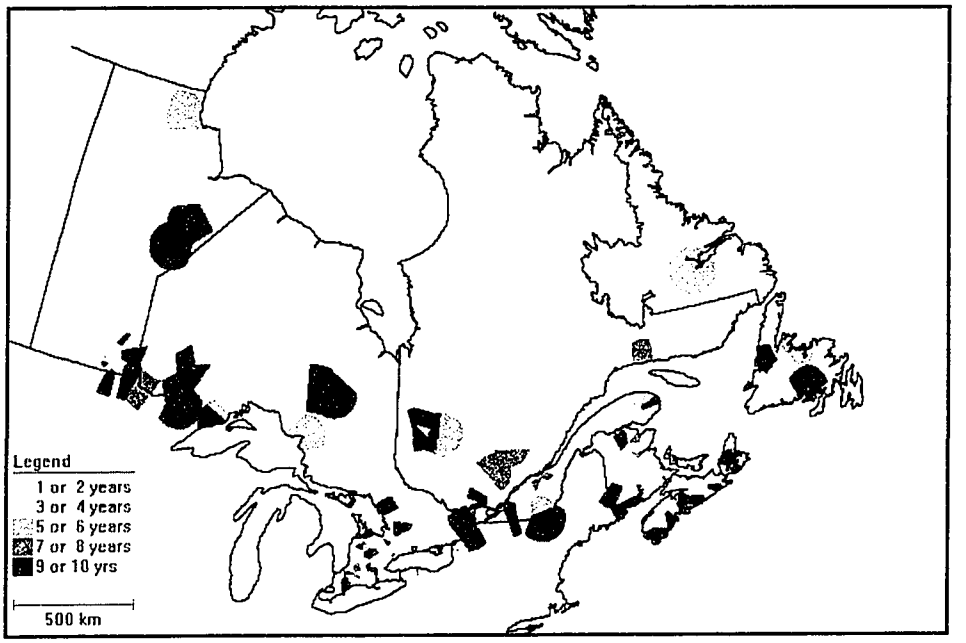

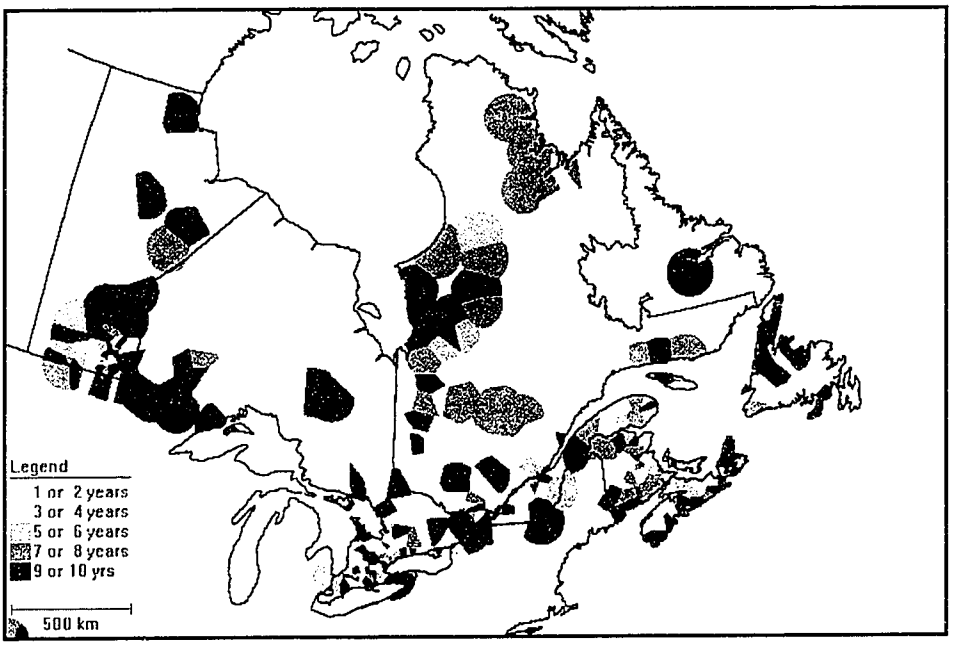

1950 to 1960 and 1960 to 1970

Figure C2: Years of Record for Gauged Areas

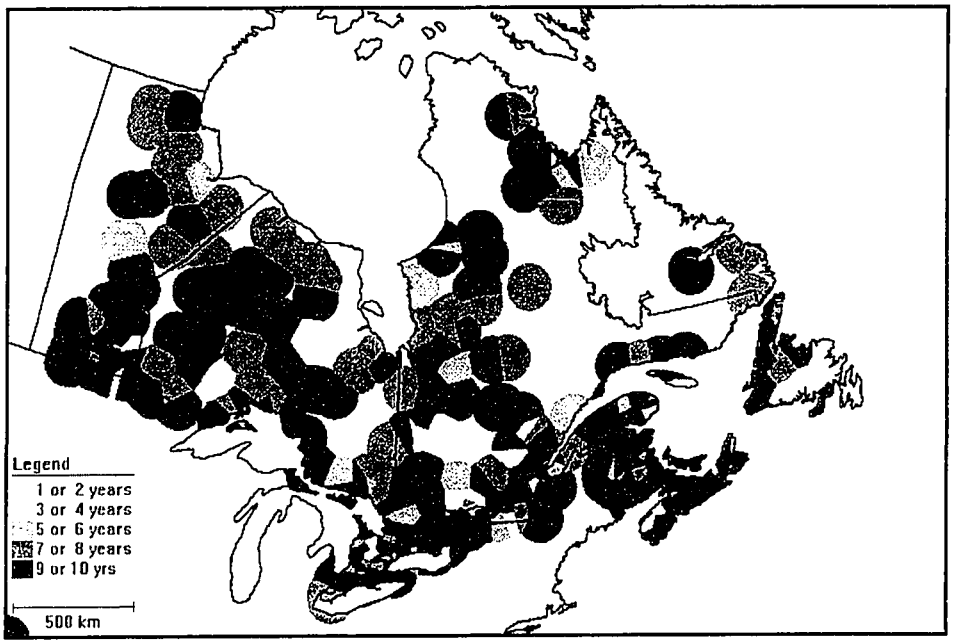

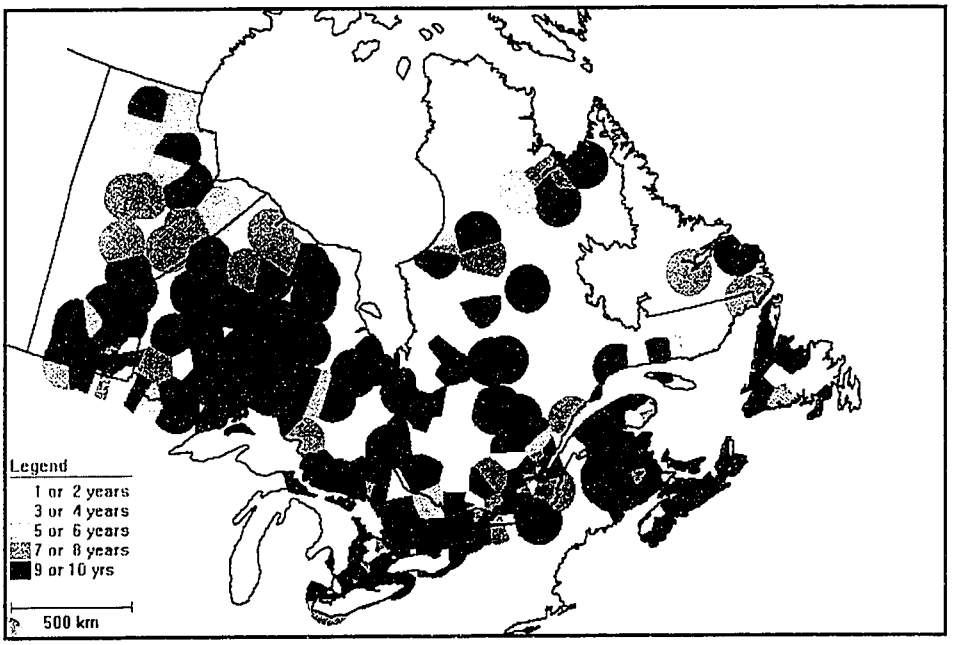

1970 to 1980 and 1980 to 1990

Figure C2: Years of Record for Gauged Areas

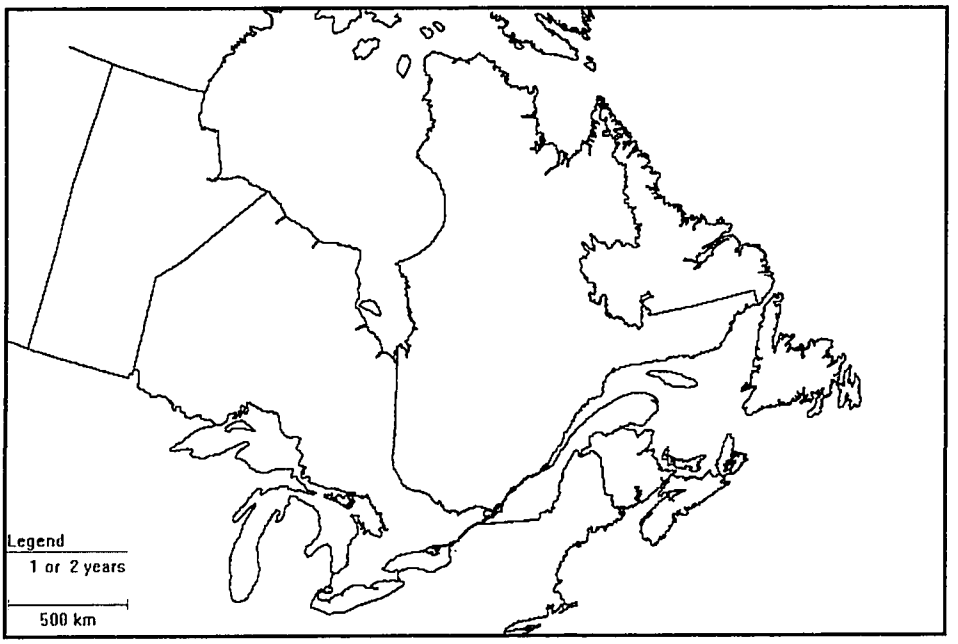

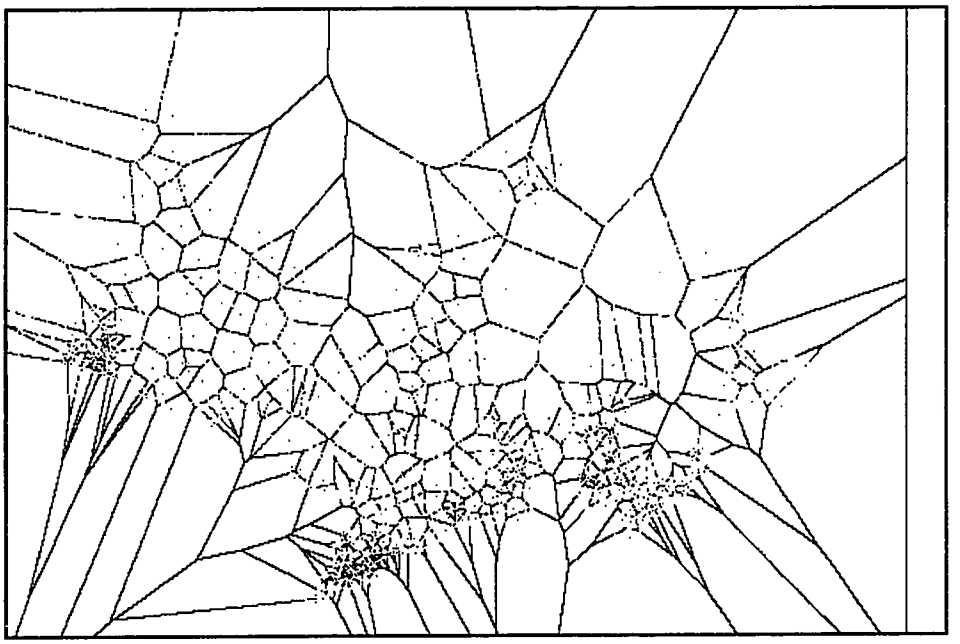

1990 to 1992 and Voronoi Polygons

Figure C2: Years of Record for Gauged Areas

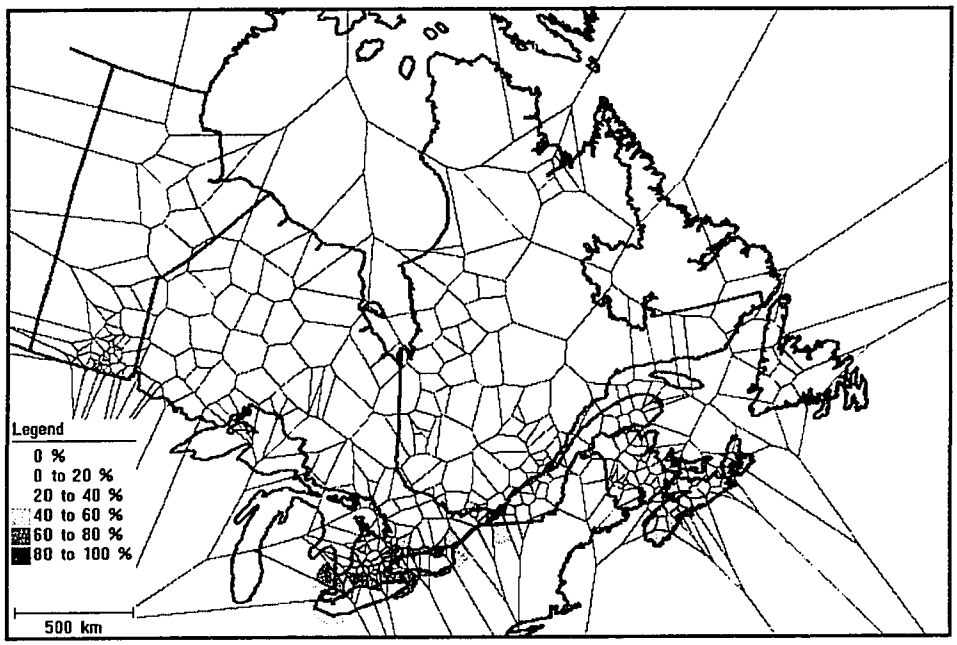

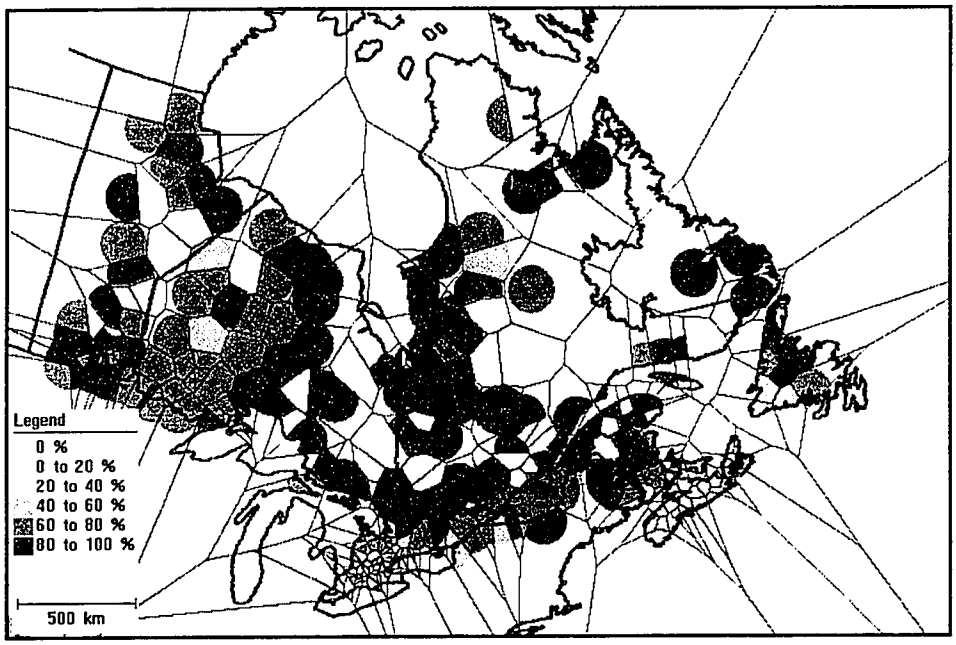

Spring and Summer Floods

Figure C3: Seasonal Flood Frequency

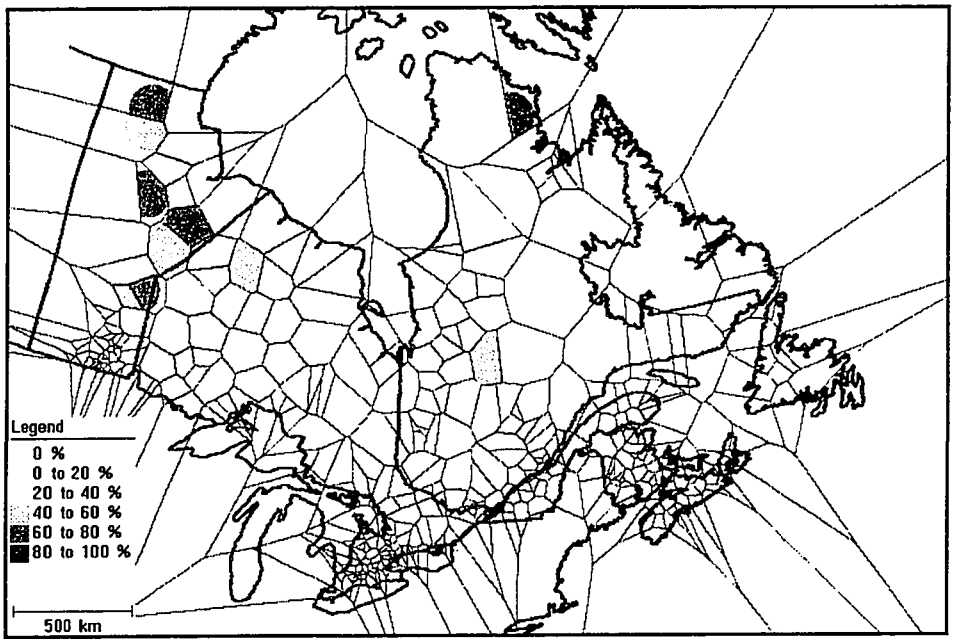

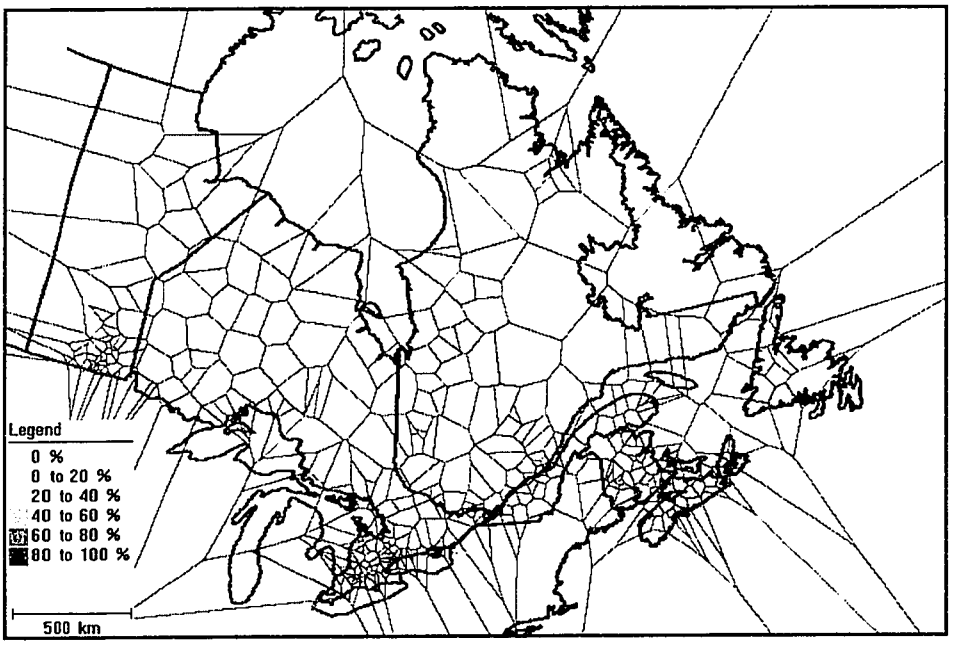

Fall and Winter Floods

Figure C3: Seasonal Flood Frequency

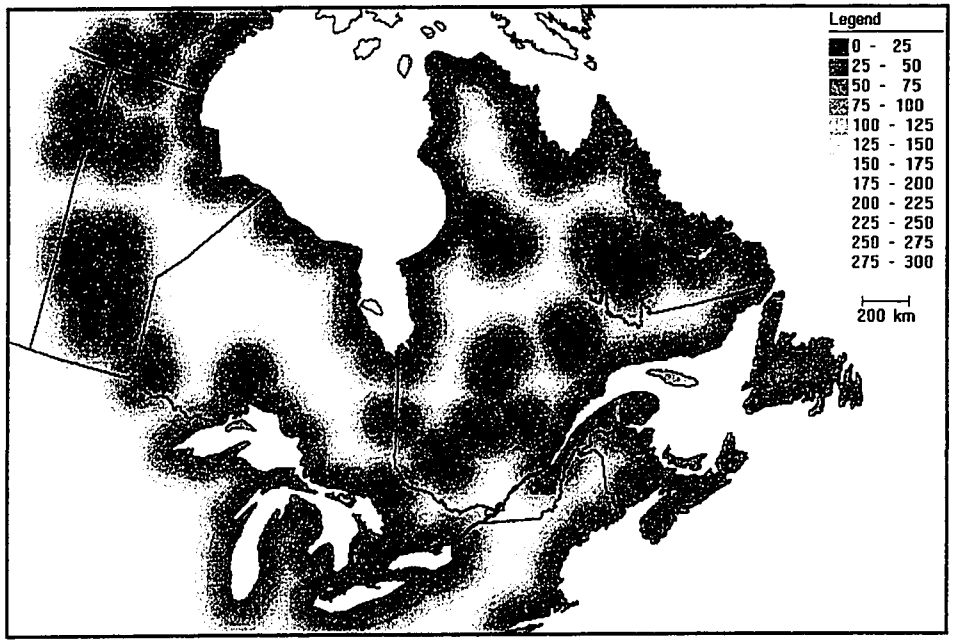

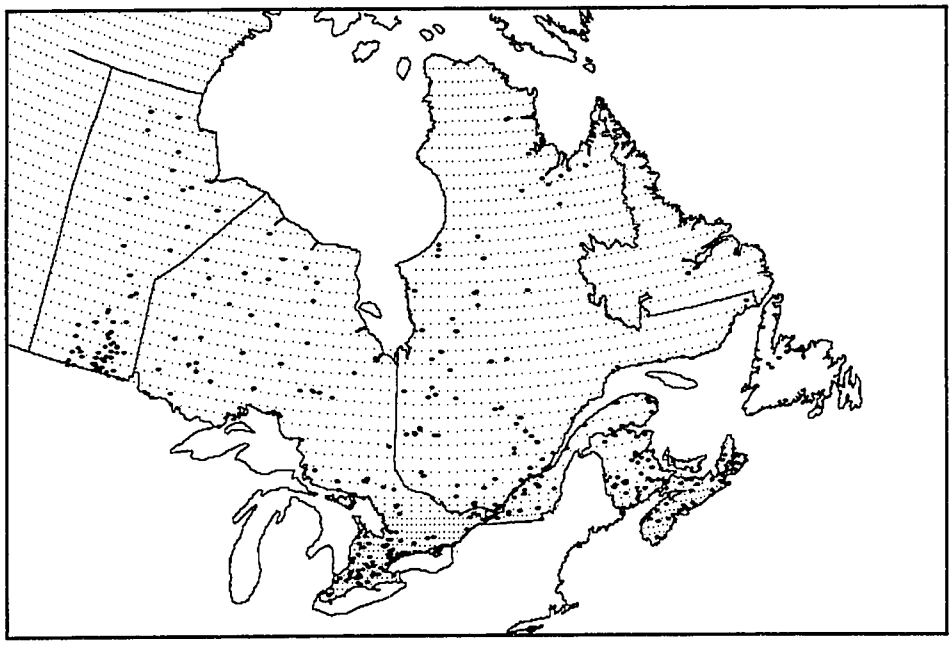

25 km Buffers to 300 km, Gauge Locations and Sampling Grid

Figure C4: Distance from Water Bodies and Map Sampling Grid

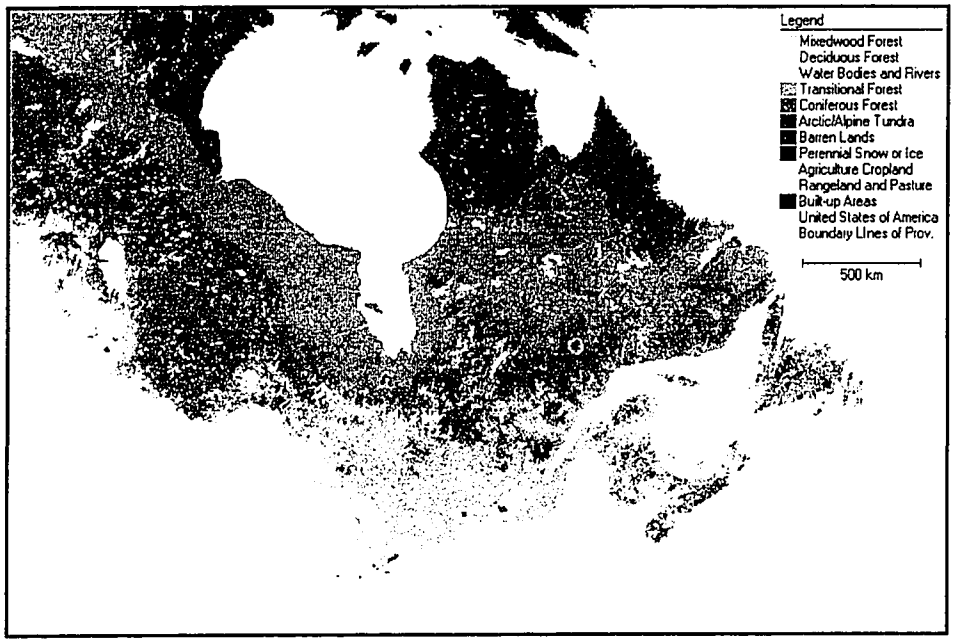

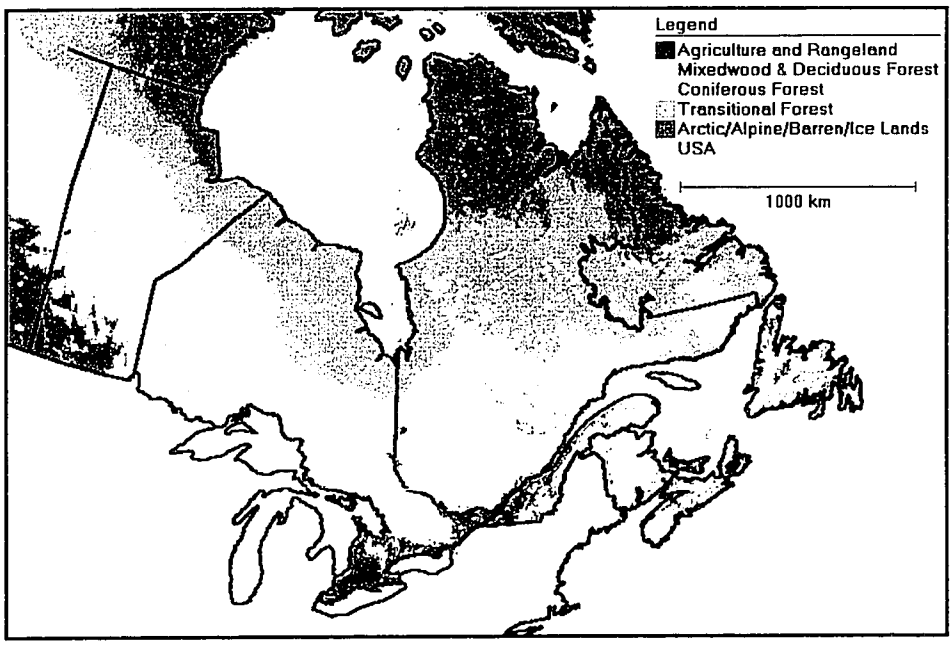

Figure C5: Detailed Land Use and Simplified Vegetation

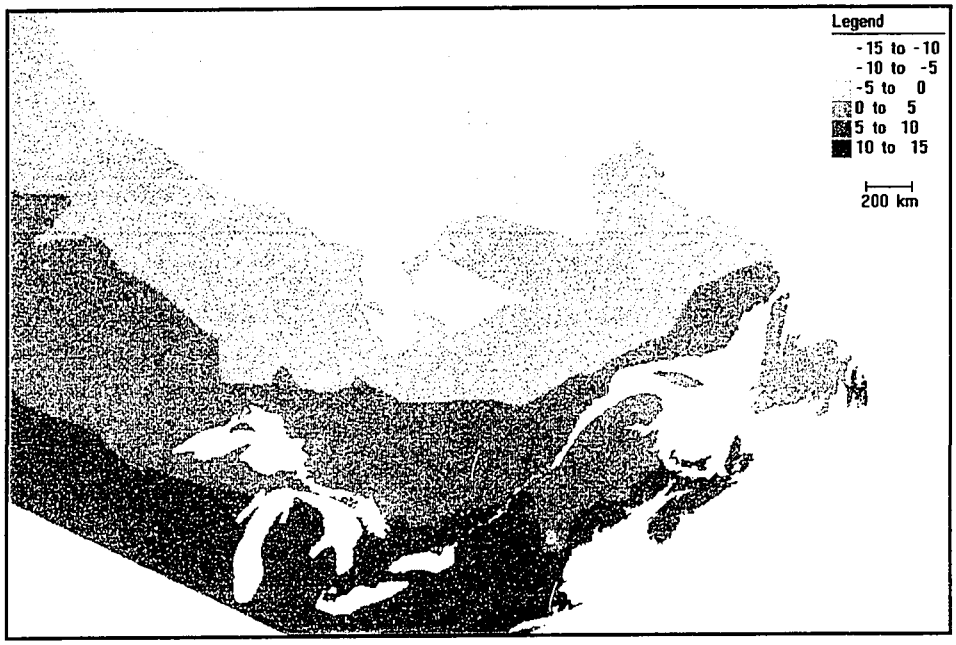

Figure C6: Average Annual Temperature and Total Precipitation

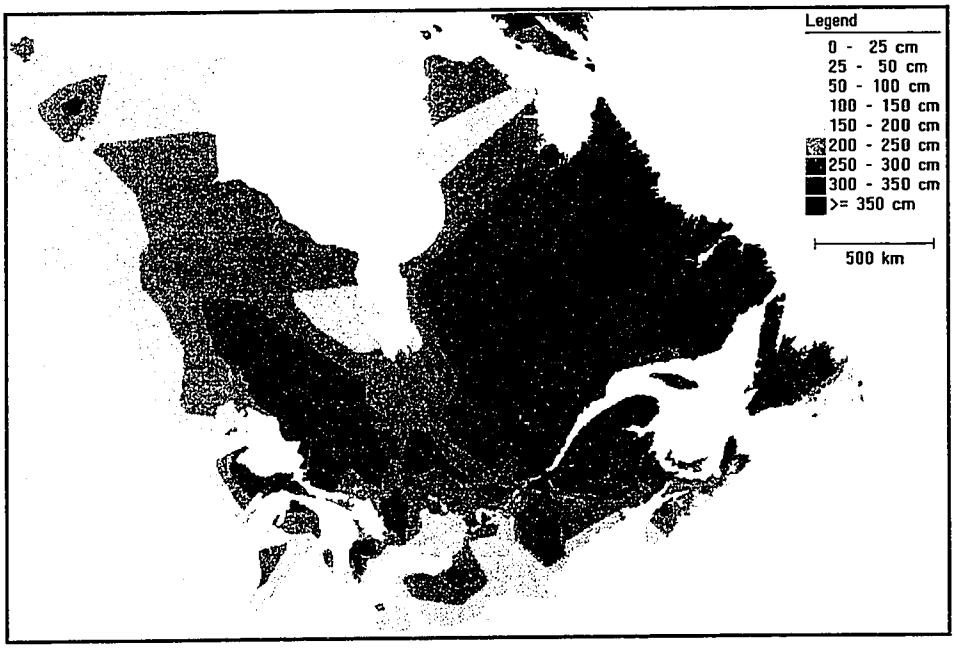

Figure C7: Average Annual Rain and Snow Precipitation

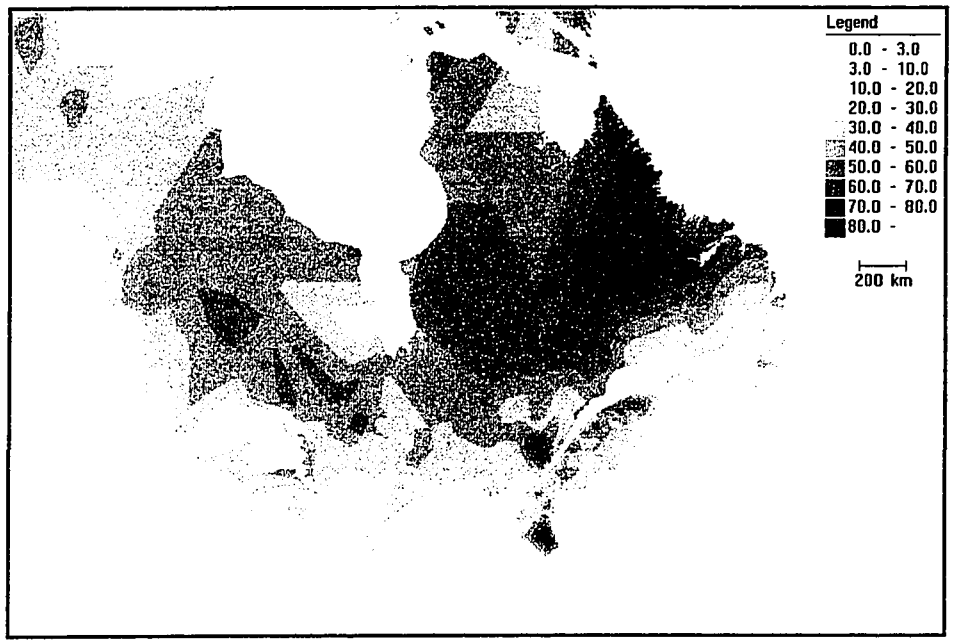

November and December

Figure C8: Average Monthly Snowfall

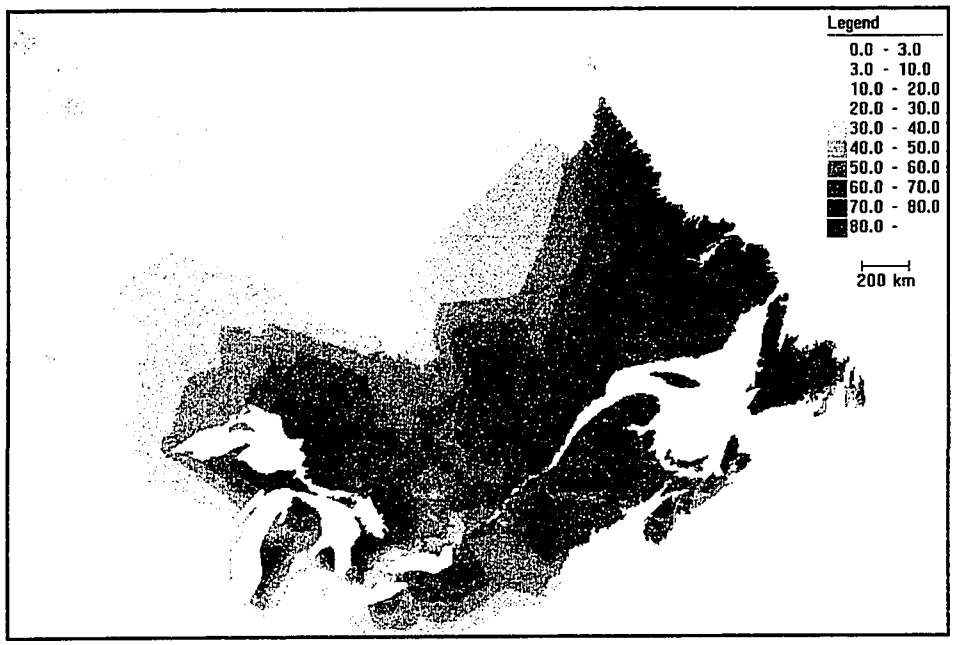

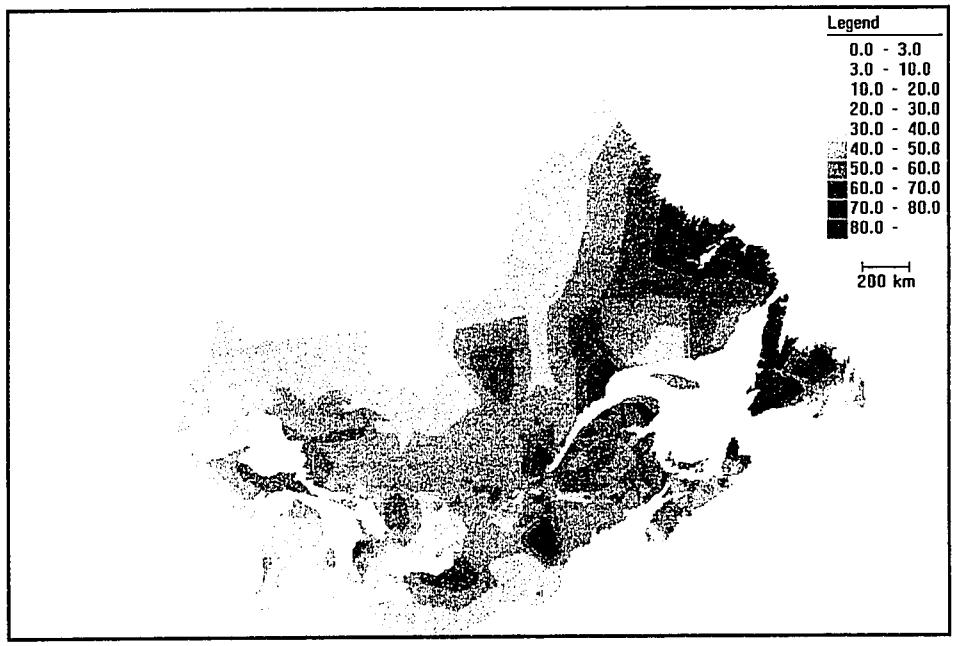

January and February

Figure C8: Average Monthly Snowfall

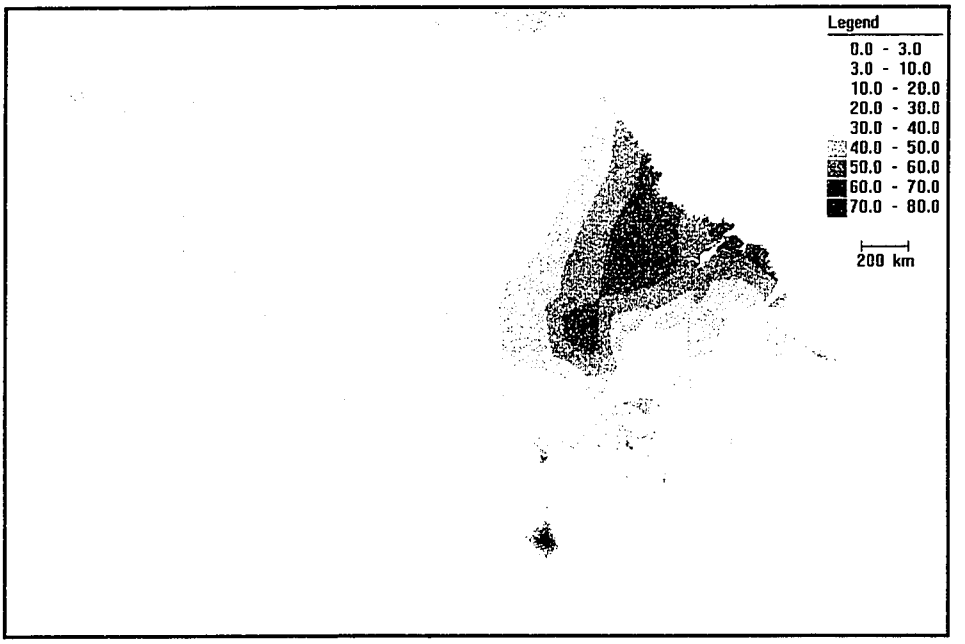

March and April

Figure C8: Average Monthly Snowfall

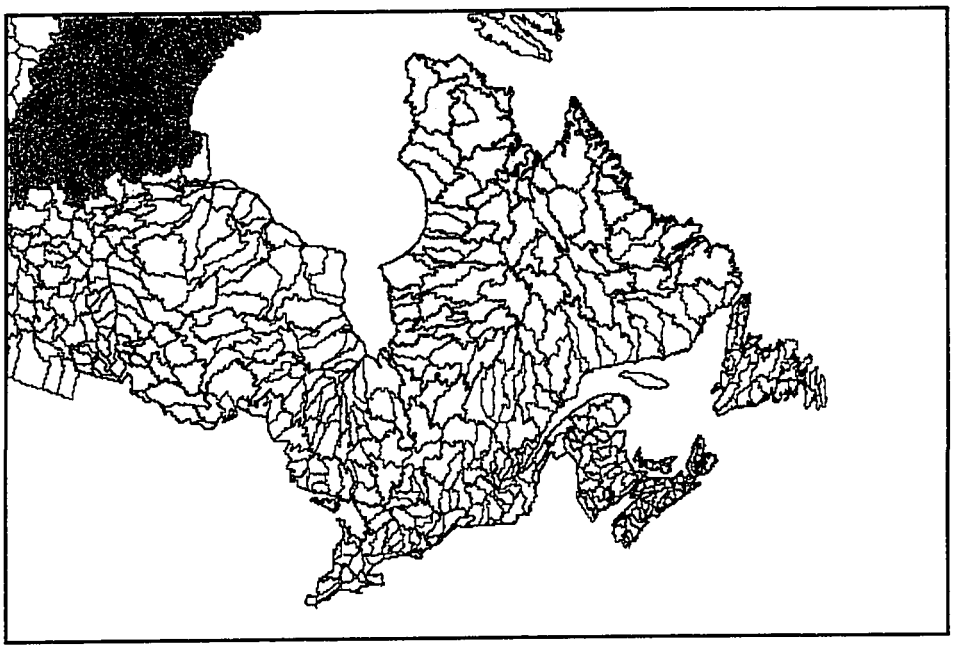

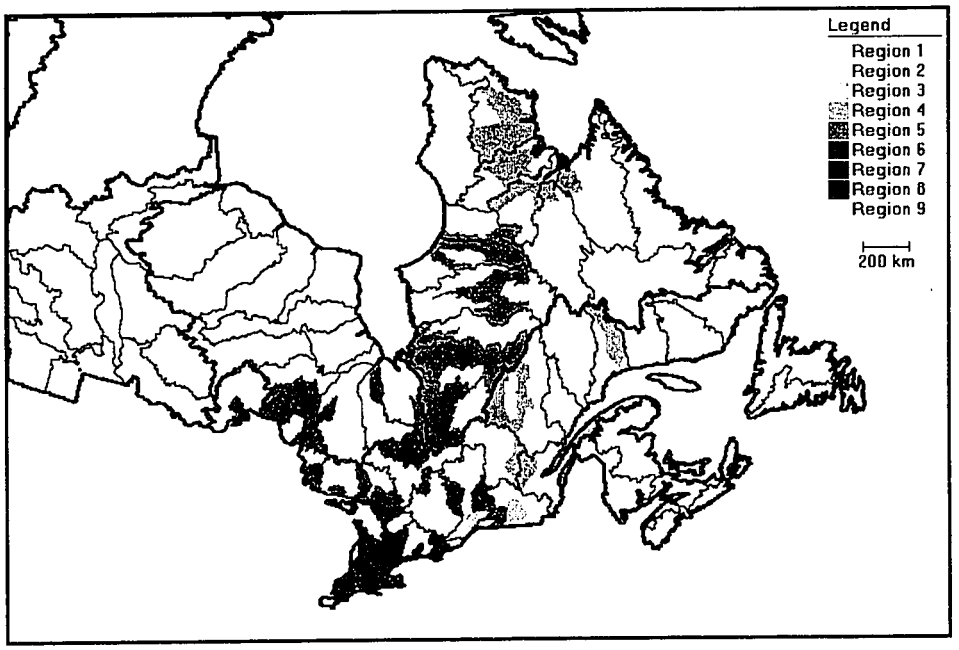

Second-Order Drainage Basin Divides and Initial Region Assignments

Figure C9: Delineation of Homogeneous Regions

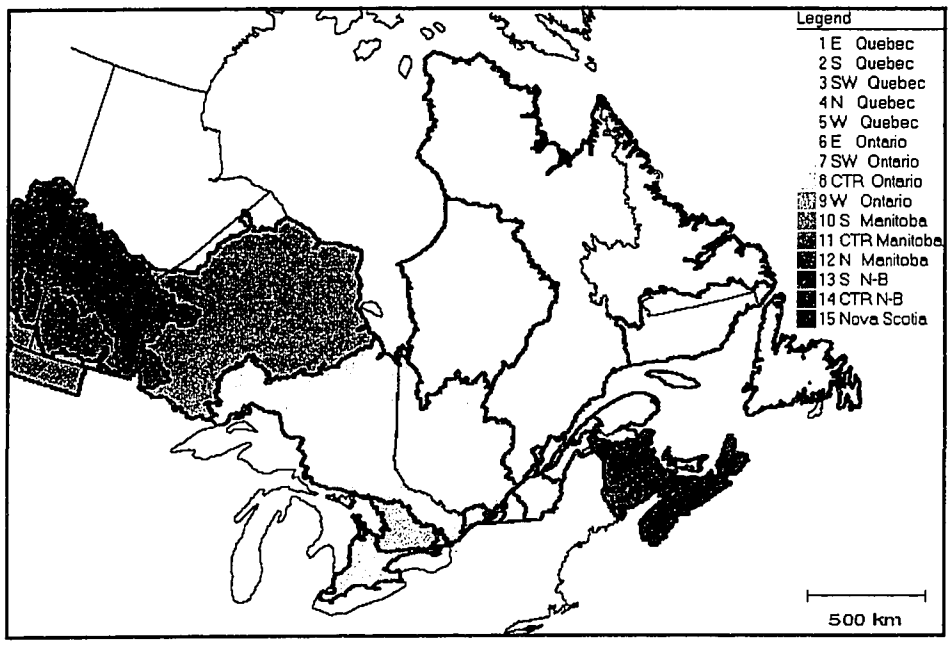

Regional Alternatives 1 and 2

Figure C9: Delineation of Homogeneous Regions

IMAGE EVALUATION TEST TARGET (QA-3)

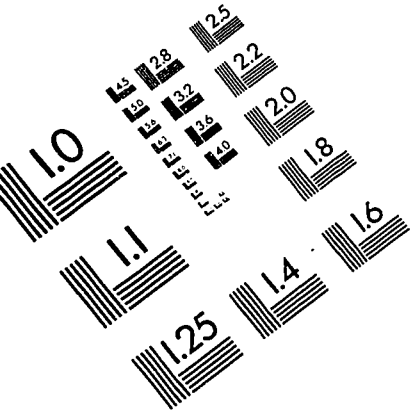

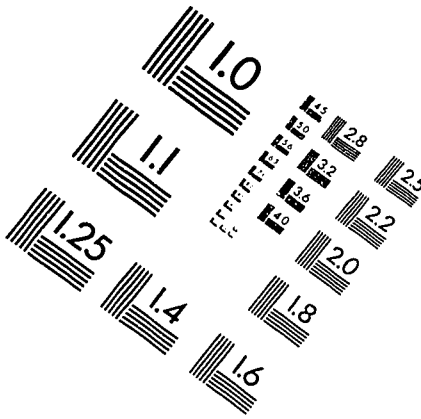

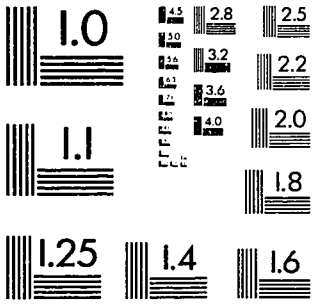

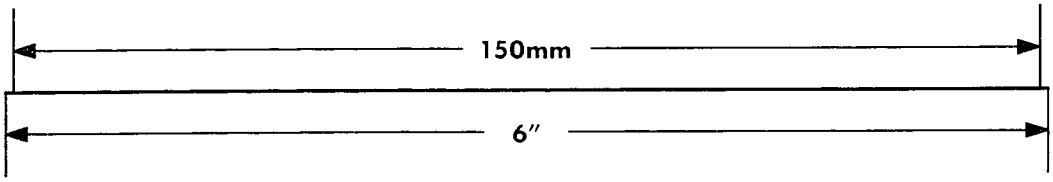

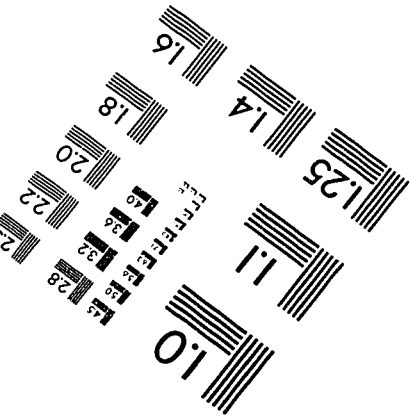

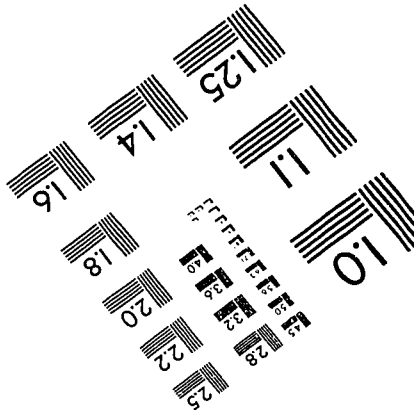

APPLIED IMAGE, Inc
1653 East Main Street
Rochester, NY 14609 USA
Phone: 716/482-0300
Fax: 716/288-5989